UNITED STATES DEPARTMENT OF COMMERCE
HARRY L. HOPKINS, Secretary
NATIONAL BUREAU OF STANDARDS
Lyman J. Briggs, Director

✦

Journal of Research

of the

National Bureau of Standards

✦

Volume 24, Number 1
January 1940

[Published with approval of the Director of the Budget]

UNITED STATES
GOVERNMENT PRINTING OFFICE
WASHINGTON : 1940

For sale by the Superintendent of Documents, Washington, D. C. - - - - - Price 30 cents
$3.50 per year on subscription

The prices of the separate Research Papers appearing in this JOURNAL are given on the front cover page. If 100 or more copies of any separate are ordered, a discount of 25 percent is allowed. Those who desire copies of separate Research Papers should send their orders and remittances without delay to the Superintendent of Documents, U. S. Government Printing Office, Washington, D. C. This will aid him to determine the number of copies to be printed for sale. Research Papers are not printed from electrotypes, and usually no more reprints can be had when the first and only printing is exhausted.

U. S. DEPARTMENT OF COMMERCE NATIONAL BUREAU OF STANDARDS

RESEARCH PAPER RP1266

Part of Journal of Research of the National Bureau of Standards, Volume 24, January 1940

INFRARED ARC SPECTRUM OF GERMANIUM

By C. C. Kiess

ABSTRACT

For theoretical reasons it is known that a portion of the arc spectrum of germanium must lie in the infrared. The more intense lines in this region have now been recorded on the specially sensitized plates of the Eastman series with the grating spectrographs of the National Bureau of Standards. Most of the new lines have been classified as combinations between the previously known $^3P^o$ and $^1P^o$ terms of the $5s$ configuration with new triplet and singlet terms of the $5p$ configuration. The yellow lines observed by Lunt in spark and discharge tube sources are found to be lines of Ge I and, in analogy with similar lines of C I and Si I, probably owe their origin to the $5s$-$6p$ transition.

CONTENTS

	Page
I. Introduction	1
II. Experimental procedure	2
III. Results	2

I. INTRODUCTION

The element germanium shares with gallium and scandium the distinction of having its existence foretold and its properties described prior to its actual discovery. In 1871 Mendeléeff announced his periodic classification of the chemical elements and predicted three new members to occupy the gaps in the table as it then existed. The final verification of his predictions occurred in 1886, when Winkler discovered a new element, germanium, with the properties ascribed by Mendeléeff to ekasilicon. The element is rare and only small amounts have been prepared in a pure state.

Investigations of the spectra emitted by germanium atoms in various states of excitation are summarized in volume 7 of Kayser's Handbuch der Spectroscopie. Since the preparation of this work in 1927, several more papers have appeared—three papers by Lang [1] and one by Rao and Narayan,[2] who describe the series of Ge II, Ge III, and Ge IV; a paper by Rao,[3] who describes the arc spectrum in the Schumann region and gives a revised term analysis of Ge I; and a paper by Sibaiya,[4] who finds that certain lines of Ge I reveal no hyperfine structure.

Rao's analysis of Ge I describes that portion of the spectrum that is built up on the terms ^3P, ^1D, and ^1S of the basic configuration $4s^2\ 4p^2$ of the neutral atom. That part of the spectrum resulting from combinations between high terms and lower terms of various

[1] R. J. Lang, Phys. Rev. **30**, 762 (1927); Proc. Nat. Acad. Sci. **14**, 32 (1928); Phys. Rev. **34**, 696 (1929).
[2] K. R. Rao and A. L. Narayan, Proc. Roy. Soc. (London) [A] **119**, 607 (1928).
[3] R. K. Rao, Proc. Roy. Soc. (London) [A] **124**, 465 (1929).
[4] L. Sibaiya, Current Sci. **6**, 152 (1937).

excited states has not yet been described. Prominent among the terms of the excited states are $5s\ ^3P$ and $5s\ ^1P$. In analogy with the structures that have been found for C I [5] and Si I,[6] we may expect for Ge I groups of lines in the infrared and in the yellow that represent the combinations between the higher terms of the $4s^2\ 4p\ np$ configurations with the $5s$ terms. It is the purpose of this paper to describe the results that have been obtained in a survey of the germanium arc spectrum throughout the yellow, red, and infrared regions photographically accessible.

II. EXPERIMENTAL PROCEDURE

The spectrograms upon which the present investigation is based were secured with the grating spectrographs of the National Bureau of Standards. For the infrared region, the grating ruled by Anderson with 7,500 lines per inch was employed. For the shorter regions, gratings ruled by Wood with 15,000 and 30,000 lines per inch were employed. For each spectral region to be recorded, the appropriate sensitized plate of the Eastman series was used.

The light source was an arc between copper or silver electrodes to which small amounts of GeO_2 were added. The arc was maintained at 6 or 7 amperes from 220-volt d-c mains, and operated with a fair degree of steadiness during the exposure periods, which ranged from 10 or 15 minutes for the yellow region to 3 hours for the infrared. Exposures to the iron arc were juxtaposed to the germanium exposures to furnish the wave-length standards required in the reductions of the measurements. The values of the standards were selected from the lists adopted by the International Astronomical Union [7] or from those measured by Meggers.[8]

III. RESULTS

The new wave lengths of Ge I are presented in table 1, in which each entry represents the mean of two to six measurements. The infrared lines are sharp, only a few presenting a slightly hazy or widened appearance. This latter characteristic is indicated in the table by the letter *h*. On the other hand, the yellow lines are diffuse, many of them exhibiting an asymmetrical shading toward longer wave lengths. The intensities assigned to the lines are the usual visual estimates, and are not comparable between widely separated regions of the spectrum.

[5] A. Fowler and E.W.H. Selwyn, Proc. Roy. Soc. (London) [A] **118,** 34 (1928); F. Paschen and G. Kruger, Ann. Physik [5] **7,** 1 (1930).
[6] C. C. Kiess, J. Research NBS **21,** 185 (1938) RP1124.
[7] Trans. Int. Astron. Union **3,** 77 (1928).
[8] W. F. Meggers, J. Research NBS **14,** 33 (1935) RP755.

TABLE 1.—*Wave lengths in the arc spectrum of germanium*

λ_{air} A	Intensity	ν_{vac} cm^{-1}	Term combination
11144. 80	2	8970. 34	$5s\ ^3P^o_2 - 5p\ ^3P_1$
11125. 28	25	8986. 08	$5s\ ^3P^o_2 - 5p\ ^3D_3$
11040. 09	1	9055. 42	$5s\ ^1P^o_1 - 5p\ ^3S_1$
11030. 88	2	9062. 98	$5s\ ^3P^o_1 - 5p\ ^3D^1$
10947. 51	30	9132. 00	$5s\ ^3P^o_1 - 5p\ ^3D_2$
10734. 14	25	9313. 52	$5s\ ^3P^o_0 - 5p\ ^3D_1$
10731. 80	1	9315. 55	
10576. 70	5	9452. 15	
10459. 70	1	9557. 89	
10405. 05	40	9608. 09	$5s\ ^3P^o_2 - 5p\ ^3P_2$
10382. 54	20	9628. 90	$5s\ ^1P^o_1 - 5p\ ^1D_2$
10305. 24	1	9701. 15	
10201. 00	8	9800. 27	$5s\ ^3P^o_1 - 5p\ ^3P_0$
10039. 48	20	9957. 95	$5s\ ^3P^o_2 - 5p\ ^3S_1$
9957. 65	1	10039. 78	
9844. 16	0	10155. 52	
9625. 72	35	10385. 99	$5s\ ^3P^o_1 - 5p\ ^3P_1$
9492. 59	10	10531. 65	$5s\ ^3P^o_2 - 5p\ ^1D_2$
9398. 93	20	10636. 59	$5s\ ^3P^o_0 - 5p\ ^3P_1$
9233. 40	1*h*	10826. 57	$5p\ ^3D_3 - 7s\ ^3P^o_2$
9096. 13	25	10990. 67	$5s\ ^1P^o_1 - 5p\ ^1S^o_0$
9068. 87	15	11023. 72	$5s\ ^3P^o_1 - 5p\ ^3P_2$
8789. 87	5	11373. 62	$5s\ ^3P^o_1 - 5p\ ^3S_1$
8367. 85	3	11947. 22	$5s\ ^3P^o_1 - 5p\ ^1D_2$
8256. 14	4*h*	12108. 87	
8031. 15	8*h*	12448. 10	
7833. 56	7*h*	12762. 08	
7511. 55	2*h*	13309. 17	$5s\ ^3P^o_1 - 5p\ ^1S_0$
6557. 74	3*h*	15244. 93	$5s\ ^1P^o_1 - 6p\ ^3D_2$
5967. 78	4*hl*	16752. 02	
5802. 23	50*hl*	17229. 99	$5s\ ^1P^o_1 - 6p\ ^1D_2$
5801. 18	4*h*	17233. 10	
5718. 08	1*hl*	17483. 55	
5701. 84	3*hl*	17533. 47	$5s\ ^3P^o_1 - 6p\ ^3D_1$
5692. 06	50*hl*	17563. 47	$5s\ ^3P^o_1 - 6p\ ^3D_2$
5664. 90	15*hl*	17647. 68	
5664. 27	12*hl*	17649. 64	
5656. 08	25*hl*	17675. 20	
5621. 59	20*hl*	17783. 64	$5s\ ^3P^o_0 - 6p\ ^3D_1$
5616. 00	1*h*	17801. 34	
5606. 94	25*h*	17830. 10	
5564. 88	15*hl*	17964. 86	
5513. 35	5*hl*	18132. 77	$5s\ ^3P^o_2 - 6p\ ^1D_2$
5265. 91	2*h*	18984. 80	

When the wave numbers of the new infrared lines were differenced, it was seen that they exhibited the separations of the ^3P and ^1P terms of the $5s$ configuration. This led to the detection of the $5p$ terms, as listed in table 2, with numerical values based on those given by Rao. For the present, the component $^3P_0$ must be regarded as provisional owing to the nonappearance of other combinations necessary to establish it with certainty. The absence of the term $5p\ ^1P$ must also be regarded as surprising in view of the intensity with which the analogous term appears in Si I and C I.

TABLE 2.—*np terms of Ge* I

Term symbol	$n=5$		$n=6$	
	Term value	$\Delta\nu$	Term value	$\Delta\nu$
$^3D_3$	17454. 25		--------	
		1269. 59		
$^3D_2$	18723. 84		10292. 53	
		69. 04		30. 07
$^3D_1$	18792. 88		10322. 60	
$^3P_2$	16832. 20		--------	
		637. 70		
$^3P_1$	17469. 90		--------	
		585. 68		
$^3P_0$	18055. 58		--------	
$^3S_1$	16482. 28			
$^1D_2$	15908. 70		8307. 50	
$^1P_1$	--------		--------	
$^1S_0$	14546. 82		--------	

The green and yellow lines between 5200 and 6000 A are identical with those previously observed by Lunt.[9] In his experiments with sparks between metallic electrodes and with discharges through Geissler tubes containing $GeCl_4$, these lines appeared under conditions favorable for the excitation of the neutral atom. The recent experiments at the National Bureau of Standards make it certain that they are emitted by neutral and not ionized atoms. Apparently they are the counterparts of similar groups in Si I and C I and represent the transition $5s$—$6p$. However, the satellite lines necessary to establish the multiplets with certainty are not present, and the classifications given for some of them, in table 1, must be regarded as provisional. The terms on which these tentative assignments are based were suggested by the occurrence among these lines of the $5s$ differences 250, 903, and 2,318 cm^{-1}.

The new terms that have resulted from this investigation belong to the np electron configurations. They are presented in table 2. According to Hund's theory, the terms $^3P_0$, $^3P_1$, $^3D_1$, and $^3D_2$ owe their origin to the binding of a p electron to the $^2P^\circ_{0½}$ state of Ge^+; the others, including all the singlets, have $^2P^\circ_{1½}$ as their parent term.

[9] J. Lunt, Monthly Notices Roy. Astron. Soc. 85, 38 (1924).

The $5p\ ^3D$ terms show clearly that they originate in the manner required by theory; the $5p\ ^3P$ terms exhibit this feature to a lesser degree. Accepting these facts as a guide, it would be possible to derive a complete set of terms for the $6p$ configuration; but for the present it seems more desirable to await the evidence of future observations.

While the work described in this paper was in progress, the wave lengths of some Ge II lines, in the yellow and red, were measured several times. These lines appeared only at the poles of the arc and were clearly distinguishable from the Ge I lines. The mean values of these determinations are presented at this time, in table 3, to complete the observational record.

TABLE 3.—*Wave lengths of some* Ge II *lines*

Wave length	Intensity	Wave number	$\Delta\nu$	Term combination
7145. 42	7	13991. 13	359. 49	$4p'\ ^2D_{1½}-5p\ ^2P^0_{0½}$
7049. 45	10	14181. 60		$4p'\ ^2D_{2½}-5p\ ^2P^0_{1½}$
6966. 42	1	14350. 62		$4p'\ ^2D_{1½}-5p\ ^2P^0_{1½}$
6484. 26	7*h*	15417. 71	359. 62	$5p\ ^2P^0_{1½}-6s\ ^2S_{0½}$
6336. 46	4*h*	15777. 33		$5p\ ^2P^0_{0½}-6s\ ^2S_{0½}$
6021. 09	20	16603. 70	359. 68	$5s\ ^2S_{0½}-5p\ ^2P^0_{0½}$
5893. 42	25	16963. 38		$5s\ ^2S_{0½}-5p\ ^2P^0_{1½}$

WASHINGTON, November 28, 1939.

U. S. DEPARTMENT OF COMMERCE NATIONAL BUREAU OF STANDARDS

RESEARCH PAPER RP1267

Part of Journal of Research of the National Bureau of Standards, Volume 24, January 1940

COLORIMETRIC DETERMINATION OF ARSENIC IN FERROUS AND NONFERROUS ALLOYS[1]

By Clement J. Rodden

ABSTRACT

A method is described for the determination of arsenic and has been applied successfully to iron, steel, copper-base alloys, tin- and lead-base bearing metals, and pig lead. The arsenic is first separated from the other constituents of the material by distillation as the trichloride. It is then oxidized to arsenic acid and converted to a blue arsenic-molybdenum compound by treatment with a solution containing hydrazine sulfate and ammonium molybdate. The transmittancy of the colored solution is measured with a photoelectric colorimeter, and the amount of arsenic read from a curve obtained by using known amounts of arsenic. Alternatively, the color may be matched against standards by means of a visual colorimeter. The method is reasonably rapid and is applicable to amounts of arsenic as small as 2 micrograms.

CONTENTS

		Page
I.	Introduction	7
II.	Apparatus	8
III.	Weight of sample	9
IV.	Procedure	9
V.	Results	11

I. INTRODUCTION

Arsenic in ferrous and nonferrous alloys is usually separated from other elements by distilling it as arsenic trichloride and is then determined by (a) weighing as the sulfide, (b) converting the arsenious sulfide to silver arsenate and titrating the silver with potassium thiocyanate, or (c) neutralizing the hydrochloric acid in the distillate and titrating with iodine or potassium bromate.[2] Other methods have been used, especially for white metals; for example, arsenic is sometimes separated as the element from a hydrochloric-acid solution of the metal or alloy by reduction with sodium hypophosphite,[3] stannous chloride,[4] or calcium hypophosphite.[5] The arsenic thus obtained is dissolved in an excess of standard iodine solution and the excess iodine titrated with standard sodium arsenite solution. Alternatively, the arsenic may be converted to arsenious acid and titrated with bromate.[6]

[1] Presented before the Division of Microchemistry at the 98th Meeting of the American Chemical Society, Boston, Mass., September 11 to 15, 1939.

[2] G. E. F. Lundell, J. I. Hoffman, and H. A. Bright, Chemical Analysis of Iron and Steel (John Wiley & Sons, Inc., New York, N. Y., 1931). Methods of Chemical Analyses of Metals, (American Society for Testing Materials, 1936).

[3] L. Brandt, Chem.-Ztg. **37**, 1445, 1496 (1913).

[4] S. B. Evans, Analyst **57**, 492 (1932).

[5] E. I. Fogel'son and N. V. Kalmuikova, Zavodskaya Lab. **5**, 584 (1936).

[6] C. W. Anderson, Ind. Eng. Chem., Anal. Ed. **9**, 569 (1937).

For the determination of small amounts of arsenic in biological material, Morris and Calvery [7] recommend a modification of Denigès' method,[8] whereby a blue complex arsenic-molybdenum compound is formed. In the method to be described, the formation of this blue color is the basis for the determination of arsenic, which has previously been removed from interfering elements by distillation as arsenic trichloride. Antimony, which might distill in part under certain conditions, does not interfere.

The transmittancy of the colored solution is measured with a photoelectric colorimeter (or comparator). The quantity of arsenic is read from a standard curve drawn from data obtained by treating known amounts of arsenic in the same manner as is described for the unknown. The method has been applied to many types of ferrous and nonferrous alloys. It is more rapid than the usual macromethods and is especially useful with materials of very low arsenic content, such as pig lead.

II. APPARATUS

The Scherrer all-glass distilling apparatus,[9] shown in figure 1, was used to distill the arsenic trichloride. *C* is a 200-ml distilling flask, the neck of which is 2.5 cm in diameter. It is provided with an exit tube, a thermometer well, and an inlet tube for conveying the acids and carbon dioxide to the distilling flask. Both the thermometer well and the inlet tube reach within 3 mm of the bottom of the flask. The distance between the bottom of the flask and the exit tube leading to the condenser is 17 cm.

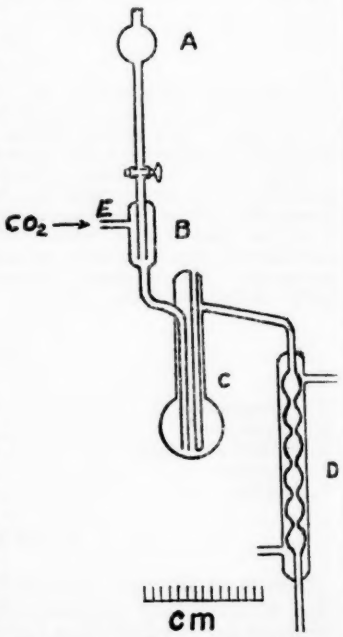

FIGURE 1.—*Distilling apparatus.*

The apparatus is clamped to a ring stand. *C* rests on an asbestos board (about 18 by 18 cm) having a round hole 4.5 cm in diameter.

The photoelectric colorimeter was constructed according to the design of Brice [10] and consists of a balanced circuit using barrier-layer type photoelectric cells. The cylindrical absorption cells are 18 mm in internal diameter with the distance between the faces 2 cm.

Examination of the colored solution with a hand spectroscope showed absorption in the red, and for this reason a Jena OG_2 filter which transmits from 550 mμ through the red was used.

A visual colorimeter, such as the Duboscq type, may also be used for determining the amount of arsenic by matching against solutions containing known amounts of arsenic.

[7] H. J. Morris and H. O. Calvery, Ind. Eng. Chem., Anal. Ed. **9**, 447 (1937).
[8] G. Denigès, Pregl Festschrift, p. 27 (Mikrochemie, 1929).
[9] John A. Scherrer, J. Research NBS **16**, 253 (1936) RP871; **21**, 95 (1938) RP1116.
[10] B. A. Brice, Rev. Sci. Instr. **8**, 279 (1937). Also private communications.

III. WEIGHT OF SAMPLE

Nonferrous alloys, particularly bearing metals, are prone to segregate, as is shown by the variation in results of macroanalyses of journal bearings.[11] The composition of the large-sized particles of many alloys often differs from that of the small ones, and it is usually inconvenient or impossible to decrease the size of all the particles to the point where it becomes certain that a small sample (say less than 10 mg) is truly representative of the material. Experiments with samples of brass and bronze, as prepared for macroanalyses, have shown that there is a sufficient difference in composition of the chips to cause serious error if the analysis is made on a 5- to 10-mg sample (4 to 5 chips), but when 100-mg samples are taken, no such errors are encountered.

A 100-mg sample is therefore recommended as the minimum for materials in the form of small chips,[12] unless tests have shown that there is no segregation, or the amount of sample is limited. For convenient comparison in the cells and instrument used, the sample should contain at least 2 micrograms of arsenic. A 100-mg sample of commercial steel, with arsenic contents ranging from 0.005 to 0.02 percent, fulfills this condition. The same weight of sample can be used for cast irons. However, with high-arsenic irons (arsenic $>$0.03 percent) it is necessary to dilute the colored solution, as described later.

If the arsenic content is such that 100 mg of material does not give sufficient arsenic, the weight of the sample may be increased. For example, with lead of high purity (arsenic about 0.0005 percent) a 5-g sample is required in order to obtain the optimum amount of arsenic.

IV. PROCEDURE

Carbon steel.—Place a 0.1-g sample in a 50-ml beaker, dissolve the steel in 10 ml of diluted nitric acid (1+1), and evaporate the solution to dryness on a hot plate at a temperature not exceeding 130° C. Cool, add 5 ml of hydrochloric acid (sp gr 1.18), and transfer the solution to the distilling apparatus (fig. 1) with the aid of a 10-ml portion of hydrochloric acid. Add 2 ml of hydrobromic acid. Mix 0.3 g of hydrazine sulfate with 10 ml of hydrochloric acid (sp gr 1.18), start the current of carbon dioxide and transfer the mixture to the distilling apparatus. Insert a thermometer in the well of the distilling flask and provide a receiver (150-ml tall-form beaker) containing 10 ml of water into which the end of the condenser dips. Pass a stream of carbon dioxide through the apparatus at the rate of two or three bubbles per second, and boil the solution gently until the temperature reaches 111° C. This requires approximately 15 minutes; the flask will contain about 10 ml of solution at this stage. Without interrupting the stream of carbon dioxide or the heating, remove the receiver and rinse the end of the condenser with distilled water. Add 10 ml of nitric acid (sp gr 1.42) to the distillate, place the beaker on a steam bath, and evaporate the solution to dryness. Heat the beaker and contents in an oven at 130° C for ½ to 1 hour to remove all traces of nitric acid. Add 10 ml of hydrazine sulfate-molybdenum solution[13] for each 30

[11] J. A. Scherrer and G. E. F. Lundell, BS J. Research 5, 891 (1930) RP237.
[12] Particle size between Nos. 18 and 40 sieves, U. S. Standard.
[13] The hydrazine sulfate-molybdenum solution is prepared as follows: Dissolve 1 g of ammonium molybdate in 100 ml of 5 *N* sulfuric acid. Dissolve 0.15 g of hydrazine sulfate in 100 ml of water. Dilute 10 ml of the molybdate solution to 90 ml with water, add 1 ml of the hydrazine sulfate solution, and dilute with water to 100 ml.

micrograms of arsenic, and heat the solution on a steam bath for 10 to 15 minutes. Cool, and dilute with hydrazine sulfate-molybdenum solution so that the solution contains no more than 3.0 micrograms of arsenic per milliliter.[14] This is done conveniently in 10- to 250-ml volumetric flasks. Measure the transmittancy of the solution with a photoelectric colorimeter, using the hydrazine sulfate-molybdenum solution in the comparison cell. Read the amount of arsenic from a standard curve which has been drawn from data obtained by treating known amounts of arsenic by the same procedure as is described for the unknown, and correct the result for a blank carried through the

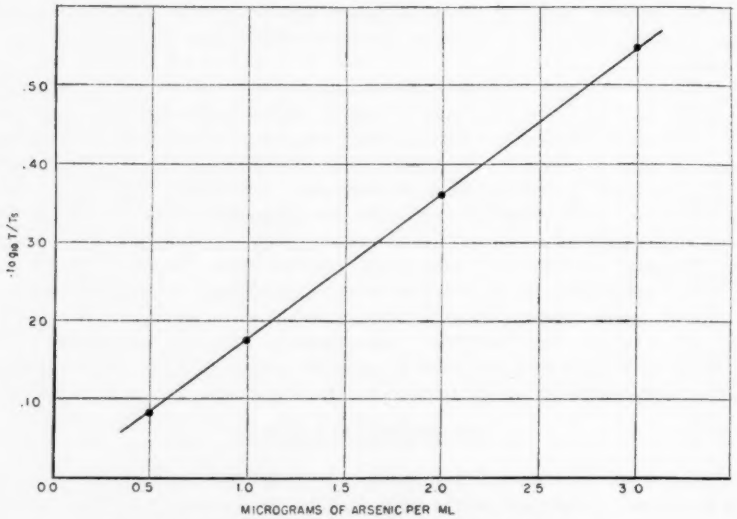

FIGURE 2.—*Curve showing conformance to Beer's Law.*

T = Transmittancy of solution containing arsenic.
T_0 = Transmittancy of blank hydrazine-sulfate-molybdate solution.

entire procedure.[15] The standard curve is constructed by plotting micrograms of arsenic with respect to transmittancy.

The transmittancy measurements of solutions containing from 0.5 to 3.0 micrograms of arsenic per milliliter are reproducible to about 0.1-percent transmittancy.

Experiments showed that the transmittancy of the solutions containing the arsenic-molybdenum compound did not change over a period of 24 hours. Figure 2 indicates that the colored solutions obey Beer's law in the region from 0.5 to 3.0 micrograms of arsenic per milliliter.

If a photoelectric colorimeter is not available, use a visual colorimeter to compare the color with that obtained from known amounts of arsenic. A Jena OG_2 filter over the eyepiece of the colorimeter facilitates matching.

[14] If the approximate amount of arsenic is unknown, 10 ml of hydrazine sulfate-molybdenum solution is added, the solution is heated, cooled, and the transmittancy measured as directed. If the arsenic content exceeds 3 micrograms per milliliter, 15 ml more of the reagent is added, and the solution is again heated, cooled, and the transmittancy measured. This operation is repeated until the arsenic content does not exceed 3 micrograms per milliliter.

[15] With the reagents used, the blank ranged from 0 to 0.0002 percent of arsenic on the basis of a 100-mg sample.

High-chromium steel.—Dissolve a 0.1-g sample in 10 ml of a mixture of equal parts of nitric and hydrochloric acids. Evaporate to dryness and proceed as with carbon steel.

Cast iron.—Proceed as with carbon steel.

Ferromanganese.—Proceed as with carbon steel.

Brass, bronze, bearing metals.—Dissolve a 0.1-g sample in 5 ml of nitric acid (sp gr 1.42). Cool, add 8 ml of diluted sulfuric acid (1+1), and evaporate the solution to fumes of sulfuric acid. Cool, and add 5 ml of water. Transfer to the distilling apparatus, and complete the determination as in carbon steel.

Pig lead.—Transfer a 5-g sample to a 400-ml beaker, add 100 ml of diluted nitric acid (1+3), and heat on a steambath. When solution is complete, cool, add 15 ml of sulfuric acid (sp gr 1.84), and evaporate to fumes of sulfuric acid. Cool, add 20 ml of water, and transfer to the distilling apparatus with 50 ml of hydrochloric acid (sp gr 1.18). Add 10 ml of hydrobromic acid. Then add 1 g of hydrazine sulfate to the distilling apparatus with an additional 50-ml portion of hydrochloric acid (sp gr 1.18). Distill as with carbon steel, catching the distillate in 10 ml of water contained in a 250-ml beaker. Distill until approximately 90 ml of distillate has passed over. Add 30 ml of nitric acid (sp gr 1.42) to the distillate, evaporate to dryness on the steambath, and complete the determination as in carbon steel.

V. RESULTS

Table 1 shows the results obtained on some National Bureau of Standards Standard Samples of ferrous and nonferrous alloys and on two samples of pig lead prepared by the American Society for Testing Materials for cooperative analysis.

TABLE 1.—*Results obtained for arsenic in some ferrous and nonferrous alloys*

Arsenic		Material	Arsenic		Material
Present [a]	Found		Present [a]	Found	
Percent	*Percent*		*Percent*	*Percent*	
0.009	0.008 .009 .009	A. O. H. steel, NBS Standard Sample 34a.	0.031	.023 .026 [b] .025	Tin-base bearing metal, NBS Standard Sample 54a.
.011	.008 .009	Stainless steel (13 percent, chromium), NBS Standard Sample 73.	.069	.059 .061	Lead-base bearing metal, NBS Standard Sample 53a.
.012	.011 .011 .012	Ingot iron, NBS Standard Sample 55.	.19	.17 .18 [c] .23	Phosphor-bronze bearing metal, NBS Standard Sample 63.
.071	.068 .070 .071	Cast iron, NBS Standard Sample 7c.	----------	[d] 0.0010 .0015	Sheet brass, NBS Standard Sample 37b.
.26	.24 .25	Cast iron, NBS Standard Sample 6d.	----------	[d] .0018 .0018 .0019	Pig lead.
.024	.024 .025	Ferromanganese, NBS Standard Sample 68.	----------	[d] .00040 .00046	Pig lead.

[a] Values reported by determinations with conventional methods.
[b] By comparing color with Duboscq-type colorimeter.
[c] Analysis made on a 6-mg sample—value obtained indicative of nonhomogeneity of small samples.
[d] Values given to show the sensitivity and reproducibility of method.

WASHINGTON, November 1, 1939.

U. S. DEPARTMENT OF COMMERCE NATIONAL BUREAU OF STANDARDS

RESEARCH PAPER RP1268

Part of Journal of Research of the National Bureau of Standards, Volume 24, January 1940

DETERMINATION OF URONIC ACIDS IN CELLULOSIC MATERIALS

By Roy L. Whistler, Albert R. Martin, and Milton Harris [1]

ABSTRACT

Methods for the determination of uronic acids, based on the estimation of the amount of carbon dioxide evolved by these acids in a given length of time during treatment with a boiling solution of hydrochloric acid, were found to fail when cellulose or other carbohydrate material was present, since these substances also decomposed with the evolution of some carbon dioxide. An investigation of the rates of evolution showed that pure uronic acids evolved carbon dioxide at a rapid rate and that the evolution was complete in several hours. Carbohydrates, free of uronic acids, evolved carbon dioxide at a much slower rate, which remained approximately constant during the entire treatment with acid. It is shown that this difference in rates can be used as the basis for estimating uronic acids, even when they are mixed with large proportions of cellulosic materials. A detailed description of the apparatus and its manipulation is given.

CONTENTS

		Page
I.	Introduction	13
II.	Description of apparatus and method	14
III.	Experimental results and discussion	17
IV.	References	23

I. INTRODUCTION

As part of a Bureau program of research relating to the structure of cotton fibers, it was necessary to measure the uronic acid content of cotton, both before and after the application of a variety of treatments. Such analyses necessitated the measurement of small quantities of uronic acids when mixed with large proportions of other carbohydrate material.

Uronic acids in contact with boiling solutions of hydrochloric acid undergo complete decarboxylation.

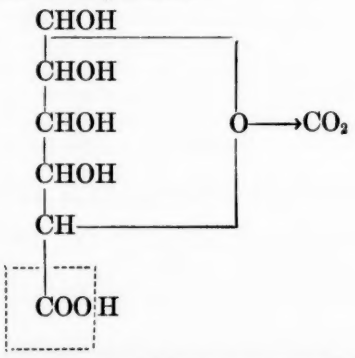

[1] Research Associates at the National Bureau of Standards, representing the Textile Foundation.

Proceeding from this observation, Lefevre and Tollens [1] [2] developed a method for the quantitative determination of uronic acids. The decarboxylation of the uronic acid was accomplished by boiling it in a solution of hydrochloric acid of specific gravity 1.06. A stream of carbon dioxide-free air drawn through the apparatus carried the evolved carbon dioxide from the reaction flask through a reflux condenser into a Peligot tube containing water to remove traces of hydrochloric acid, then through a drying tube, and finally into a weighed potash bulb. This procedure has since undergone numerous modifications [2 to 11]. The subsequent methods differ for the most part in the manner in which the carbon dioxide is collected and determined, and in the length of time necessary to bring the reaction to completion. The length of time recommended as necessary for complete decarboxylation has ranged from 3½ to 10 hours.

Although these methods gave good results when applied to pure uronic acids, considerable difficulty was encountered when they were used on such materials as cotton fibers or other carbohydrate mixtures. Under the drastic conditions employed in the analysis, it was found that uronic acid-free carbohydrates decomposed with the evolution of carbon dioxide. For example, when pure glucose was treated with a boiling 12-percent solution of hydrochloric acid, carbon dioxide was continuously evolved; the evolution was appreciable even after 30 hours. A study of the rates of evolution of carbon dioxide revealed that in the case of pure uronic acids there occurred an initial rapid evolution of carbon dioxide which ceased after several hours. On the other hand, carbohydrates which did not contain uronic acid groups evolved carbon dioxide at a much slower but approximately constant rate during the entire treatment with acid. A mixture of uronic acids with other carbohydrate material gave an initial rapid evolution of carbon dioxide followed by a slower but steady evolution of the gas.

During the time that the present work was in progress, there appeared three papers [12, 13, 14] from other laboratories, reporting findings relative to the evolution of carbon dioxide from a number of pure sugars and polysaccharides. Norman [13] pointed out that the presence of uronic acid groups could be inferred from the rate of evolution of carbon dioxide (a fact which we had noted independently) and stated that no quantitative significance could be attached to the small yields of carbon dioxide from polysaccharides.

In the present investigation, a critical study was made of the factors which influence the rates of evolution of carbon dioxide from uronic acids, glucose, and cellulose fibers during treatment with hydrochloric acid. As a result of these studies, it has been possible to develop a new method for the precise estimation of small quantities of uronic acids in the presence of cellulosic materials.

II. DESCRIPTION OF APPARATUS AND METHOD

The apparatus which was developed in this investigation is shown in figure 1. Two assemblies of the type shown were employed simultaneously; the same source of carrier gas and the same oil bath were used for both.

[2] Figures in brackets indicate the literature references at the end of this paper.

Nitrogen, which is used as the carrier gas for the evolved carbon dioxide, enters the apparatus through an empty safety bottle, *A*. It next passes through an alkaline solution of pyrogallol, *B*. The inlet tube in this bottle is drawn out to a small orifice which produces very fine bubbles. From *B* the gas passes through two absorption towers, *C*, filled with soda lime, into a second safety bottle, *D*, which is provided with a mercury manometer, *E*, and then enters the reaction flask, *F*, by way of a side arm whose outlet is 10 to 15 mm above the surface of the liquid in the flask. The size of the flask depends upon the type of material and the size of the sample to be analyzed. In most of the experiments a 500-ml reaction flask was used. From the reaction flask the gas passes through a 40-cm reflux condenser, *G*, and into a bubbling tower, *H*, containing approximately 60 ml of concentrated sulfuric acid. The sulfuric acid serves to remove interfering decomposition products which are carried over from the reaction flask.[3] The gas next passes through

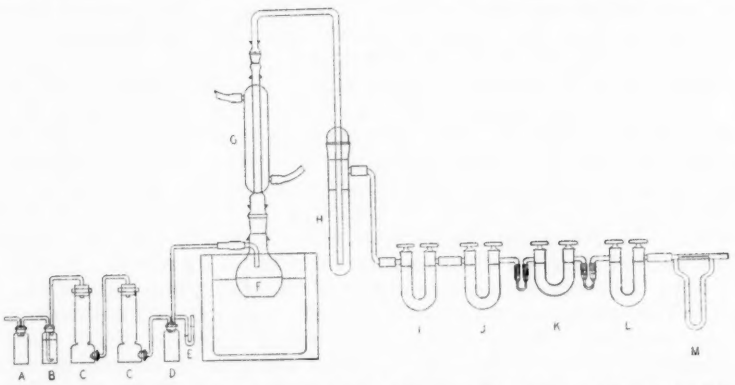

FIGURE 1.—*Apparatus for determination of the rate of evolution of carbon dioxide from uronic acids or materials containing uronic acids during treatment with hydrochloric acid.*

(The apparatus is not drawn to scale. See text for dimensions.)

the U-tube, *I*, which is filled with anhydrous copper sulfate,[4] then through the tube, *J*, which contains phosphorus pentoxide, and finally through the carbon dioxide-absorption tube, *K*, containing ascarite, backed by phosphorus pentoxide. The absorption tubes, *K*, are connected into the train by means of mercury-cup seals [15]. This type of connection makes possible a rapid exchange of the absorption tubes. Tube *K* is protected by a soda-lime tube, *L*, which is followed by a calibrated flowmeter, *M*, for estimating the rate of flow of nitrogen through the apparatus.

The reaction flask is immersed in a vessel containing about 16 liters of hydrogenated cottonseed oil. A bath temperature of 130° C was found to be optimum for maintaining a steady but gentle boiling of the reaction mixture. The bath is brought to the operating temperature by means of two electric immersion heaters, one of 500 and one of 1,000 watts. When the desired temperature is reached,

[3] An aniline-hydrochloric acid mixture may also be used to remove volatile products, but in our work it was found to be less efficient than H_2SO_4.

[4] A precaution necessary in systems where chlorine or hydrogen sulfide might be formed.

the 500-watt heater alone is sufficient to maintain thermal constancy within ±0.2° C. The time required to raise the temperature of the bath to 130° C is approximately 50 minutes.

The sample to be analyzed is placed in the reaction flask, *F*. The optimum size of the sample depends upon its uronic acid content. When working with a material such as cotton, which contains a relatively small proportion of uronic acids, it is advisable to use samples of approximately 10 g, although good results may be obtained with smaller samples. A sample of this size is readily covered by 300 ml of the hydrochloric acid solution. Varying the ratio of acid solution to sample within reasonable limits does not affect the results. Thorough wetting of the sample by the acid solution is accomplished by evacuating the air in the flask with a filter pump.

The flask is placed in position in the oil bath so that the oil level is 3 to 4 mm lower than the liquid level inside of the flask. This precaution is taken to prevent the baking of small bits of sample which may be splashed against the sides of the flask. Nitrogen, at the rate of about 10 liters per hour, is passed through the apparatus until the ascarite tube, *K*, shows no further gain in weight. This operation requires about 30 minutes, during which time the temperature of the oil bath is slowly raised to 50° C. When the apparatus is free of carbon dioxide, both heating units are turned on and the temperature brought to 130° C. This procedure is always carefully followed in order to assure the same preliminary heating for all samples. The point of zero time is taken as the time at which the bath reaches 130° C. At that time the ascarite tube, *K*, is removed for weighing and a second weighed ascarite tube inserted in its place. At the end of 1 hour the second tube is removed for weighing and replaced by the first. This process is repeated at intervals of 1 hour for the duration of the analysis. When analyses are made on pure uronic acids or materials rich in uronic acids, a small amount of carbon dioxide is evolved by the time the temperature of the bath reaches 130° C. In these cases, this amount is measured and added to that evolved during the first hour.

Previous investigators have suggested that the tube entering the reaction flask, *F*, extend into the reaction mixture in order to prevent bumping. However, it was found that there is no tendency to bump when a 12-percent solution of acid and an oil-bath temperature of 130° C are used. On the other hand, it is found advantageous to have this tube terminate above the surface of the liquid. With this arrangement there is no tendency toward different amounts of agitation resulting from slight variations in the rate of flow of the carrier gas. Furthermore, there is less tendency for the gas stream to carry interfering products from the reaction mixture into the sulfuric acid tower, *H*. That no secondary reaction occurs from the action of sulfuric acid on the volatile substances, which interferes with the determination, was demonstrated by substituting a U-tube cooled in a mixture of solid carbon dioxide and trichloroethylene for the sulfuric acid tower, *H*. Identical results were obtained under both conditions.

The length of time required to sweep the carbon dioxide from the reaction flask into the absorption tubes was determined by the use of a known quantity of pure sodium carbonate. The sample was weighed in a glass tube, and the ends were sealed with paraffin. The tube was placed in an acid solution in the reaction flask and the train

swept out with nitrogen. The temperature of the bath was then raised until the paraffin plugs loosened and allowed the acid to come in contact with the sample of carbonate. Since the reaction is extremely rapid, it was easy to determine the moment at which the carbon dioxide was released into the system. This procedure was repeated several times, a different rate of nitrogen flow being used in each case. It was found that with a gas flow of 10 liters per hour, all the carbon dioxide was absorbed by the ascarite in less than 30 minutes.

III. EXPERIMENTAL RESULTS AND DISCUSSION

The rate of evolution of carbon dioxide from pure galacturonic acid monohydrate in 11-, 12-, and 13-percent solutions [5] of hydrochloric

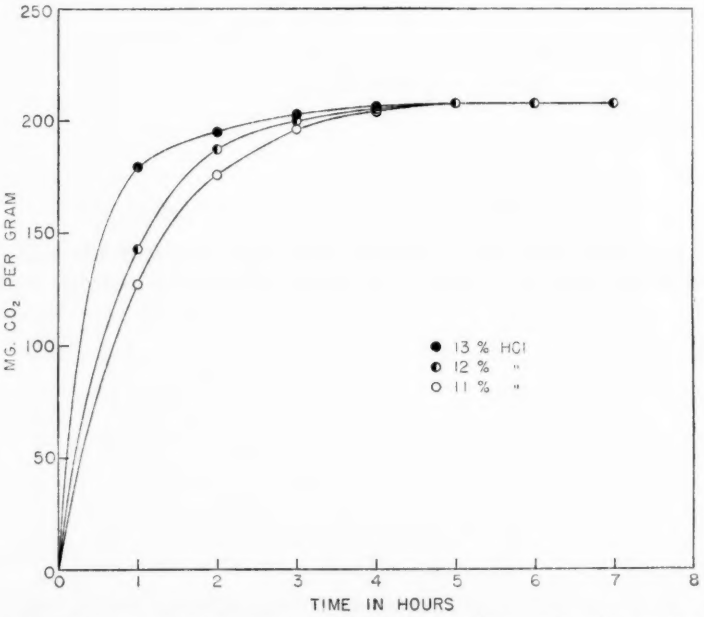

FIGURE 2.—*Rate of evolution of carbon dioxide from galacturonic acid monohydrate.*

acid is shown in figure 2. The curves show that an initial, rapid evolution of carbon dioxide occurs and that the evolution ceases after about 4 hours. A total of 208 mg of carbon dioxide per gram of galacturonic acid monohydrate was obtained (the theoretical yield is 207.5 mg). Increasing the concentration of acid increases the rate of evolution but does not affect the total amount of gas evolved.

Similar treatment of pure glucose in solutions of hydrochloric acid gives very different results, as shown in figure 3. The amounts of carbon dioxide evolved are small [6] compared with the amounts obtained from galacturonic acid under similar conditions. The rate of evolution increases with increasing acid concentration; but unlike the case of the galacturonic acid, the evolution of gas continues, except in the

[5] These solutions contained 110, 120, and 130 g of hydrogen chloride per liter of solution.
[6] Because of the small amount of CO_2 evolved, 10-g samples of glucose were used for each analysis.

most concentrated acid solutions, at an approximately constant rate for the duration of the analysis.

The amount of carbon dioxide obtained from pure glucose is very

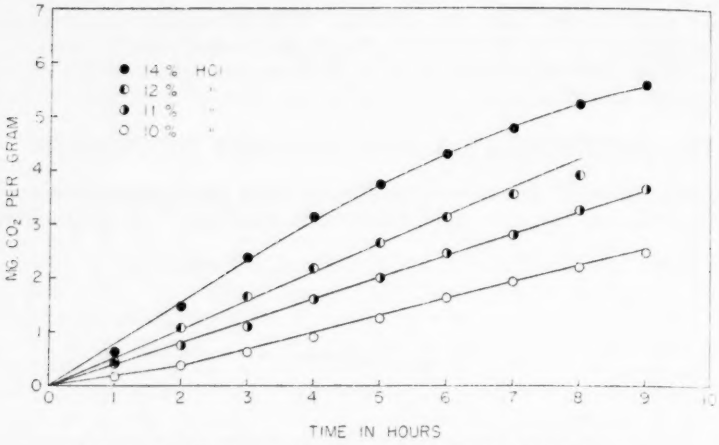

FIGURE 3.—*Rate of evolution of carbon dioxide from glucose.*

small compared with that obtained from pure galacturonic acid; but it is obvious that in naturally occurring cellulosic materials, such as

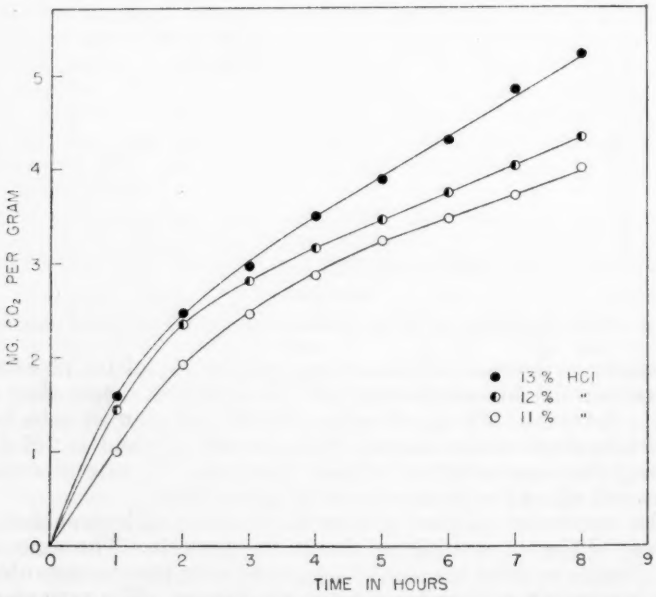

FIGURE 4.—*Rate of evolution of carbon dioxide from dewaxed cotton.*

cotton, which contain only small amounts of uronic acids, the amount of carbon dioxide evolved by that portion of the material which does not contain uronic acid groups may be an appreciable part of the total.

This is shown by the curves for dewaxed cotton [7] in figure 4. An examination of these curves indicates that they are probably composites of curves of the types found in figures 2 and 3. The rapid evolution of carbon dioxide during the first 3 hours, as indicated by the steep slopes of the curves, is characteristic of uronic acids. After the 3-hour period the evolution of gas does not cease but continues at a slower but constant rate characteristic of carbohydrates which do not contain uronic acid groups. As in the previous experiments, the rate of evolution of gas increases with increasing acid concentrations.

On the basis of the results shown in figures 2, 3, and 4, a 12-percent solution (3.290 *N*) of hydrochloric acid was chosen as a satisfactory concentration for the decarboxylation of uronic acids in the presence

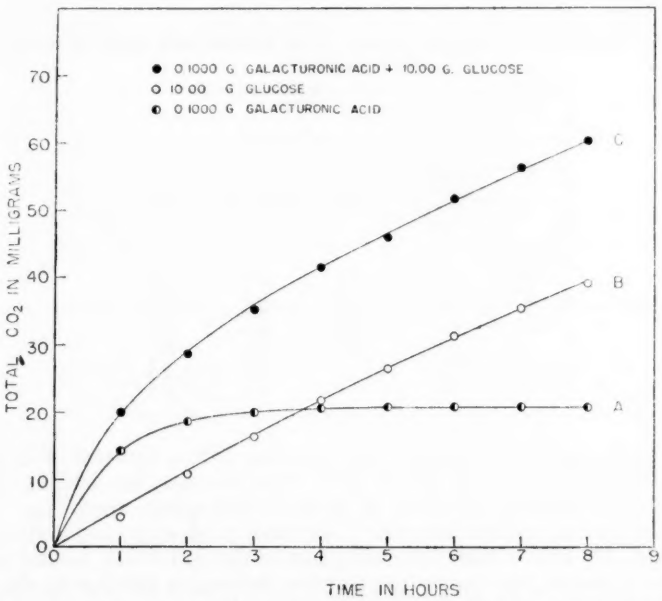

FIGURE 5.—*Rate of evolution of carbon dioxide from glucose, galacturonic acid, and a mixture of both.*

of other carbohydrate material.[8] In lower concentrations of acid the decarboxylation of the uronic acids proceeds too slowly for convenience, whereas in acids of higher concentration the decomposition of the carbohydrate itself is too rapid and erratic. *Since the rate of evolution of carbon dioxide is appreciably affected by variations in acid strength, it is essential that the same concentration (within 0.02 percent) of acid be used in all comparative studies.*

That the results obtained with dewaxed cotton probably represent the behavior of a mixture of uronic acids and other carbohydrate materials was further indicated by studying the evolution of carbon dioxide from glucose, galacturonic acid, and a known mixture of the two. The results are shown in figure 5. Curve *C*, which represents

[7] Dewaxed cotton refers to cotton which has undergone 24-hour extractions each with alcohol and with diethyl ether.

[8] This concentration was used in all subsequent experiments.

the total amount of carbon dioxide evolved from a mixture of 10.00 g of glucose and 0.100 g of galacturonic acid monohydrate, is similar in shape to the curves in figure 4. The total amount of carbon dioxide evolved by the mixture at any time, as shown by curve *C*, is equal to the sum of the amounts evolved by each of the components in the same time, as shown by curves *A* and *B*. The good agreement of the data is seen in table 1.

Conversely, it follows that the amount of carbon dioxide evolved from uronic acid groups in this or similar mixtures can be readily estimated from the differences between the ordinates of the parallel portions of the curves *B* and *C*. The average of these differences, taken from the data in table 1, is 20.5 mg of carbon dioxide (theory, 20.75 mg).

TABLE 1.—*Evolution of carbon dioxide from galacturonic acid, glucose, and a mixture of both*

Time	1	2	3	4
	0.100 g of galacturonic acid (monohydrate)	10.00 g of glucose	1+2 calculated	1+2 found
Hours	*mg*	*mg*	*mg*	*mg*
1	14.3	4.5	18.8	20.0
2	18.7	10.8	29.5	28.7
3	20.0	16.4	36.4	35.2
4	20.6	21.8	42.4	41.5
5	20.8	26.4	47.2	46.0
6	20.8	31.3	52.1	51.7
7	20.8	35.4	56.2	56.3
8	20.8	39.1	59.9	60.3

The curves shown in figure 6 were obtained from samples of dewaxed cotton and from cotton which had been purified by boiling for 7½ hours in a 1-percent solution of sodium hydroxide according to the methods recommended for the preparation of standard cotton cellulose [16, 17, 18]. With the exception of the induction period during the first 2 hours, the curve for purified cotton is similar in shape to that for glucose. It shows no initial, rapid rise, characteristic of the uronic acids, and indicates that cotton purified in this manner is free from a measurable amount of uronic acids. The amount of carbon dioxide evolved from the uronic groups in the dewaxed cotton is obtained by taking the average distance between the parallel portions of the curves, which gives a value of 2.4 mg of carbon dioxide per gram of cotton.

It has generally been assumed that the uronic acids in native cotton are contained in the pectic [9] substance of the fiber. Further evidence for this assumption is shown in figure 7. The carbon dioxide-rate curve of the pectin [10] is very similar in shape to that obtained for galacturonic acid (fig. 2), and reaches a maximum at 208 mg of car-

[9] Pectic substance has been defined by the ACS committee on nomenclature of pectin [19] as a complex carbohydrate derivative which is characterized by the presence of galacturonic acid units.

[10] The pectin used in these experiments was obtained from the cotton by the well-known method of extraction with ammonium oxalate. A description of the preparation and properties of this pectin is being prepared for publication.

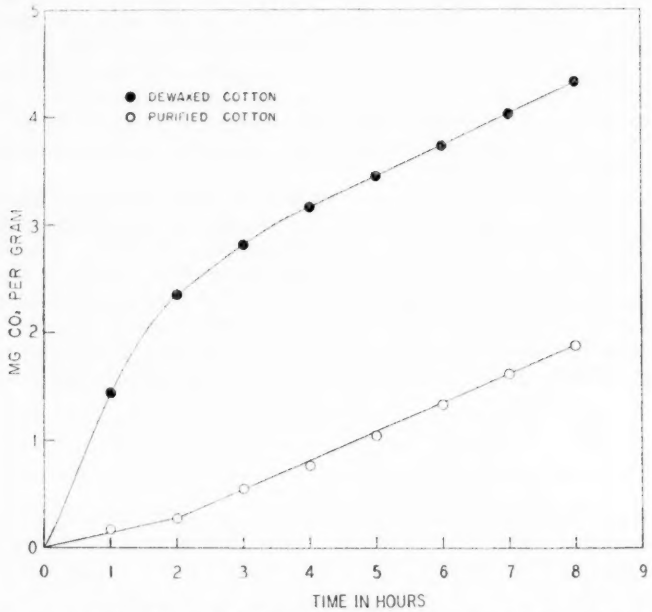

FIGURE 6.—*Rate of evolution of carbon dioxide from samples of dewaxed and purified cotton.*

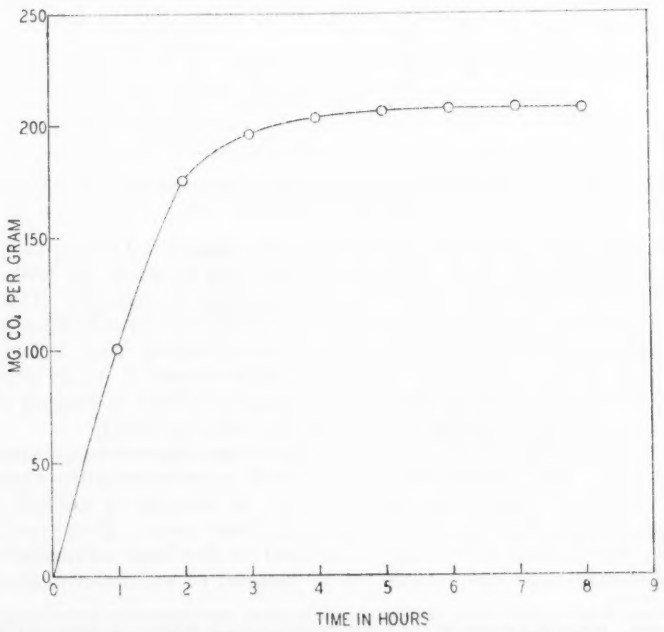

FIGURE 7.—*Rate of evolution of carbon dioxide from a sample of pectin from cotton.*

bon dioxide per gram of pectin. From this value a factor of 4.8 [11] for converting carbon dioxide, formed from uronic acids, to the pectin extracted from cotton is obtained. The pectin content of the cotton used in the present work may then be roughly estimated by multiplying 2.4 mg (from the curves in fig. 6) by 4.8, which gives a value of 11.5 mg of pectin per gram, or 1.15 percent. As is to be expected, this value is higher than previously reported values obtained by isolation methods [20, 21].

The uronic acid contents of a number of other cellulosic fibers were also determined. Table 2 shows the results obtained from decorticated ramie, retted flax, and purified samples of both. Purification was accomplished by treatment of the fibers with a boiling 1-percent solution of sodium hydroxide for 4 hours by the methods described for cellulose. The data for the decorticated ramie and retted flax are similar to those obtained for dewaxed cotton, inasmuch as they show an initial, rapid evolution of carbon dioxide, which becomes

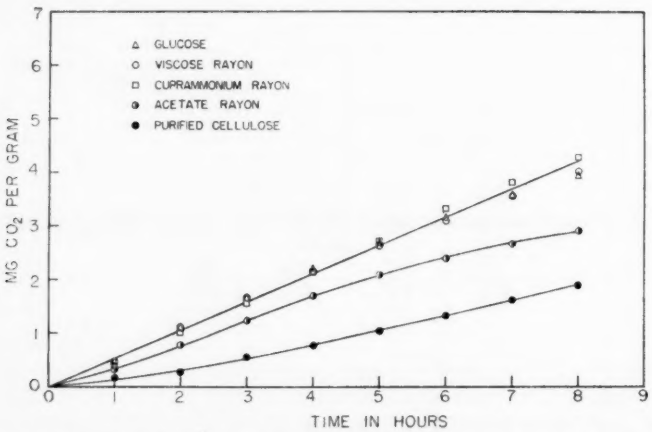

FIGURE 8.—*Rate of evolution of carbon dioxide from samples of rayon, glucose, and purified cotton*

slower but approximately constant after 4 hours. During the first 4 hours considerably more carbon dioxide was evolved by both ramie and flax than was evolved in the same period by cotton. The value for the amount of carbon dioxide evolved by the uronic acid groups, obtained by subtracting the value for the purified from that for the unpurified fiber, reaches a maximum after about 4 hours and then remains constant. An average of 10.4 and 10.2 mg of carbon dioxide per gram of ramie and flax, respectively, was obtained.

The results obtained from three different samples of rayon are shown in figure 8. The curves for viscose and cuprammonium rayon are nearly identical with that for glucose. A sample of acetate rayon evolved carbon dioxide at a somewhat lower rate. However, if the data for the acetate rayon are calculated on the basis of milligrams of carbon dioxide per gram of cellulose instead of cellulose acetate, the

[11] This factor is valid only if it is assumed that the pectin has not been appreciably altered during removal from the fiber. Justification for the use of such a factor will depend on obtaining similar results on samples of pectin removed from cotton by several different methods. Work along this line is in progress.

results are very similar to those for the viscose or cuprammonium rayon. The curves for these samples indicate that they are free of uronic acids.

TABLE 2.—*Amount of carbon dioxide evolved from the uronic acid groups of ramie and flax fibers*

Duration of treatment	Ramie			Flax		
	Decorticated	Purified	Uronic acid-carbon dioxide	Retted	Purified	Uronic acid-carbon dioxide
Hours	*mg/g*	*mg/g*	*mg/g*	*mg/g*	*mg/g*	*mg/g*
1	5.4	0.3	5.1	5.4	0.3	5.1
2	8.5	.5	8.0	8.7	.7	8.0
3	10.1	.6	9.5	10.2	1.0	9.1
4	10.9	.7	10.2	11.2	1.4	9.8
5	11.4	1.0	10.3	11.7	1.6	10.1
6	11.9	1.4	10.5	12.2	1.9	10.3
7	12.0	1.7	10.3	12.5	2.3	10.2
8	12.4	2.0	10.4	12.8	2.6	10.2
9	12.7	2.3	10.4	13.1	3.0	10.1

A carbon dioxide-rate curve for purified cotton cellulose is included for comparison. It is of interest to note that the slope of this curve is quite different from that of glucose or the regenerated fibers.

IV. REFERENCES

[1] K. V. Lefevre and B. Tollens, Ber. deut. chem. Ges. **40,** 4513 (1907).
[2] A. W. van der Haar, Anleitung zum Nachweis, zur Trennung und Bestimmung der Monosaccharide und Aldehydesauren, p. 71 (Gebrüder Borntraeger, Berlin, 1920).
[3] D. R. Nanji, F. T. Paton, and A. R. Ling, J. Soc. Chem. Ind. **44,** 253T (1925).
[4] W. H. Dore, J. Am. Chem. Soc. **48,** 232 (1926).
[5] R. B. McKinnis, J. Am. Chem. Soc. **50,** 1911 (1928)
[6] F. Ehrlich and F. Schubert, Ber. deut. chem. Ges. **62,** 1974 (1929).
[7] A. D. Dickson, H. Otterson, and K. P. Link, J. Am. Chem. Soc. **52,** 775 (1930).
[8] C. M. Conrad, J. Am. Chem. Soc. **53,** 1999 (1931).
[9] G. Klein, Handbuch der Pflanzenanalyse **3,** 121 (Julius Springer, Vienna, 1932).
[10] H. W. Buston, Analyst, **57,** 207 (1932).
[11] B. Burkhart, L. Baur, and K. P. Link, J. Biol. Chem. **104,** 171 (1934).
[12] W. G. Campbell, E. L. Hirst, and G. T. Young, Nature **142,** 912 (1938).
[13] A. G. Norman, Nature **143,** 284 (1939).
[14] H. Colin and S. Lemayne, Bu.l. soc. chim. biol. **20,** 343 (1939).
[15] W. F. Hillebrand and G. E. F. Lundell, Applied Inorganic Analysis, p. 623 (John Wiley & Sons, New York, N. Y., 1929).
[16] Report of the Committee of the Division of Cellulose Chemistry of the American Chemical Society, Ind. Eng. Chem. **15,** 748 (1923).
[17] A. B. Corey and H. L. Grey, Ind. Eng. Chem. **16,** 853, 1130 (1924).
[18] R. K. Worner and R. T. Mease, J. Research NBS **21,** 609 (1938) RP1146.
[19] American Chemical Society Committee on Nomenclature of Pectin of the Agricultural Food Division. Definitions. J. Am. Chem. Soc. (Proc.) **49,** 37 (1927).
[20] S. A. Harris and H. J. Thompson, Contributions from Boyce Thompson Institute **9,** 1 (1937).
[21] J. T. Marsh and F. C. Wood, An Introduction to the Chemistry of Cellulose, p. 12 (Chapman and Hall, London, 1938).

WASHINGTON, October 25, 1939.

U. S. Department of Commerce National Bureau of Standards

RESEARCH PAPER RP1269

Part of Journal of Research of the National Bureau of Standards, Volume 24, January 1940

THERMAL EXPANSION OF SOME CHROMIUM-VANADIUM STEELS

By Peter Hidnert

ABSTRACT

Data on the linear thermal expansion of several SAE chromium-vanadium steels have been published previously. The present paper gives the results of an investigation at this Bureau on the linear thermal expansion of two other SAE chromium-vanadium steels (SAE 1625 and 6150) in the annealed condition and in the quenched and tempered condition. These steels were investigated at various temperatures between 20° and 650°C. The coefficients of expansion of the hardened sample tempered at 400°F (204°C) or 800°F (427°C) are less than the coefficients of expansion of the annealed sample. Tempering at 1,200°F (650°C) increased the expansion to that of the annealed sample. For the range from 20° to 650°C, the average coefficients of expansion of all of the samples investigated vary from 13.8×10^{-6} to 14.8×10^{-6} per degree centigrade.

CONTENTS

		Page
I.	Introduction	25
II.	Materials investigated	25
III.	Apparatus	27
IV.	Results	27
V.	References	30

I. INTRODUCTION

Coefficients of linear thermal expansion of SAE 6115,[1] 6135, and 6140 [1] chromium-vanadium steels, have been determined by Souder and Hidnert [1, 2] [2] and republished in 1939 in the Metals Handbook of the American Society for Metals. The present paper gives the results of an investigation of the linear thermal expansion of other SAE chromium-vanadium steels which are strictly in accordance with SAE specifications.

Chromium-vanadium steels are used for a variety of purposes. Publications by Vanadium Corporation of America [3] and Priestley [4] give information about the mechanical properties and uses of these steels.

II. MATERIALS INVESTIGATED

The chemical composition and the heat treatment of five samples that were investigated are given in table 1. Two of these samples are SAE 6125 chromium-vanadium steels and the other three samples SAE 6150 chromium-vanadium steels.

[1] Chemical composition not strictly in accordance with SAE specification.
[2] The numbers in brackets indicate the references at the end of this paper.

TABLE 1.—*Coefficients of linear expansion of chromium-vanadium steels*

Sample	SAE No.	Chemical composition							Heat treatment	Test	Average coefficients of expansion per °C							Change in length after heating and cooling [a]
		C	Mn	Si	P	S	Cr	V			20° to 100°C	20° to 200°C	20° to 300°C	20° to 400°C	20° to 500°C	20° to 600°C	20° to 650°C	
		%	%	%	%	%	%	%			×10⁻⁶	×10⁻⁶	×10⁻⁶	×10⁻⁶	×10⁻⁶	×10⁻⁶	×10⁻⁶	%
1610 [b]	6125	0.22	0.75	0.27	0.019	0.033	0.96	0.17	Annealed at 1,650° F for 3 hours and furnace cooled.	1	12.2	12.7	13.3	13.7	14.1	14.4	14.6	+0.001
1611 [b]	6125	.22	.75	.27	.019	.033	.96	.17	Heated for ½ hour at 1,475° F, quenched in oil and tempered 4 hours at 400° F.	1	12.0	12.5	12.9	13.0	13.3	13.7	13.8	−.044
										2	12.1	12.6	13.2	13.7	14.1	14.4	14.6	.000
1612 [c]	6150	.53	.80	.15	.015	.020	1.02	.17	Annealed at 1,575° F for 3 hours and furnace cooled.	1	12.4	12.8	13.4	13.9	14.2	14.5	14.7	−.006
1613 [c]	6150	.53	.80	.15	.015	.020	1.02	.17	Heated for ½ hour at 1,575° F, quenched in oil, heated for 3 hours at 800° F and air cooled.	1	11.8	12.4	13.1	13.6	13.9	14.1	14.2	−.042
										2	12.5	12.9	13.5	14.0	14.3	14.7	14.8	+.000
1614 [c]	6150	.53	.90	.15	.015	.020	1.02	.17	Heated for ½ hour at 1,575° F, quenched in oil, heated for 3 hours at 1,200° F and air cooled.	1	12.3	12.7	13.4	13.9	14.3	14.7	14.8	+.002

[a] Determined from the expansion curve on heating and the contraction curve (or observation) on cooling. The plus sign indicates an increase in length, and the minus sign a decrease in length.

[b] Samples 1610 and 1611 from basic open-hearth heat (about 100 tons); forged from 1¼-inch diameter rolled bar to ⅝-inch diameter; heat treated as indicated in column marked "Heat treatment;" machined to ⅜-inch diameter by 12½ inches long.

[c] Samples 1612, 1613, and 1614 from basic electric-furnace heat (15 tons), which was rolled to 4-inch square billets. The billets were then treated as follows: (a) Chipped and ground; (b) rolled to ⅝-inch rounds; (c) open-annealed at 1,380° F (½ hour); (d) cold-drawn 0.580 inch round; (e) pack annealed at 1,350° F (6 hours), cooling with furnace to 1,200° F, and then air cooled in container—total time 34 hours; (f) heat treated as indicated in column marked "Heat treatment;"; and (g) machined to ⅜-inch diameter by 12½ inches long.

III. APPARATUS

The samples were investigated at various temperatures between 20° and 650° C with the precision comparator type of thermal-expansion apparatus described by Souder and Hidnert [5]. The white furnace shown at the left of figure 1 of their publication was used. Figure 5 of the same publication shows the details of mounting the sample in the furnace. The distance between the two sharp V notches on each sample was 300 mm.

Platinum-osmium observation wires (6½ percent osmium) were used. The diameter of each observation wire was 0.050 mm. A vane weighing 18 g was attached at the bottom of each observation wire and suspended in oil to damp out vibrations.

IV. RESULTS

The observations obtained on the linear thermal expansion of the five samples of chromium-vanadium steels at various temperatures between 20° and 650° C are shown in figures 1 and 2. Each expansion curve was plotted from a different origin. Two expansion tests were made on samples 1611 and 1613, for in the first tests the observations on cooling lie appreciably below the expansion curves obtained on heating. Results obtained in a second test represent data on material after the heat treatment incident to the first test.

In each test except the first tests on samples 1611 and 1613, the observations on cooling are very close to the expansion curve. This occurs in each case when the sample had been annealed or if the sample had been heated to 1,200° F (about 650° C) after quenching.

The average coefficients of expansion in table 1, were obtained from the expansion curves of figures 1 and 2. This table also shows the difference in length before and after each expansion test.

A comparison of the coefficients of expansion of samples 1610 and 1611 shows that the expansion of the hardened sample which had been tempered at 400° F (204° C) is less than the expansion of the annealed sample. The tempering produced by the first test to 1,200° F. (650° C) increased the expansion (in the second test) to that of the annealed sample. This effect is also indicated by the contraction curve of the first test and the expansion and contraction curves of the second test.

Similarly, for samples 1612 and 1613, it is evident that the expansion of the hardened sample which had been tempered at 800° F (427° C) is less than the annealed sample. The tempering produced by heating to 1,200° F (650° C) in the first test, also increased the expansion (in the second test) to that of the annealed sample. This effect is also indicated by the contraction curve of the first test and the expansion and contraction curves of the second test.

The tempering at 1,200° F (650° C) for sample 1614 is comparable to the heat treatment incident to the first tests on samples 1611 and 1613 and produced the same expansion as that of the corresponding annealed sample.

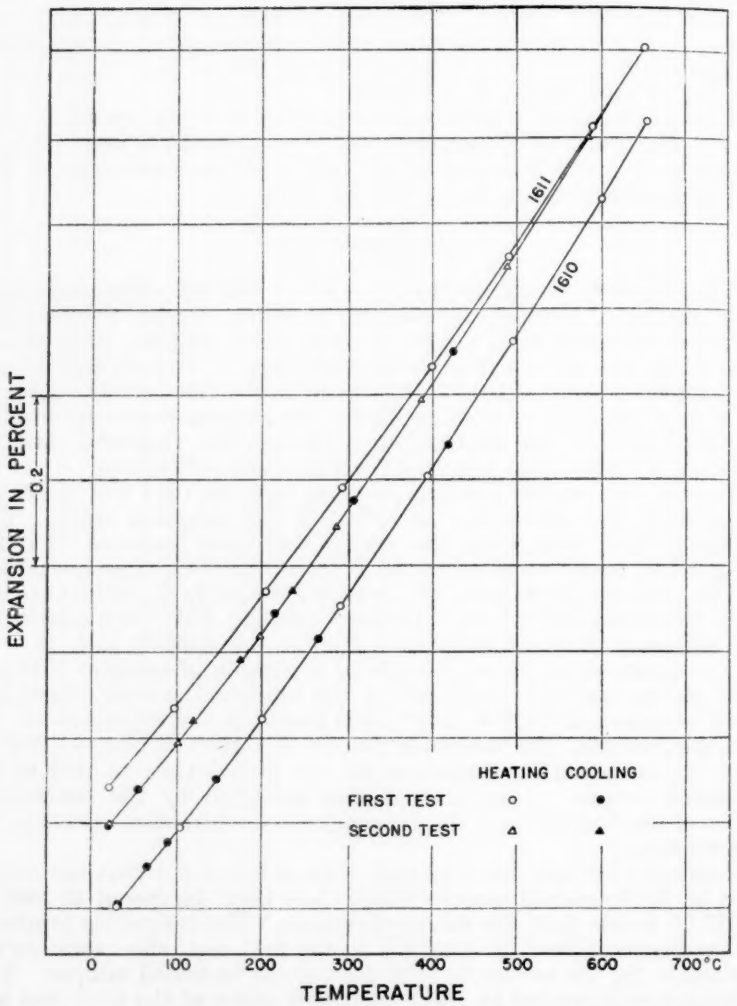

FIGURE 1.—*Linear thermal expansion of two samples of SAE 6125 chromium-vanadium steel.*

C, 0.22; Mn, 0.75; Si, 0.27; P, 0.019; S, 0.033; Cr, 0.96; V, 0.17 percent.
Sample 1610—Annealed at 1,650° F for 3 hours and furnace cooled; sample 1611—heated for ½ hour at 1,475° F, quenched in oil and tempered 4 hours at 400° F.

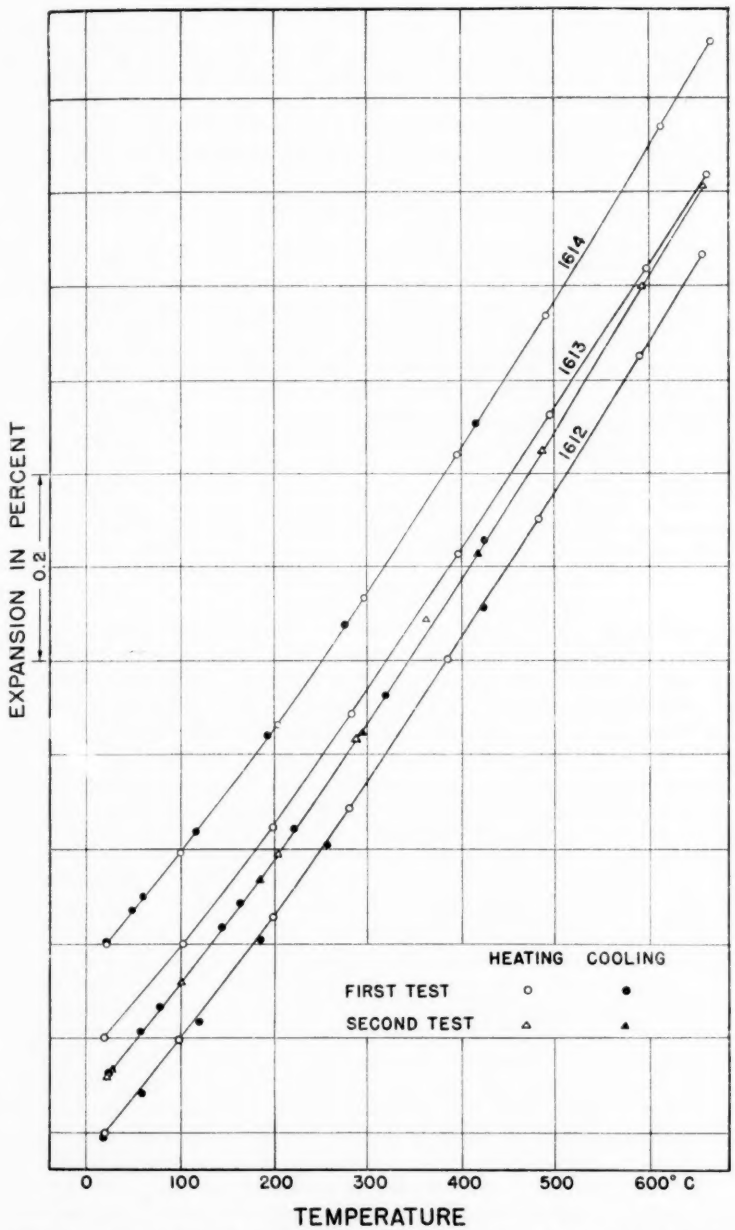

FIGURE 2.—*Linear thermal expansion of three samples of SAE 6150 chromium vanadium steel.*

C, 0.53; Mn, 0.80; Si, 0.15; P, 0.015; S, 0.020; Cr, 1.02; V, 0.17 percent.

Sample 1612—Annealed at 1,575° F for 3 hours and furnace cooled; sample 1613—heated for ½ hour at 1,575° F, quenched in oil, heated for 3 hours at 800° F and air cooled; sample 1614—heated for ½ hour at 1,575° F, quenched in oil, heated for 3 hours at 1,200° F and air cooled.

The author expresses his appreciation for the cooperation of the Vanadium Corporation of America, Bridgeville, Pa. This corporation furnished the samples of chromium-vanadium steels and information about the chemical composition and treatment. The author thanks Paul R. Stone, formerly of the National Bureau of Standards, for assistance in the computations and the preparation of the figures.

V. REFERENCES

[1] W. Souder and P. Hidnert, *Thermal expansion of a few steels*, Sci. Pap. BS **17**, 611 (1922) S433.
[2] Determinations made by P. Hidnert [J. A. Mathews, *The coefficient of expansion of alloy steels*, Trans. Am. Inst. Mech. Engrs. **67**, 133 (1922)].
[3] Vanadium Corporation of America, Vanadium Steels and Irons (booklet).
[4] W. J. Priestley, *Vanadium in steel and iron*, Metals and Alloys **9**, 193 (1938).
[5] W. Souder and P. Hidnert, *Measurements on the thermal expansion of fused silica*, Sci. Pap. BS **21**, 1 (1926) S524.

WASHINGTON, November 6, 1939.

U. S. DEPARTMENT OF COMMERCE NATIONAL BUREAU OF STANDARDS

RESEARCH PAPER RP1270

Part of Journal of Research of the National Bureau of Standards, Volume 24, January 1940

SENSITIVE ANEROID DIAPHRAGM CAPSULE WITH NO DEFLECTION ABOVE A SELECTED PRESSURE

By W. G. Brombacher, V. H. Goerke, and F. Cordero

ABSTRACT

A sensitive diaphragm capsule has been designed in which the two corrugated diaphragms nest into each other at external air pressures above a desired value. Evacuated capsules of this type have particular application in measuring pressure with radio sondes of the Diamond-Hinman-Dunmore type, where the deflection of the contact arm is fixed. At the ground level the diaphragms are designed to nest into each other and deflection does not begin until the air pressure is reduced to the value called the cut-off pressure. Several elements of two capsules each were constructed with a cut-off pressure of 140 millibars. When installed in a radio sonde in place of the usual type, which is responsive over the entire range of pressures, a sevenfold increase in sensitivity in pressure measurement was obtained at altitudes above 46,000 feet.

In measuring air pressure with radio sondes of the Diamond-Hinman-Dunmore type,[1] where the motion of the pressure contactor is a fixed distance, it is desirable, in some cases, to increase the sensitivity at high altitudes. To secure this increase in sensitivity, a disphragm capsule has been designed at the National Bureau of Standards, the two diaphragms of which, when evacuated and sealed off in accordance with the usual practice for capsules used to measure atmospheric pressure, nest into each other at air pressures greater than a selected value. At pressures less than this cut-off value, the capsule deflects normally. The nesting of the diaphragms prevents damage to the relatively sensitive diaphragms, which might be caused by excessive differential pressures. The new diaphragm element is designed so that the contact arm of the radio sonde deflects over the same distance for the pressure interval from the cut-off to zero pressures, as does the ordinary element from sea level to zero pressures.

The capsule, at zero pressure, is shown diagrammatically in figure 1. The connections needed for evacuating the capsule and for attachment to the radio sonde are not shown in figure 1. It is apparent from the form of the capsule that, as the air is evacuated from its interior, it will gradually collapse and finally, at a definite differential pressure, the two diaphragms will nest into each other and remain nested for larger external pressures. The evacuated capsule starts deflecting when the air pressure is reduced to a pressure equal to the differential pressure at which nesting took place during evacuation. This is known as the cut-off pressure.

A pressure element of this type, consisting of two diaphragm capsules installed in a Diamond-Hinman-Dunmore radio sonde made by

[1] Harry Diamond, Wilbur S. Hinman, Jr., and Francis W. Dunmore, *A method for the investigation of upper-air phenomena and its application to radio meteorography*, J. Research NBS **20**, 369 (1938) RP1082.

198881—40——3

Friez, is shown in figure 2. Two such elements were constructed. The diaphragms are 0.003 inch thick and 2.5 inches in diameter. They were formed hydraulically from soft beryllium copper, which was later hardened by heat treatment. Separate dies were used to form the upper and lower diaphragms. The complete pressure elements have a deflection of about 0.22 inch at the center for the pressure range from 140 to 0 millibars (105 to 0 mm of mercury). At greater air pressures, the diaphragms of each capsule nest into each other. As installed in the radio sonde, the first contact is made at about 140 millibars (105 mm of mercury), equivalent to an altitude of about 46,000 feet. Since the pressure element ordinarily installed in the radio sonde deflects over the range of contacts in the pressure range from 0 to 1,040 millibars, the gain in sensitivity on a pressure basis is about 7½ to 1. The effect of temperature change (0° to +30° C) on the deflections was found to be somewhat less than that to be expected on the basis of the temperature coefficient of the modulus of elasticity of beryllium copper.

In cooperation with H. Diamond and W. S. Hinman, one of the radio sondes was sent up attached to six sounding balloons, which reached an altitude of 85,500 feet. Seventy of the eighty contacts of the range operated during the flight. A temperature record was also secured. The minimum pressure obtained was 24 millibars (18

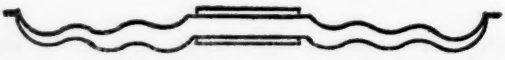

FIGURE 1.—*Capsule in which the diaphragms nest into each other as the internal pressure is decreased or the external pressure increased.*

mm of mercury). The action was satisfactory in all respects, including smooth motion of the contactor over the contacts.

Other designs may be indicated, using the formulas developed by W. A. Wildhack and V. H. Goerke.[2] Thus two beryllium-copper capsules similar to those described above, and with the same shape of corrugations but of material 0.0045 inch thick, would have the same deflection in the pressure range 0 to 256 millibars (0 to 200 millimeters of mercury).

The effect of friction at the sliding contact should be considered. If the friction at the point of contact and the deflection range of the contact arm remain constant, while the stiffness of the pressure element and the multiplication of the mechanism are varied, the differential pressure necessary to balance the friction varies directly as the stiffness and inversely as the square of the diameter of the diaphragm capsule.

If data are required at air pressures above the cut-off point of the elements described, the usual type of pressure element can also be used, but should be arranged so as to record only in this pressure range. The sensitive element contactor would be so arranged that it would traverse the same contacts at pressures below its cut-off pressure.

This diaphragm capsule was developed at the National Bureau of Standards as a part of the program of upper-air investigations undertaken in cooperation with the National Geographic Society.

WASHINGTON, November 27, 1939.

[2] Corrugated Metal Diaphragms for Aircraft Pressure Measuring Instruments. Nat. Adv. Comm. Aero. Technical Note 738 (1939).

FIGURE 2.—*New type pressure element installed in Diamond-Hinman-Dunmore radio sonde.*

A is the contact arm.

U. S. DEPARTMENT OF COMMERCE NATIONAL BUREAU OF STANDARDS

RESEARCH PAPER RP1271

Part of Journal of Research of the National Bureau of Standards, Volume 24, January 1940

PHYSICAL PROPERTIES OF SOME PURIFIED ALIPHATIC HYDROCARBONS

By Donald B. Brooks, Frank L. Howard, and Hugh C. Crafton, Jr.

ABSTRACT

In an investigation of the suitability of various paraffin hydrocarbons as constituents of aviation fuel, which is being conducted for the National Advisory Committee for Aeronautics, the Navy Bureau of Aeronautics, and the Army Air Corps, four olefin and seven paraffin hydrocarbons have been obtained in a state of high purity. Eight of these materials were synthesized, one was isolated from a commercial synthetic crude, and two were obtained from commercial sources. All were purified by distillation in automatically controlled fractionating columns of high efficiency.

The measured physical properties of these materials included freezing point, boiling point and its variation with pressure, refractive index and density and their variations with temperature.

CONTENTS

	Page
I. Introduction	33
II. Fractionating columns	34
III. Preparation of materials	34
1. Preparation of 3,3-dimethylbutene-1, 2,3-dimethylbutene-1, and 2,3-dimethylbutene-2	34
2. Preparation of 2,2-dimethylbutane	37
3. Preparation of 2,3-dimethylbutane	37
4. Preparation of 2,3,3-trimethylbutene-1 and 2,2,3-trimethylbutane	37
5. Preparation of 3-ethylpentane	38
6. Isolation of 2,3,4-trimethylpentane	39
7. Purification of *n*-heptane and 2,2,4-trimethylpentane	39
IV. Determination of physical properties	39
V. References	45

I. INTRODUCTION

The materials described herein were prepared in connection with an investigation of the suitability of various paraffin hydrocarbons as constituents of aviation fuel. This investigation is being conducted at the National Bureau of Standards for the National Advisory Committee for Aeronautics, the Navy Bureau of Aeronautics, and the Army Air Corps. In the previous paper [1] [1] of this series, the preparation and properties of purified 2,2,3-trimethylpentane were described.

Eight of the hydrocarbons described herein were synthesized, one was isolated by fractionation from a commercial synthetic crude, and two were obtained from commercial sources. All of these materials were further purified by distillation in automatically controlled fractionating columns of high efficiency.

[1] Figures in brackets indicate the literature references at the end of this paper.

II. FRACTIONATING COLUMNS

The high purity of the compounds described in this paper resulted primarily from the efficiency of the two fractionating columns used for the final purification. Both columns operate automatically and continuously throughout a distillation, whether it takes 4 days or 4 weeks.

Both columns are built entirely of Pyrex glass. The smaller is a 150-plate bubble-cap column, the fractionating elements of which follow the design of Bruun [2]. The other column is a 600- by 4-cm helix-packed column. Both columns have silvered vacuum jackets, heating elements wound around the latter, and 1 inch of asbestos insulation outside the heating elements. Five-liter still-pots are sealed on the columns. The head of each column has a thermometer well. The columns operate under total reflux with intermittent sampling automatically timed.

Other columns similar to the bubble-cap have shown efficiencies of over 80 theoretical plates for a 120-plate column; therefore, it is believed the efficiency of the 150-plate bubble-cap column is close to 100 theoretical plates. By comparison of the distillation of the same or similar materials in the two columns, it was evident that the 600- by 4-cm packed column was more efficient than the bubble-cap column.

The criteria which guided the selection of samples for measurement of physical properties were the constancy of boiling point and the refractive index of the fractions, and other factors of the particular run which experience had shown might affect the purity of the fraction.

III. PREPARATION OF MATERIALS

1. PREPARATION OF 3,3-DIMETHYLBUTENE-1, 2,3-DIMETHYLBUTENE-1, AND 2,3-DIMETHYLBUTENE-2

Flow diagram:

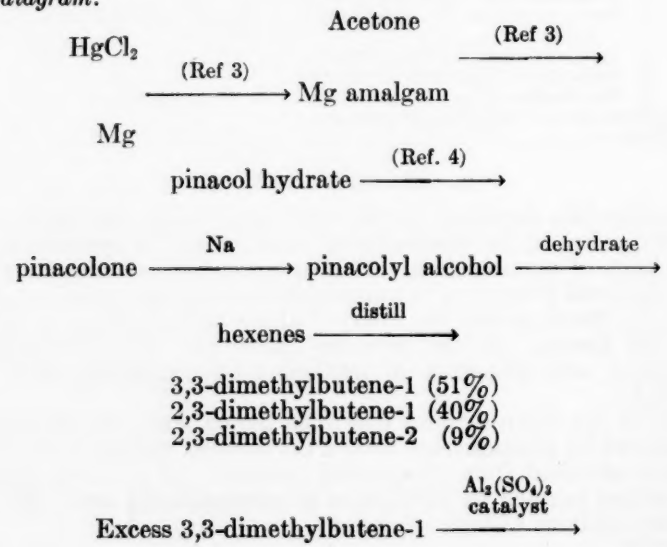

3,3-dimethylbutene-1 (7%)
2,3-dimethylbutene-1 (28%)
2,3-dimethylbutene-2 (65%)

A. Pinacol hydrate.—Pinacol hydrate was prepared from acetone and magnesium amalgam by a modification of the procedure given in Organic Syntheses [3].

A 5-liter three-necked flask was fitted with a 500-ml dropping funnel and a 150- by 2-cm condenser in the two smaller necks. Water at 5° to 10°C was circulated through the condenser jacket. The large center neck was stoppered with a cork. In the flask were placed 120 g of magnesium turnings and 500 ml of benzene.

(Technical benzene and acetone for this preparation were dried for 2 days over calcium chloride and decanted. No increase in yield was found when these materials were further purified.) A solution of 135 g of mercuric chloride in 260 ml of acetone was added all at once, and the very vigorous reaction controlled by adding portions of 700 ml of benzene as needed. In this way all the magnesium was amalgamated equally before the magnesium pinacolate had swelled up to the point where addition of mercuric chloride caused local amalgamation and separation of free mercury. After the benzene had been added, 500 ml of acetone was added slowly, and then a solution of 300 ml of benzene and 390 ml of acetone was added. The swollen magnesium pinacolate was worked down to the bottom of the flask, when necessary, by inserting a wooden paddle in the large neck of the flask and stirring. The product was worked up in the way described in Organic Syntheses [3]. Concentration of the pinacol hydrate solution was effected by distillation from a 12-liter flask heated internally with a steam coil. The vapors were condensed by passing through a ½-in. copper-coil water-cooled condenser. The yield of crude pinacol hydrate was 52 to 58 percent of the calculated amount based on magnesium. About 50 kg was prepared.

B. Pinacolone.—Pinacolone was prepared in 70-percent yield from pinacol hydrate by the method described in Organic Syntheses [4]. Double quantities were used, and the reaction was carried out in a 5-liter three-necked flask.

The crude pinacolone was distilled through a 100- by 2-cm column packed with Pyrex helices. Distillate representing 80 to 83 percent of the charge was collected between 105° and 106°C.

C. Pinacolyl alcohol.—A 12-liter round-bottomed flask was fitted with a 150- by 2-cm condenser cooled with water at 5° to 10°C. The flask was charged with 740 ml (6 moles) of purified pinacolone, 3,600 ml of ether and 2,700 ml of saturated sodium carbonate solution. Sodium (690 g, 30 moles) cut into small pieces was added through the condenser as fast as possible without causing an excessively violent reaction. This required from 6 to 7 hours. When sodium carbonate crystallized out to such an extent that the mixing caused by evolution of hydrogen was impaired, water was added, 25 ml at a time, until the salt was just dissolved.

When the reaction was complete, the layers were separated, the aqueous layer extracted once with 1,000 ml of ether, and the combined ether solutions were washed with water, dried with potassium carbonate, and distilled through a 100- by 2-cm packed column. The product collected boiled at 120° to 122° C. In this way 10,850 ml of pinacolyl

alcohol was prepared from 12,295 ml of pinacolone (88.4 percent of the calculated yield).

D. Dehydration of pinacolyl alcohol.—Pinacolyl alcohol was dehydrated by passing it through a 100- by 2-cm horizontal Pyrex-glass tube electrically heated, well lagged, and filled with alumina (Hydralo, from J. T. Baker Chemical Co.). The alcohol was added at the rate of 60 ml per hour while the tube was maintained at 297° to 305° C. The products, olefins and water, were separated, and the olefins dried

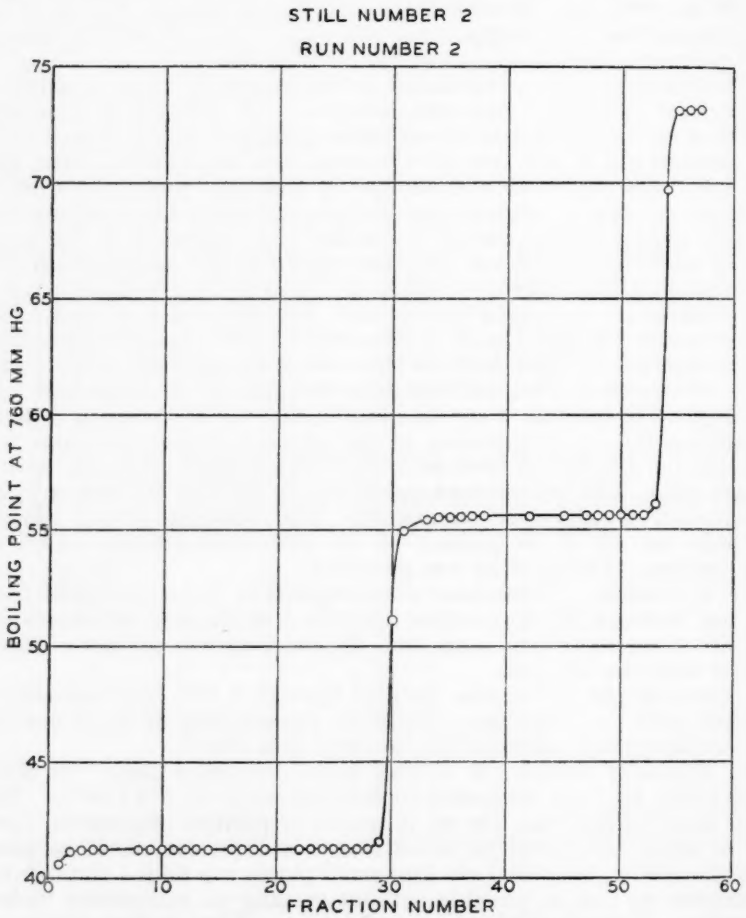

FIGURE 1.—*Fractional distillation of dimethylbutenes.*

with anhydrous sodium sulfate. In this way 7,742 ml of mixed olefins was obtained from 7,795 ml of the alcohol. The product was water-white and contained no alcohol. The mixture of olefins was distilled through the 150-plate bubble-cap column. One charge, the distillation curve of which is shown in figure 1, was separated into 57 fractions, 27 of which boiled between 41.23° and 41.24° C (head temperatures), 21 between 55.56° and 55.62° C, and 5 between 73.17°

and 73.18° C. Not including the holdup (210 ml, 3½ fractions) and four intermediate fractions, this represents 51.0 percent of 3,3-dimethylbutene-1, 39.6 percent of 2,3-dimethylbutene-1, and 9.4 percent of 2,3-dimethylbutene-2.

Since approximately equal portions of the three olefins were desired, excess 3,3-dimethylbutene-1 and intermediate fractions were passed through the catalyst tube previously described, filled with aluminum sulfate maintained at 280° to 290° C. The first portion of the effluent contained hydrogen sulfide and sulfur, but the remainder was clean. All olefins from the reaction were washed with sodium plumbite and shaken with mercury. From 3,570 ml charged, there was obtained 3,390 ml of mixed olefins. The relative proportions, as determined by distillation analysis, were: 3,3-dimethylbutene-1, 7 percent; 2,3-dimethylbutene-1, 28 percent; and 2,3-dimethylbutene-2, 65 percent. These results substantiate those found by Cramer and Glasebrook [5].

Appropriate fractions from several runs were combined and redistilled, and samples of the middle portion of each distillate were used in the determination of physical constants.

2. PREPARATION OF 2,2-DIMETHYLBUTANE

Flow diagram:

$$\text{3,3-dimethylbutene-1} \xrightarrow[\substack{\text{Raney Ni}\\\text{catalyst}}]{H_2} \text{2,2-dimethylbutane}$$

Fifteen hundred milliliters of 3,3-dimethylbutene-1 was hydrogenated at 1,500 lb/in.^{2} pressure, at 150° C, in the presence of Raney nickel catalyst. After washing, drying, and refluxing over sodium, 1,485 ml was carefully fractionated in the 600- by 4-cm packed column.

3. PREPARATION OF 2,3-DIMETHYLBUTANE

Flow diagram:

$$\text{2,3-dimethylbutene-2} \xrightarrow[\substack{\text{Raney Ni}\\\text{catalyst}}]{H_2} \text{2,3-dimethylbutane}$$

One thousand milliliters of constant-boiling 2,3-dimethylbutene-2 was hydrogenated at 1,800 lb/in.^{2} pressure, at 130° C, in the presence of Raney nickel catalyst. The product was washed, dried, refluxed over sodium, and distilled in the manner already described. The product, 987 ml, was carefully fractionated in the 600- by 4-cm packed column.

4. PREPARATION OF 2,3,3-TRIMETHYLBUTENE-1 AND 2,2,3-TRIMETHYLBUTANE

Flow diagram:

$$\textit{tert}\text{-butyl chloride} \xrightarrow[\text{ether}]{\text{Mg}} \textit{tert}\text{-butyl magnesium chloride} \xrightarrow{\text{acetone}}$$

$$\text{2,3,3-trimethylbutanol-2} \xrightarrow{\text{dehydrate}} \text{2,3,3-trimethylbutene-1}$$

$$\xrightarrow[\substack{\text{Raney Ni}\\\text{catalyst}}]{H_2} \text{2,2,3-trimethylbutane}$$

2,3,3-Trimethylbutanol-2 was prepared by the action of acetone on *tert*-butyl magnesium chloride in dry ether in yields up to 30 percent. The product was recovered, dehydrated to 2,3,3-trimethylbutene-1, and hydrogenated to 2,2,3-trimethylbutane in a manner essentially the same as that described hereinafter for the preparation of 3-ethylpentane. The carbinol boiled at 129° to 133° C, the olefin at 76° to 78° C, and the paraffin at 80° to 82° C in the preliminary separations.

A portion of the 2,3,3-trimethylbutene-1 was purified by distillation through the 150-plate bubble-cap column. From 3,000 ml of crude olefin 2,600 ml of 2,3,3-trimethylbutene-1 was recovered, which was constant-boiling (within 0.01° C) and which had a constant refractive index.

All 2,2,3-trimethylbutane was carefully washed with sulfuric acid, water, sodium bicarbonate solution, dried over calcium chloride, and distilled from sodium. The distillate boiling at 80° to 82° C was fractionated in the 600- by 4-cm packed column. Six liters of material was prepared in this way, fractions of which differed in boiling point by no more than 0.013° C and which had refractive indices (n_D^{20}) of 1.3892 to 1.3894.

5. PREPARATION OF 3-ETHYLPENTANE

Flow diagram:

$$\text{Ethyl bromide} \xrightarrow{\text{ether}} \text{ethyl magnesium bromide}$$

$$\text{Mg}$$

$$\text{ethylpropionate} \xrightarrow{\text{ether}} \text{complex} \xrightarrow[\text{HCl}]{\text{ice}} \text{triethylcarbinol} \xrightarrow{I_2} \text{3-ethylpentene-2}$$

$$\xrightarrow[\substack{\text{Raney Ni}\\\text{catalyst}}]{H_2} \text{3-ethylpentane}$$

Triethylcarbinol was made in 80- to 85-percent yield by the action of ethyl propionate on ethyl magnesium bromide in dry ether. The carbinol was isolated from the reaction mixture by decomposing the Grignard complex with ice and dilute hydrochloric acid, and extracting the aqueous layer with ether. The ether solution was distilled through a 100- by 2-cm packed column. The carbinol boiled at 140° to 142° C.

The 3-ethylpentene-2 was formed in a 94-percent yield when triethylcarbinol was slowly distilled in the presence of 0.5 percent of its weight of iodine. The product was dried with calcium chloride, refluxed over sodium, and distilled in the 100- by 2-cm column. The fraction which boiled at 95° to 97° C was collected for hydrogenation.

The 3-ethylpentane was formed in a 97-percent yield when 3-ethylpentene-2 was hydrogenated at 120° C and 1,800 to 2,200 lb/in.^{2} pressure in the presence of Raney nickel catalyst. The product was thoroughly washed with concentrated sulfuric acid, water, 5-percent aqueous sodium bicarbonate, and finally washed several times with water. It was dried with calcium chloride, refluxed over sodium, and distilled through the 100- by 2-cm. column. The fraction which boiled between 92° and 94.5° C was collected for further purification. A total of 2,650 ml was prepared in this way.

The material was further purified by careful fractionation in the 600- by 4-cm packed column. Each fraction was withdrawn after the temperature at the head of the column (corrected to 760 mm Hg) had become constant. In this way 1,750 ml of hydrocarbon was collected at still head temperatures within a range of 0.012° C. All fractions of this portion had a refractive index ($n_D^{21.20}$) of 1.3928.

6. ISOLATION OF 2,3,4-TRIMETHYLPENTANE

This octane was prepared by fractionation of a mixture of isomeric octanes supplied through the kindness of Gustav Egloff, of the Universal Oil Products Co. The isomeric octanes were first distilled in a batch still having a 240- by 4-cm column packed with locket chain. Fractions of about 4.5 liters so obtained were distilled in a 150-plate bubble-cap still, recombined according to refractive index, and redistilled.

7. PURIFICATION OF *n*-HEPTANE AND 2,2,4-TRIMETHYLPENTANE

Samples from the purest batches of certified *n*-heptane (California Chemical Co.) and "isooctane" (2,2,4-trimethylpentane) (Röhm & Haas Co., Inc.) were carefully fractionated in a 150-plate bubble-cap column.

IV. DETERMINATION OF PHYSICAL PROPERTIES

The apparatus and technique employed in the measurements of physical properties have already been described in the first report [1] of this series.

In previous work [1, 6, 7] it has been found that data obtained in the distillation of a sample through the 10-in. jacketed column used in determining the boiling point of the sample furnished a rough index of its purity. The distillation data on each sample were obtained at two or more total pressures differing by 7 to 28 mm Hg, one of these values being close to 760 mm Hg. From the rate of change of temperature with pressure so found, the data obtained when the pressure was near 760 mm Hg were corrected to that value. As pressure readings were taken only at intervals during a distillation, minor fluctuations not recorded caused an unevenness in the corrected data amounting to three or four thousandths of a degree. The corrected distillation data obtained in the present work are plotted in figures 2 to 9 and 11 to 13.

The two lower-boiling hexenes, 3,3-dimethylbutene-1 and 2,3-dimethylbutene-1, figures 2 and 3, appear to be of fairly high purity. By comparison, the 2,3-dimethylbutene-2, figure 4, is of very low purity.

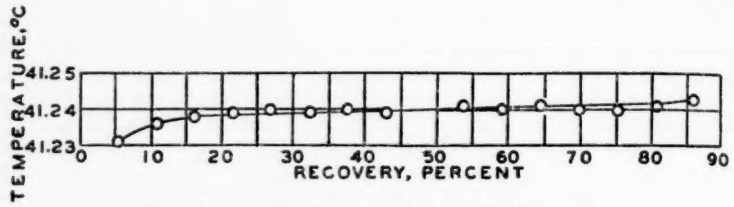

FIGURE 2.—*Distillation of 3,3-dimethylbutene-1.*

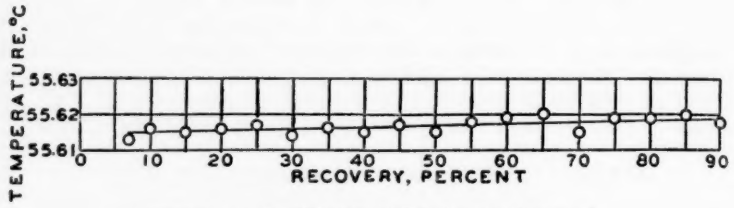

FIGURE 3.—*Distillation of 2,3-dimethylbutene-1.*

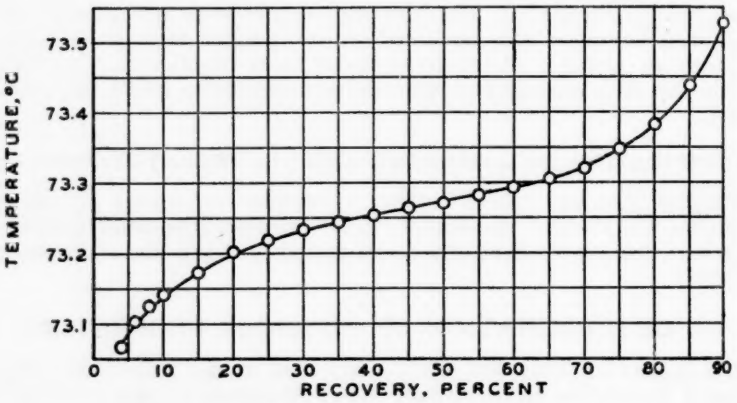

FIGURE 4.—*Distillation of 2,3-dimethylbutene-2.*

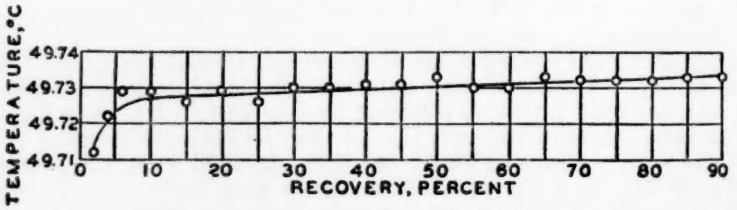

FIGURE 5.—*Distillation of 2,2-dimethylbutane.*

The two dimethylbutanes, figures 5 and 6, are of about as high purity as the lower-boiling hexenes. The 3-ethylpentane, figure 7,

is of very high purity, no rise of temperature being observed during distillation from 6 percent to 90 percent recovered.

The 2,3,3-trimethylbutene-1, figure 8, appears to be of lower purity than the hexenes. Its paraffin homologue, 2,2,3-trimethylbutane, figure 9, like the 3-ethylpentane, shows no rise of temperature in distillation above 3 percent recovered. A freezing-point determina-

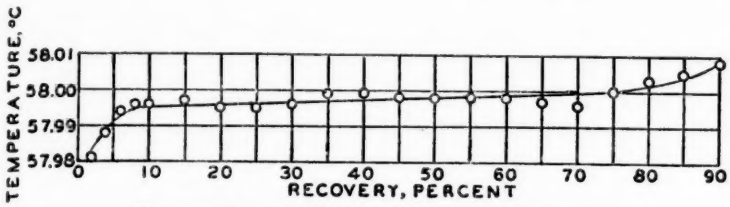

FIGURE 6.—*Distillation of 2,3-dimethylbutane.*

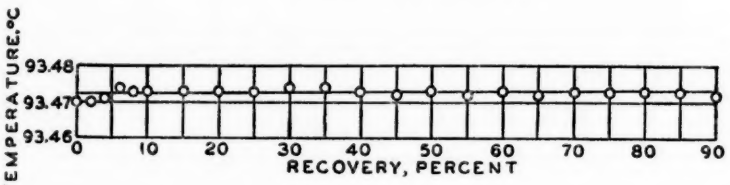

FIGURE 7.—*Distillation of 3-ethylpentane.*

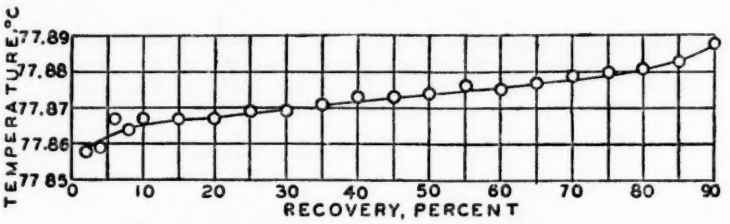

FIGURE 8.—*Distillation of 2,3,3-trimethylbutene-1.*

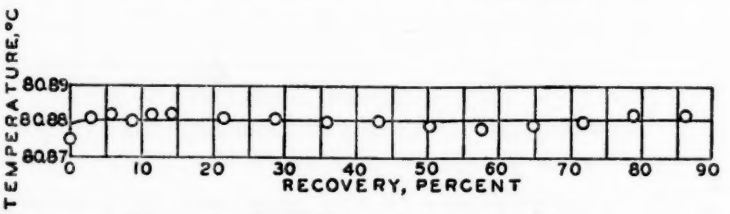

FIGURE 9.—*Distillation of 2,2,3-trimethylbutane.*

tion on this material is plotted in figure 10. A freezing-point determination on another sample, to which 2 percent of normal heptane had been added, showed the lowering to be 2.17° C per mole-percent of impurity.

The distillation curves of normal heptane, figure 11, and of 2,2,4-trimethylpentane, figure 12, offer no especial points of interest. Figure 13, the distillation curve of 2,3,4-trimethylpentane, is of interest in

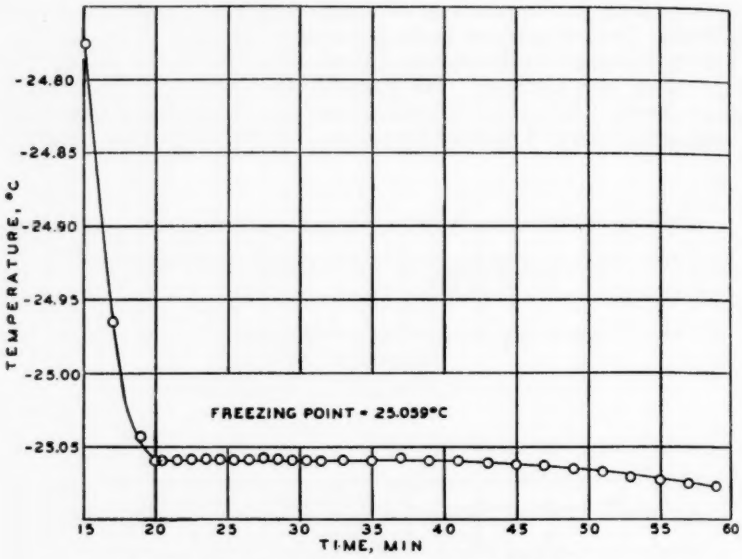

FIGURE 10.—*Freezing curve of 2,2,3-trimethylbutane.*

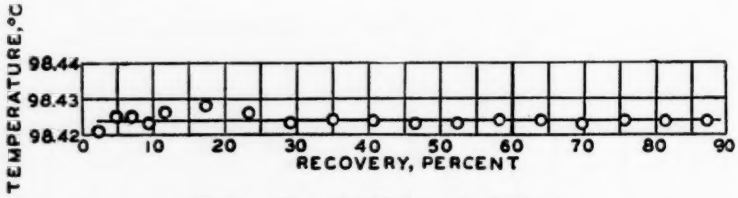

FIGURE 11.—*Distillation of n-heptane.*

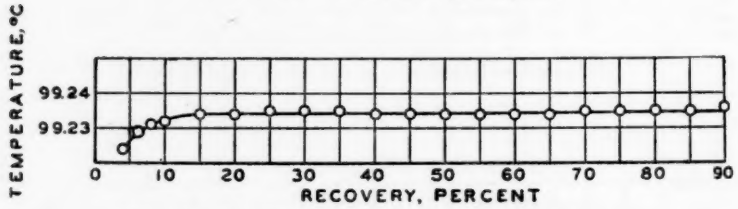

FIGURE 12.—*Distillation of 2,2,4-trimethylpentane.*

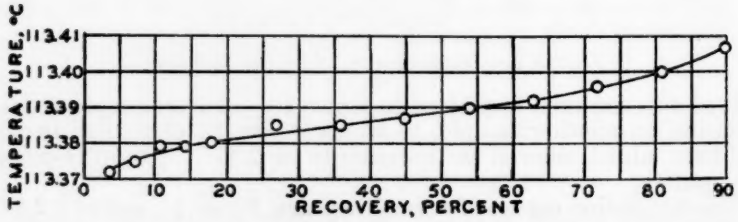

FIGURE 13.—*Distillation of 2,3,4-trimethylpentane.*

that this material was isolated by fractional distillation from a synthetic crude containing 5 to 10 percent of hexanes and heptanes, the balance being octanes including the four trimethylpentanes, at least two dimethylhexanes, and small amounts of unidentified octanes. Without recourse to fractional crystallization, a product was obtained, 80 percent of which distilled within a range of 0.03° C. The freezing and melting curves of 2,3,4-trimethylpentane are shown in figure 14.

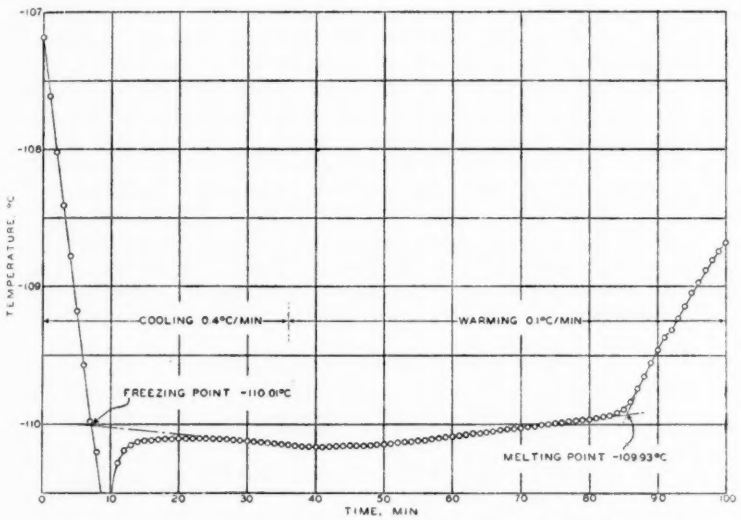

FIGURE 14.—*Freezing and melting curves of 2,3,4-trimethylpentane.*

TABLE 1.—*Boiling-point data on 2,2,3-trimethylbutane*

Barometric pressure	Observed boiling point	Computed boiling point	Difference, observed − computed
mm Hg	° *C*	° *C*	*deg.*
740.74	80.006	80.005	+0.001
750.20	80.434	80.436	−.002
758.67	• 80.819	80.819	.000
764.41	81.082	81.076	+.006
767.44	81.207	81.211	−.004

• This value was obtained on a sample from a different batch of 2,2,3-trimethylbutane.

TABLE 2.—*Empirical constants in vapor pressure equations*

Compound	*A*	*B*
3,3-Dimethylbutene-1	17.04606	3,274
2,3-Dimethylbutene-1	17.18944	3,471
2,3-Dimethylbutene-2	17.63641	3,812
2,3,3-Trimethylbutene-1	16.96984	3,628
2,2-Dimethylbutane	17.06023	3,367
2,3-Dimethylbutane	17.19986	3,499
2,2,3-Trimethylbutane	17.01002	3,674
3-Ethylpentane	17.45112	3,966
2,2,3-Trimethylpentane	17.13021	4,020
2,3,4-Trimethylpentane	17.25410	4,105

Boiling-point determinations were made on 2,2,3-trimethylbutane at several barometric pressures, the values being given in the first two columns of table 1. Since the heat of vaporization could be assumed to be constant over the small range of temperatures shown in the second column of the table, the equation

$$\log p = A - B/T, \tag{1}$$

where p=pressure; T=absolute temperature; and A, B=empirical constants, should fit the data satisfactorily. The constants A and B were evaluated from the data by the method of least squares, and are given in table 2 for nine of these compounds and for 2,2,3-trimethylpentane, the properties of which have been described earlier [1]. Values are not given for *n*-heptane and 2,2,4-trimethylpentane, as the cubic equations of Smith and Matheson [9] are more accurate.

The third column of table 1 gives the boiling points computed from the formula so found, and the last column shows the difference between observed and computed values. These differences are of the magnitude to be expected if the standard deviation of a boiling-point determination is ±0.003° C. This value is only one-third as large as that found in earlier work with this apparatus [7]. Refinements in technique are believed to be responsible for the reduction.

TABLE 3.—*Properties of preparations* [a]

Compound	Freezing point	Boiling point at 760 mm Hg	dt/dP	Refractive index		dn/dt (20° to 25° C)	Density		dD/dt (20° to 25° C)
				n_D^{20}	n_D^{25}		20° C	25° C	
	° C	° C	*deg/mm Hg*			*per deg*	*g/ml*	*g/ml*	*g/ml deg*
3,3-Dimethylbutene-1	−115.53	41.239	0.0397	1.37604	1.37295	−0.000618	0.65293	0.64786	−0.001014
	−114.7	*41.2*		*1.37660*		*−.000598*	*.65198*		[b] *−.000908*
2,3-Dimethylbutene-1	−140.1	55.615	.0410	1.39022	1.38724	−.000596	.67801	.67322	−.000958
	−139 to −133	*55.8*		*1.3915*			*.6825*		
2,3-Dimethylbutene-2	−75.4	73.24	.0414	1.4121	1.4092	−.00057	.7088	.7045	−.00086
	−74.2	*73.5*		[c] *1.4116*			*.7054*		[b] *−.000580*
2,3,3-Trimethylbutene-1	−111.40	77.874	.0447	1.40292	1.40004	−.000576	.70501	.70054	−.000860
		78		[d] *1.402*			*.7029*		[b] *−.00116*
2,2-Dimethylbutane	−100.06	49.731	.0407	1.36864	1.36592	−.000543	.64902	.64432	−.000940
	−98.2	*49.7*		*1.36887*		*−.000541*	*.64944*		[b] *−.000916*
2,3-Dimethylbutane	−129.79	57.999	.0412	1.37490	1.37212	−.000556	.66150	.65699	−.000921
	−128.8	*58.0*		*1.37499*		*−.000540*	*.66201*		[b] *−.000869*
2,2,3-Trimethylbutane	−25.059	80.879	.0449	1.38947	1.38683	−.000528	.69000	.68576	−.000848
	−25.0	*80.8*		*1.38943*			*.69014*		[b] *−.000880*
3-Ethylpentane	−118.65	93.473	.0446	1.39337	1.39084	−.000506	.69818	.69377	−.000882
	−118.8	*93.5*		[c] *1.3937*			*.69860*		*−.000884*
n-Heptane	−90.60	98.424	[e] (.0449)	1.38764	1.38511	−.000506	.68368	.67943	−.000849
	−90.5	*98.4*		*1.38774*		[c] *−.00014*	*.68375*		*−.000858*
2,2,4-Trimethylpentane	−107.37	99.233	[e] (.0465)	1.39155	1.38915	−.000480	.69189	.68778	−.000822
	−107.45	*99.3*		*1.39187*			*.69194*		*−.000844*
2,3,4-Trimethylpentane	−109.97	113.391	.0479	1.40431	1.40193	−.000476	.71903	.71507	−.000791
	[f]	*113.4*		*1.4046*			*.7195*		

[a] The values given in the upper row of figures for each compound are those obtained in this work and are believed to be accurate within a few units in the last decimal place given. The lower row of figures (in italics) are taken from Egloff [8] for comparison.
[b] Over a wider range of temperatures.
[c] At 18° C.
[d] Estimated.
[e] Probably a typographical error.
[f] "Glassy at low temperatures."
[g] Copied from reference [7].

The physical properties of the compounds included in this investigation are given in table 3. The upper row of figures for each compound are the values obtained in this work. For comparison, values taken from Egloff [8] are give below in italics. The boiling point of each compound at 760 mm Hg barometric pressure was found by substituting in eq 1 the observed data for the compound, evaluating the constants A and B, and solving the resulting formula for $p=760$. The values so obtained deviate from those shown in figures 2 to 9 and 11 to 13 by one or two thousandths of a degree, the latter having been corrected to 760 mm Hg by linear interpolation only. Refractive indices and densities were obtained at temperatures close to 20° and 25°C and were corrected to 20° and 25° C by assuming the variations with temperature to be linear. All weighings made in the density determinations were corrected to vacuum.

V. REFERENCES

[1] Donald B. Brooks, Frank L. Howard, and Hugh C. Crafton, Jr., J. Research NBS **23,** 637 (1939) RP1259.
[2] Johannes H. Bruun, Ind. Eng. Chem., Anal. Ed., **8,** 224 (1936).
[3] Organic Syntheses, collective vol. 1, p. 448 (1932). (John Wiley & Sons, New York, N. Y.)
[4] Organic Syntheses, collective vol. 1, p. 451. (John Wiley & Sons, New York, N. Y.)
[5] P. L. Cramer and A. L. Glasebrook, J. Am. Chem. Soc. **61,** 230 (1939).
[6] Donald B. Brooks, Robetta B. Cleaton, and Frank R. Carter, J. Research NBS **19,** 319 (1937) RP1027.
[7] Donald B. Brooks, J. Research NBS **21,** 847 (1938) RP1160.
[8] Gustav Egloff, Physical Constants of Hydrocarbons, vol. 1 (Reinhold Publishing Corp., New York, N. Y., 1939.)
[9] Edgar Reynolds Smith and Harry Matheson, J. Research NBS **20,** 641 (1938) RP1097.

WASHINGTON, November 21, 1939.

U. S. DEPARTMENT OF COMMERCE NATIONAL BUREAU OF STANDARDS

RESEARCH PAPER RP1272

Part of Journal of Research of the National Bureau of Standards, Volume 24, January 1940

MATHEMATICAL THEORY OF IRROTATIONAL TRANSLATION WAVES

By Garbis H. Keulegan and George W. Patterson

ABSTRACT

This paper is the first of a series dealing with the motion of flood waves and other waves of translation in open channels. The case treated is that of waves for which the forces of fluid friction are negligible with respect to the inertia and gravitational forces. The irrotational motion of a perfect liquid in a horizontal rectangular canal when the original surface is disturbed is investigated on the assumption that the horizontal velocity in a cross section is approximately uniform. The results are also applicable to motion in a canal of uniform slope containing water originally moving with a uniform velocity. Special emphasis is laid on disturbances which are propagated without change of form, and in these cases formulas are derived for the wave profile and velocity of propagation. Formulas are also derived which give the deformation, energy, motion of the center of gravity, and moment of instability of an arbitrary intumescence. Consideration is given to the maximum height of a wave of permanent form. Formulas have been compared with the available experimental data. Of special interest is the comparison of the shape of the undulations composing the head of an initial surge with the characteristics of the cnoidal wave.

CONTENTS

	Page
List of symbols	48
I. Introduction	49
II. Irrotational motion	53
1. Dynamical equations of motion	53
2. Displacement and deformation of a liquid element	54
3. Kinematical relations	55
4. Irrotational motion	56
5. Invariance of the circulation in a moving circuit	57
6. Impulsive generation of motion	59
7. Pressure equation	60
8. Solution of problems in irrotational motion	61
III. Formulation of the wave problem—Waves in water of small depth	61
IV. Long waves of negligible height and curvature	63
1. Velocity of propagation	63
2. Energy of an intumescence	65
3. Displacement of the particles	66
4. Effect of an arbitrary initial disturbance	66
5. Reflection and transmission of waves	67

198881—40——4

Page

V. Waves of appreciable height and curvature 69
1. Two definitions of velocity of propagation 69
2. Mean velocity of particles 70
3. Effect of curvature and height on velocity of propagation of a volume element 72
4. Deformation of the wave profile 74
5. Motion of the center of gravity of a wave 75
6. Variation in energy of an intumescence 76
7. The moment of instability of an intumescence 77
8. Solitary waves 78
9. Cnoidal waves 81
10. Moment of instability of a solitary wave 85
11. Moment of instability and wave formation 87
12. Negative waves 88
13. Intumescences of finite height but negligible curvature 89
14. Horizontal channel in communication with the ocean 90
15. Waves due to sudden increase of discharge 91
16. Effect of channel velocity distribution 91
17. Initial waves 95
18. Favre's experiments on the undulations in a positive surge 97
19. Theory of breakers 99
VI. References 100

LIST OF SYMBOLS

c	velocity of propagation of long wave of negligible height and curvature.
c_1	velocity of wave approaching a discontinuity in a channel cross section. Also a constant of integration.
c_2	velocity of transmitted wave after passing a discontinuity in a channel cross section. Also a constant of integration.
cn (x, k)	Jacobian elliptic function, cosine amplitude.
ρgE	total energy of a wave per unit width of channel [MLT^{-2}].
$E_1(k)$	complete elliptic integral of the second kind.
$f(\ ), F(\ ),$	with or without subscripts—functional symbols.
$F(x, k)$	incomplete elliptic integral of the first kind.
$F_1(k)$	complete elliptic integral of the first kind.
g	acceleration of gravity.
$g(\ ), G(\ )$	functional symbol.
h	height of main body of discharge wave (section V–17); vertical displacement of water surface.
h_1	vertical displacement of surface as wave approaches discontinuity in channel cross section (section IV–5).
h_2	vertical displacement of surface after wave passes discontinuity in channel cross section (section IV–5).
h_1	maximum height of solitary wave, maximum depth of negative wave, maximum height of initial discharge wave.
h_1, h_2	maximum height and depth, respectively, of cnoidal wave.
$h_2 = H\eta_2$.	
h_a	maximum height of initial discharge wave.
h'	average height of discharge wave.
H	undisturbed depth of liquid in channel.
$H(\ )$	functional symbol.
k	modulus of elliptic integral.
l	length of section of channel (section IV–4).
l, m, n	direction cosines.
M_s	moment of instability [L].
M'_1, M_2, M'_2, M_s	momenta per unit width [MT^{-1}].
p	pressure [$ML^{-1}T^{-2}$].
p_a	atmospheric pressure.
q	speed of particle (section II–5, 7, 8).
q	discharge per unit width in a cross section [L^2T^{-1}] (section V–2).
Q	total volume per unit width of a solitary wave [L^2].
s	length of arc.

$\mathrm{sn}\,(x, k)$ Jacobian elliptic function, sine amplitude.
t time.
u, v, w x component, y component, z component, respectively, of velocity.
u_0 x component of velocity at bottom of channel, also first approximation to velocity in cross section.
u_0, v_0, w_0 velocity components prior to impulse (section II–6).
u_1, u_2 velocities of particles in a wave before and after passing a discontinuity in a channel cross section (section IV–5).
v_1, u_2, U_1, U_2 local and mean velocities in two cross sections (section V–16).
u_1 velocity of particle at apex of wave (section V–19).
U mean velocity of particles in cross section.
U_0 mean velocity in a section where $h=0$.
V volume [L^3] (section II–3); volume per unit width [L^2] (sections IV–3, V–5).
x Cartesian coordinate, specifically, parallel to channel in bottom plane.
y Cartesian coordinate, specifically, lateral to channel in the horizontal plane.
z Cartesian coordinate, specifically, drawn upward with origin at bottom of channel.
$\alpha=3/H^3$ (section V–10); a ratio (section V–14).
$\gamma_1, \gamma_2, \gamma_3$ rates of angular dilatation [T^{-1}].
Γ circulation [L^2T^{-1}].
$\epsilon_1, \epsilon_2, \epsilon_3$ rates of linear dilatation [T^{-1}].
ϵ a small quantity.
ξ, η, ζ components of vorticity [T^{-1}] (sections II–1, 4, 5).
ζ dimensionless x coordinate of free surface.
η, ξ z and x coordinates, respectively, of center of gravity of volume above undisturbed surface (sections V–5, 6, 12, 17).
η dimensionless z coordinate of free surface$=h/H$ (sections V–8, 9); Boussinesq number (section V–16).
$\eta', \eta'', \eta''' = -\eta_3$ three roots of the differential equation of the permanent wave.
η_1 maximum relative height of a solitary wave (section V–8); maximum relative height of a cnoidal wave (section V–9, 18).
η_2 maximum relative depression of a cnoidal wave.
$\theta\,(\ )$ functional symbol.
λ wave length of a cnoidal wave (sections V–9, 18).
ρ density of liquid [ML^{-3}].
σ partial volume per unit width of an intumescence [L^2].
Σ volume per unit width of an intumescence.
ϕ velocity potential [L^2T^{-1}].
ϕ_0 velocity potential prior to application of impulse (section II–6); velocity potential, first approximation.
$\psi\,(\ )$ functional symbol.
ω velocity of propagation of an element of volume of an intumescence.
ω_0 velocity of propagation of an element of wave height, negligible surface curvature.
ω_1 velocity of propagation of an element of wave height, appreciable surface curvature.
ω_c velocity of propagation of a cnoidal wave.
ω_q velocity of propagation of discharge.
ω impulsive pressure [$ML^{-1}T^{-1}$].
Ω gravitational potential [L^2T^{-2}].

I. INTRODUCTION

The growing importance of predicting the occurrence of floods and the rate of travel and height of flood waves as they pass down rivers has led in recent years to a marked increase in the literature on this subject. However, in no language can there be found a comprehensive presentation of the mathematical treatment of the problem of such waves. Instead, various authors at different times and in dif-

ferent countries have treated separate aspects of the problem, so that the student of the subject must read many papers in several languages to obtain a satisfactory grasp of the problem. There is definite need for a systematic treatment of the results of these different methods of attack, presenting in coordinated form the results that have been attained up to the present time.

It is for this reason that the National Bureau of Standards, at the suggestion of the United States Weather Bureau, has commenced the preparation of a series of papers dealing with the mathematical theory of flood waves and other waves of translation. It is not the purpose of these papers to furnish a practical method of predicting the rate of flood-wave travel and the rate of attenuation of the wave in an actual river channel with its complex flow conditions. Instead, the purpose is to furnish a sound mathematical theory on which attempts to solve the practical problems of flood prediction can be based.

The present paper, the first of the series, deals with the motion of translation waves in channels of uniform, rectangular cross section when the forces of fluid friction are negligible with respect to the inertia and gravitational forces. Later papers in the series as now planned are in various stages of completion and will deal with the following topics: The effect of turbulence and channel slope and configuration on the motion of translation waves; the theory of quasi-permanent regime and the methods of prediction of flood waves; and recent advances in the problem of the deformation of an intumescence.

The different regimes of the flow of water in canals and natural watercourses may be characterized as *uniform*, *varied*, or *unsteady*.

In the *uniform* regime the depth and mean velocity are invariable with respect to both time and space. This regime is attained in sufficiently long stretches of natural courses, provided the slope and discharge are constant, and the channel has a uniform cross section.

In *varied* flow the depth and mean velocity are unchanging with respect to time, but not with respect to space. Examples are flow in the backwater region of a dam, flow in a canal connecting reservoirs at different elevations, and flow in transition sections.

On the other hand, the *unsteady* regime is characterized by a depth and velocity which vary with respect to both time and space. *Gravity waves* and *capillary waves* belong to this class of phenomena, the former being the more important of the two, considered from the point of view of applied science. Gravity waves fall into two classes—*surface waves* and *translation waves*. In *surface waves*, which occur in relatively deep waters, the motion decreases rapidly from the surface downward. The wave motion is sinusoidal, the individual particles periodically traverse closed paths, and the vertical accelerations are always appreciable. In *translation waves*, on the other hand, the motion of all the particles in a cross section is sensibly the same at any given instant. As a translation wave passes, the liquid particles are permanently displaced by an amount proportional to the volume of the wave. Waves of this type are frequently encountered in channels and rivers. *Tidal waves* are examples of the same phenomenon in seas and oceans.

Perhaps the simplest classification of translation waves is that obtained by considering the physical condition governing the motion. Two extreme cases are immediately apparent. First, we have the

case in which the effect of friction is negligible. In these waves the volume and the length are small; and the latter fact explains why the effect of friction can be neglected, so that the weight and inertia become the factors controlling the motion. If the curvature of the wave surface is negligible, the velocity of propagation of the wave height, ω_0, is given by the Lagrange velocity law, $\omega_0=\sqrt{gH}$, where g is the acceleration of gravity and H is the channel depth. On the other hand, if the maximum curvature and the height above the undisturbed level of the free surface are appreciable, then the velocity of propagation of the wave height ω_1 equals ω_0 times a factor slightly different from unity, the exact value of the factor being a function of the height and the derivatives of the wave surface. We call such disturbances *potential intumescences* or *irrotational translation waves.* They can be generated by suddenly immersing a solid body in the liquid or suddenly adding a small mass of liquid; they may also be formed by the sudden motion of a body immersed in the liquid. In these cases the disturbed position of the surface is entirely above the original surface; that is, the waves have a positive elevation. The *solitary wave* is a familiar example. Waves can also be produced by abruptly removing from the channel a small quantity of water or an object already in the channel. These waves have a negative elevation. Surges produced in channels by an abrupt change of flow at either end also belong in this category.

At the other extreme, we find the *quasi-permanent* regime of rivers, or what are commonly called *flood waves.* These are also translation waves, but they are waves in which friction is the all-important factor, the effects of weight and inertia being negligible. The waves are very long, which accounts for the predominant effect of friction. It is illuminating to compare flood waves and potential intumescences on the basis of their velocities of propagation. When discussing flood waves, it is convenient to utilize the idea of the velocity of propagation of discharge, ω_q. According to the Kleitz-Seddon law [1][1] this velocity is given by dq/dH, the slope of the rating curve, q, being the discharge per unit width occurring at the normal stage, H. In a rectangular channel $\omega_q=3U/2$, if the Chezy resistance law is used. A comparison of the two wave velocities gives $\omega_0^2/\omega_q^2=(4/9)(gH/U^2)$. Since in rivers the ratio gH/U^2 is a large number, the conclusion is that ω_0 is many times larger than ω_q. This difference of velocities is significant.

It should be understood that in reality there exists a continuous transition between the two extreme types of waves described above. There are other phenomena occupying an intermediate position, in which the effects of inertia, height, and friction are of the same order of magnitude. These phenomena are also of engineering interest, particularly in connection with hydroelectric plants. When the turbines of such plants are suddenly shut down, a positive intumescence is generated in the supply canal and travels upstream, increasing in length as it goes. A negative intumescence is simultaneously produced in the discharge canal, and this travels downstream, decreasing in length. These waves may be of considerable height (1 meter or so) and are attenuated by the forces of friction. Friction cannot be neglected, because of the long distances which the waves travel.

[1] Figures in brackets indicate the literature references at the end of this paper.

Similarly, when the turbines are suddenly started, the same phenomenon occurs, but the signs of the intumescences are reversed. If the pressure and velocity variations caused by these waves are large, these effects must be considered in designing channel walls, bottom, and embankments. Waves like the above, except that they are generally propagated in still water, occur in canal reaches adjacent to locks when the latter are operated. The positive and negative waves that are generated are quite long, traverse large distances, and, although they undergo a deformation of form owing to the action of friction, the wave length remains the same [2]. There are also a few special cases of flood waves occurring in mountainous regions, in which the inertia effects are important. Massé [3] has given the name of *average intumescences* to the phenomena described above.

The present paper deals exclusively with potential intumescences. Since friction is negligible for these waves, and since they are generated in a liquid either initially at rest or in uniform motion, then by the Lagrange-Cauchy theorem the motion of the liquid particles is irrotational. This fact justifies the mathematical approach selected for this paper.

A brief presentation of the elements of irrotational theory is given in section II, primarily to emphasize the basic dynamical and kinematical principles involved. Section III is a formulation of the basic differential equations whose solutions constitute the solution of the problem.

The general theory is applied in sections IV and V, which deal with solutions of the equations to a first and to a second approximation. In the first approximation, the height and curvature of the waves are assumed negligible, and a complete solution is found in which the waves are propagated without change of form. In the treatment of the second approximation, which constitutes the main body of the paper, more general assumptions are made, leading to involved differential equations which can be solved easily only for particular cases. The deformation of the wave profile during propagation and the motion of the center of gravity of the intumescence play an important role in this analysis. These points are discussed after the introduction of the concept of velocity of propagation of a volume element, originally due to Boussinesq. There are three integrals invariant with respect to time associated with intumescences of appreciable curvature—the volume, the energy, and the moment of instability—which are discussed in considerable detail.

The main emphasis is on the intumescence whose wave profile is propagated without change of form, and the particular solution is obtained for this case. If the liquid is undisturbed at infinity, we have the well-known solitary wave which has been investigated experimentally. If the liquid is in motion at infinity and this motion is indeterminate, we have the less familiar *cnoidal waves*. In the former case, there is an interesting principle discovered by Boussinesq—namely, for all intumescences of equal energy, the solitary wave is unique in possessing the minimum moment of instability. This theorem is significant in that it explains the frequent occurrence and ease of formation of the solitary wave.

In discussing the velocity of propagation of surges, an attempt is made to determine the effect of the channel velocity distribution. The characteristics of the initial wave in a surge are not without

interest, and this wave is considered in the light of both theory and experiment.

The concluding section touches on the problem of limiting wave heights and the breaking of waves.

In the preparation of this paper, extensive use has been made of Lamb's comprehensive text [4] and of a classic paper by Boussinesq [5]. Whenever appropriate experimental data have been available, the authors have attempted to discuss the agreement between theory and experiment. The principal sources of data have been the well-known researches of Bazin [6] and Russell [7, 8] and a recent paper by Favre [2].

II. IRROTATIONAL MOTION

1. DYNAMICAL EQUATIONS OF MOTION

We consider an elementary parallelepiped $\delta x \delta y \delta z$ having its corner nearest the origin of the rectangular axes of reference at the point (x, y, z). Designating the component velocities at the point (x, y, z) by u, v, w, and the density of the liquid by ρ, we have for the kinetic reaction in the x direction of the liquid in the parallelepiped

$$\rho \frac{du}{dt} \delta x \delta y \delta z, \tag{1}$$

which is equal to the x component of all the forces acting on the liquid in the parallelepiped. If the pressure at the point (x, y, z) is p, we have for the x component of the force due to pressure,

$$-\frac{\partial p}{\partial x} \delta x \delta y \delta z. \tag{2}$$

Denoting the potential of gravity at (x, y, z) by Ω, we have for the x component of force due to the weight of liquid,

$$-\rho \frac{\partial \Omega}{\partial x} \delta x \delta y \delta z. \tag{3}$$

Equating eq 1 to eq 2 plus eq 3, dividing by $\rho \delta x \delta y \delta z$, and applying the same reasoning in the remaining two directions, we obtain

$$\left.\begin{aligned} \frac{du}{dt} &= -\frac{1}{\rho}\frac{\partial p}{\partial x} - \frac{\partial \Omega}{\partial x}, \\ \frac{dv}{dt} &= -\frac{1}{\rho}\frac{\partial p}{\partial y} - \frac{\partial \Omega}{\partial y}, \\ \text{and} \quad \frac{dw}{dt} &= -\frac{1}{\rho}\frac{\partial p}{\partial z} - \frac{\partial \Omega}{\partial z}. \end{aligned}\right\} \tag{4}$$

To introduce the local variations of the velocity components, we consider u, v, w as functions of x, y, z, and t. With this understanding we write the identity

$$\frac{du}{dt} = \frac{\partial u}{\partial x}\frac{dx}{dt} + \frac{\partial u}{\partial y}\frac{dy}{dt} + \frac{\partial w}{\partial z}\frac{dz}{dt} + \frac{\partial u}{\partial t}, \tag{5}$$

where dx/dt, for example, represents the time variation of the position x of the liquid parallelepiped; that is, the velocity component u, and

$\partial u/\partial t$ represents the time variation of u at the fixed point (x, y, z). Interpreting the quantities dy/dt and dz/dt in the same manner, we write from eq 5:

$$\left.\begin{aligned}\frac{du}{dt}&=\frac{\partial u}{\partial t}+u\frac{\partial u}{\partial x}+v\frac{\partial u}{\partial y}+w\frac{\partial u}{\partial z}.\\ \text{Similarly,}\\ \frac{dv}{dt}&=\frac{\partial v}{\partial t}+u\frac{\partial v}{\partial x}+v\frac{\partial v}{\partial y}+w\frac{\partial v}{\partial z},\\ \text{and}\\ \frac{dw}{dt}&=\frac{\partial w}{\partial t}+u\frac{\partial w}{\partial x}+u\frac{\partial w}{\partial y}+w\frac{\partial w}{\partial z}.\end{aligned}\right\} \tag{6}$$

It should be noted that du/dt represents the acceleration of a particular element of the fluid followed in its motion relative to the axes x, y, z. The symbol d/dt has in general this significance.

2. DISPLACEMENT AND DEFORMATION OF A LIQUID ELEMENT

We consider the same elementary parallelepiped, $\delta x\ \delta y\ \delta z$, having its corner nearest the origin at the point (x, y, z). Designating the component velocities at some instant at the point (x, y, z) by u, v, w, we find for the relative velocities at the point $(x+\delta x, y+\delta y, z+\delta z)$ at the same instant, by Taylor's theorem,

$$\left.\begin{aligned}\delta u&=\frac{\partial u}{\partial x}\delta x+\frac{\partial u}{\partial y}\delta y+\frac{\partial u}{\partial z}\delta z,\\ \delta v&=\frac{\partial v}{\partial x}\delta x+\frac{\partial v}{\partial y}\delta y+\frac{\partial v}{\partial z}\delta z,\\ \text{and}\\ \delta w&=\frac{\partial w}{\partial x}\delta x+\frac{\partial w}{\partial y}\delta y+\frac{\partial w}{\partial z}\delta z.\end{aligned}\right\} \tag{7}$$

If we write

$$\left.\begin{aligned}&\epsilon_1=\frac{\partial u}{\partial x},\ \epsilon_2=\frac{\partial v}{\partial y},\ \epsilon_3=\frac{\partial w}{\partial z},\\ &\gamma_1=\frac{\partial w}{\partial y}+\frac{\partial v}{\partial z},\ \gamma_2=\frac{\partial u}{\partial z}+\frac{\partial w}{\partial x},\ \gamma_3=\frac{\partial v}{\partial x}+\frac{\partial u}{\partial y},\\ \text{and}\\ &\xi=\frac{\partial w}{\partial y}-\frac{\partial v}{\partial z},\ \eta=\frac{\partial u}{\partial z}-\frac{\partial w}{\partial x},\ \zeta=\frac{\partial v}{\partial x}-\frac{\partial u}{\partial y},\end{aligned}\right\} \tag{8}$$

the relative velocities may be written

$$\left.\begin{aligned}\delta u&=\epsilon_1\delta x+\frac{1}{2}(\gamma_3\delta y+\gamma_2\delta z)+\frac{1}{2}(\eta\delta z-\zeta\delta y),\\ \delta v&=\epsilon_2\delta y+\frac{1}{2}(\gamma_1\delta z+\gamma_3\delta x)+\frac{1}{2}(\zeta\delta x-\xi\delta z),\\ \text{and}\\ \delta w&=\epsilon_3\delta z+\frac{1}{2}(\gamma_2\delta x+\gamma_1\delta y)+\frac{1}{2}(\xi\delta y-\eta\delta x).\end{aligned}\right\} \tag{9}$$

The following physical interpretation is now evident. The motion of an elementary parallepiped having the point (x, y, z) for its corner nearest the origin may be considered as made up of three parts. The first part represents a motion of translation of the whole element with the component velocities u, v, w. The second part represents the relative displacement of the particles within the parallelepiped and describes its deformation. The *linear dilatations* ϵ_1, ϵ_2, ϵ_3 give the rate of increase of the edges of the element δx, δy, δz, respectively, during the motion. The *angular dilatations* γ_1, γ_2, γ_3 give the rate of change of the angles of the edges of the parallepiped, taken two at a time. The third part represents a rotation of the whole element about an instantaneous axis having as components the angular velocities $(1/2)\ \xi$, $(1/2)\ \eta$, $(1/2)\ \zeta$. The vector (ξ, η, ζ) is referred to as the *vorticity* of the liquid at the point (x, y, z).

When, throughout a finite portion of a fluid mass, the component vorticities ξ, η, ζ vanish, the motion of that portion is called *irrotational*.

3. KINEMATICAL RELATIONS

Since ϵ_1, ϵ_2, ϵ_3 are the rates of dilation of the edges of a cubical element, it can be readily shown that the change, dV, of the volume of the liquid mass, $\Delta V = \delta x\, \delta y\, \delta z$, due to the displacement of the particles per unit time is

$$dV = (\epsilon_1 + \epsilon_2 + \epsilon_3) V. \tag{10}$$

We also have the relation,

$$\rho_0 V = (\rho_0 + \Delta\rho)(V + dV), \tag{11}$$

derived from the principle of conservation of mass. ρ_0 is the initial density of liquid and $\Delta\rho$ the change in the density during the motion of the element. If the liquid is incompressible, $\Delta\rho = 0$, and we obtain from eq 11, $dV = 0$, and from eq 10

$$\frac{\partial u}{\partial x} + \frac{\partial v}{\partial y} + \frac{\partial w}{\partial z} = 0, \tag{12}$$

which is a kinematical relation that is satisfied in the region occupied by an incompressible liquid. Equation 12 is known as the *equation of continuity* for an incompressible liquid.

At the boundary of the liquid the equation of continuity is replaced by a different relation. We shall consider the relation in its most general form. Let $F(x, y, z, t) = 0$ be the equation of the bounding surface. Let u, v, w be the velocity components of a liquid particle on the boundary, having the position (x, y, z) at time t. At time $t + \Delta t$ the position of the particle is

$$(x + u\Delta t,\ y + v\Delta t,\ z + w\Delta t).$$

Since the particle does not leave the boundary [4, p. 7], we must have, because of the equation of the boundary,

$$F(x + u\Delta t,\ y + v\Delta t,\ z + w\Delta t,\ t + \Delta t) = 0.$$

When the latter expression is expanded by means of Taylor's theorem, we obtain the relation

$$\frac{dF}{dt} = \frac{\partial F}{\partial t} + u\frac{\partial F}{\partial x} + v\frac{\partial F}{\partial y} + w\frac{\partial F}{\partial z} = 0, \tag{13}$$

which is the general boundary condition.

Two special forms are to be noted. At a fixed boundary

$$lu+mv+nw=0, \tag{14}$$

where l, m, n represent the direction cosines of the normal to the boundary. At a surface of discontinuity

$$l(u_1-u_2)+m(v_1-v_2)+n(w_1-w_2)=0, \tag{15}$$

where the suffixes are used to distinguish the velocities at the two sides of the surface.

4. IRROTATIONAL MOTION

In a large and important class of hydrodynamical phenomena, the vorticities ξ, η, ζ vanish—that is:

$$\left.\begin{aligned} \xi&=\frac{\partial w}{\partial y}-\frac{\partial v}{\partial z}=0, \\ \eta&=\frac{\partial u}{\partial z}-\frac{\partial w}{\partial x}=0, \\ \text{and}\quad \zeta&=\frac{\partial v}{\partial x}-\frac{\partial u}{\partial y}=0. \end{aligned}\right\} \tag{16}$$

As a result of this restriction, the expressions for the velocity components, u, v, w, are very much simplified.

We consider now the function ϕ, defined by the differential equation

$$-d\phi=udx+vdy+wdz. \tag{17}$$

According to a theorem in differential equations, the necessary and sufficient conditions for $d\phi$ to be an exact differential, that is, for $d\phi$ to be expressed as

$$d\phi=\frac{\partial \phi}{\partial x}dx+\frac{\partial \phi}{\partial y}dy+\frac{\partial \phi}{\partial z}dz, \tag{18}$$

are the relations in eq 16. Comparing eq 18 with eq 17, we write for the velocity components of a liquid particle of zero vorticity:

$$\left.\begin{aligned} u&=-\frac{\partial \phi}{\partial x}, \\ v&=-\frac{\partial \phi}{\partial y}, \\ \text{and}\quad w&=-\frac{\partial \phi}{\partial z}. \end{aligned}\right\} \tag{19}$$

The function ϕ is called a *velocity potential* from its analogy with potentials arising in some other branches of physics. As the velocity potential exists if and only if the flow is irrotational, the latter flow is also called *potential flow*.

If the liquid, in addition to being in irrotational motion, is also incompressible, then the velocity potential ϕ satisfies Laplace's equation,

$$\frac{\partial^2 \phi}{\partial x^2}+\frac{\partial^2 \phi}{\partial y^2}+\frac{\partial^2 \phi}{\partial z^2}=0. \tag{20}$$

This can be seen by substituting the expressions for the velocities given in eq 19 in the equation of continuity, eq 12. Thus, for the conditions of flow assumed here, (the irrotational motion of an incompressible liquid) the complete determination of the velocities at all points reduces to the selection of the harmonic function ϕ satisfying the boundary conditions.

5. INVARIANCE OF THE CIRCULATION IN A MOVING CIRCUIT

The following theorem on irrotational motion is of great importance: *If the motion of any portion of a perfect fluid is irrotational at any one moment, it will continue to be irrotational, provided the external forces have a potential and the density of the fluid be either constant or a function of pressure only.*

One of the methods for establishing the theorem is to consider the circulation around a closed curve of particles and inquire into the variation of the circulation as the particles of the curve move into new positions. By the *circulation* around the circuit, C, is meant the line integral at any time, t,

$$\Gamma = \oint_c (udx+vdy+wdx), \tag{21}$$

of the velocity vector taken around C, a closed path of particles in the liquid. The circulation of the circuit of the same particles at time $t+dt$ is

$$\Gamma+\frac{d\Gamma}{dt}dt,$$

where

$$\frac{d\Gamma}{dt} = \oint_c \frac{d}{dt}(udx+vdy+wdz). \tag{22}$$

To evaluate $d\Gamma/dt$ we take an element of circuit C of length δs and consider the time-rate of variation of the quantity $u\delta x$ as the particles on the element move into new positions. Differentiating the product $u\delta x$, we obtain

$$\frac{d}{dt}(u\delta x) = \frac{du}{dt}\delta x + u\frac{d}{dt}\delta x. \tag{23}$$

The first term in the right-hand member contains the x component of the acceleration of a particle on ds, given by the first of the following dynamical equations of motion

$$\left.\begin{aligned} \frac{du}{dt} &= -\frac{1}{\rho}\frac{\partial p}{\partial x} - \frac{\partial \Omega}{\partial x}, \\ \frac{dv}{dt} &= -\frac{1}{\rho}\frac{\partial p}{\partial y} - \frac{\partial \Omega}{\partial y}, \\ \frac{dw}{dt} &= -\frac{1}{\rho}\frac{\partial p}{\partial z} - \frac{\partial \Omega}{\partial z}. \end{aligned}\right\} \tag{24}$$

and

Here p is the pressure, ρ the density of liquid, and Ω the potential of the external forces at the point under consideration. The second term is readily transformed into

$$u\frac{d}{dt}(\delta x)=u\delta\frac{dx}{dt}=u\delta u, \tag{25}$$

since dx/dt is the velocity u. Thus,

$$\left.\begin{aligned}\frac{d}{dt}(u\delta x)&=-\frac{1}{\rho}\frac{\partial p}{\partial x}\delta x-\frac{\partial\Omega}{\partial x}\delta x+u\delta u,\\ \text{and similarly}\\ \frac{d}{dt}(v\delta y)&=-\frac{1}{\rho}\frac{\partial p}{\partial y}\delta y-\frac{\partial\Omega}{\partial y}\delta y+v\delta v,\\ \text{and}\\ \frac{d}{dt}(w\delta z)&=-\frac{1}{\rho}\frac{\partial p}{\partial z}\delta z-\frac{\partial\Omega}{\partial z}\delta z+w\delta w.\end{aligned}\right\} \tag{26}$$

Introducing eq 26 into eq 22, we obtain

$$\frac{d\Gamma}{dt}=-\oint_c\frac{dp}{\rho}-\oint_c d\,\Omega+\frac{1}{2}\oint_c dq^2, \tag{27}$$

where $q^2=u^2+v^2+w^2$. Since Ω and q^2 are single-valued, continuous functions of x, y, z, the last two integrals in the right-hand member of the equation vanish. If ρ is a single-valued, nonvanishing, continuous function of p only, or a constant, then the first integral vanishes also. Hence, under these circumstances

$$\frac{d\Gamma}{dt}=0; \tag{28}$$

that is, the circulation around a circuit moving with the liquid remains unaltered.

By using Stokes' theorem, the circulation, Γ, around circuit C, may be related to the vorticity of the liquid particles on a surface S bounded by C. Stokes' theorem states that the line integral of any vector around a closed curve is equivalent to the flux of the curl of the vector through any surface bounded by the closed curve. Using this theorem, we now write

$$\Gamma=\int_s(l\xi+m\eta+n\zeta)dS, \tag{29}$$

where l, m, n are the direction cosines of the normal drawn inward from the surface.

It now follows from eq 28 and 29 that the property of irrotationality of a portion of the fluid is carried with the fluid. For, if initially ξ, η, ζ vanish in a region containing a fluid, then the circulation for any circuit in the same region vanishes. This is true at all subsequent times in the region containing the same particles, by eq 28 above, and the vorticities consequently remain equal to zero.

The restrictions under which the main theorem, expressed by eq 28, has been proven must be remembered. It is assumed that the external body forces have a potential, and that the density is either constant or a function of pressure only. The latter condition is violated, for example, in the case of convection currents generated by a temperature gradient. Since in the dynamical eq 24, which were employed in the proof, the viscosity terms are missing, another restriction is the condition that the effects of viscous forces are negligible in comparison with inertial forces.

6. IMPULSIVE GENERATION OF MOTION

When the boundary conditions of a mass of liquid are suddenly changed, a sudden alteration in the motion may take place. The forces introduced are of the nature of impulsive pressures, and, during the time interval that the impulses last, the effects of all the other forces are negligible.

Let ρ be the density, u_0, v_0, w_0 the components of velocity immediately before, u', v', w' those immediately after the application of the impulse, $\bar{\omega}$ the impulsive pressure at the point (x, y, z). The change of momentum parallel to x of an elementary rectangular parallelepiped having edges δx, δy, δz, and with its corner nearest the origin at (x, y, z), is $\rho\delta x\delta y\delta z(u'-u_0)$; the resultant impulsive pressure in the same direction is $-\frac{\partial\bar{\omega}}{\partial x}\delta x\delta y\delta z$. Hence,

$$\rho\delta x\delta y\delta z(u'-u_0)=-\frac{\partial\bar{\omega}}{\partial x}\delta x\delta y\delta z,$$

or

$$\left.\begin{aligned} u'-u_0&=-\frac{1}{\rho}\frac{\partial\bar{\omega}}{\partial x}\cdot\\ \text{Similarly}\qquad v'-v_0&=-\frac{1}{\rho}\frac{\partial\bar{\omega}}{\partial y},\\ \text{and}\qquad w'-w_0&=-\frac{1}{\rho}\frac{\partial\bar{\omega}}{\partial z}\cdot \end{aligned}\right\} \tag{30}$$

In these relations we have a physical interpretation of the velocity potential, ϕ. For, consider the case where u_0, v_0, w_0 are zero. A state of motion for which a velocity potential exists could be produced from rest by the application of a properly chosen system of impulsive pressures. If ϕ be the velocity potential, the desired system of impulsive pressures is $\bar{\omega}=\rho\phi+C$. The arbitrary constant in this expression shows that a uniform pressure throughout a liquid mass has no effect on the motion. If the initial state of motion be uniform, that is, if for the initial state of motion the liquid possesses the velocity potential $\phi_0=u_0x+v_0y+w_0z$, then the new state of motion possessing the velocity potential ϕ may be produced from the initial motion by the application of the impulsive pressures $\bar{\omega}=\rho(\phi-\phi_0)+C$.

7. PRESSURE EQUATION

In a case of irrotational motion the velocity potential, ϕ, determines the velocity components u, v, w, but the hydrodynamical solution of the flow is not complete as long as the pressures are unknown. The determination of the pressures is made by means of the pressure equation, which is a dynamic relation to be derived presently.

Since the motion is irrotational, the velocities u, v, w in the dynamical equations,

$$\left.\begin{aligned}\frac{du}{dt}&=-\frac{1}{\rho}\frac{\partial p}{\partial x}-\frac{\partial \Omega}{\partial x},\\ \frac{dv}{dt}&=-\frac{1}{\rho}\frac{\partial p}{\partial y}-\frac{\partial \Omega}{\partial y},\end{aligned}\right\} \tag{24}$$

and

$$\frac{dw}{dt}=-\frac{1}{\rho}\frac{\partial p}{\partial z}-\frac{\partial \Omega}{\partial z},$$

where the operator d/dt is

$$\frac{d}{dt}=\frac{\partial}{\partial t}+u\frac{\partial}{\partial x}+v\frac{\partial}{\partial y}+w\frac{\partial}{\partial z}, \tag{31}$$

may be expressed in terms of the velocity potential, ϕ. The dynamical equations are transformed into

$$\left.\begin{aligned}-\frac{\partial^2\phi}{\partial x\partial t}+\frac{1}{2}\frac{\partial}{\partial x}q^2&=-\frac{\partial \Omega}{\partial x}-\frac{1}{\rho}\frac{\partial p}{\partial x},\\ -\frac{\partial^2\phi}{\partial y\partial t}+\frac{1}{2}\frac{\partial}{\partial y}q^2&=-\frac{\partial \Omega}{\partial y}-\frac{1}{\rho}\frac{\partial p}{\partial y},\end{aligned}\right\} \tag{32}$$

and

$$-\frac{\partial^2\phi}{\partial z\partial t}+\frac{1}{2}\frac{\partial}{\partial z}q^2=-\frac{\partial \Omega}{\partial z}-\frac{1}{\rho}\frac{\partial p}{\partial z}.$$

Multiplying the first by dx, the second by dy, the third by dz, adding, and then integrating the sum, we obtain the integral

$$\int\frac{dp}{\rho}=\frac{\partial\phi}{\partial t}-\Omega-(1/2)q^2+f(t), \tag{33}$$

where $f(t)$ is an arbitrary function of time. This equation makes it possible to determine the pressure, once the velocity potential ϕ is known; it is called the *pressure equation*.

For an incompressible liquid,

$$\frac{p}{\rho}=\frac{\partial\phi}{\partial t}-\Omega-\frac{1}{2}q^2+f(t). \tag{34}$$

To determine the arbitrary function $f(t)$ we must know p and ϕ as functions of t at some definite point in the region occupied by the liquid. Generally this point is one where $\partial\phi/\partial t$ vanishes, q is a constant, and p is the atmospheric pressure p_a.

8. SOLUTION OF PROBLEMS IN IRROTATIONAL MOTION

The mathematical procedure for solving a problem of the irrotational motion of an incompressible liquid bounded in part by fixed boundaries and in part by a free surface consists in finding a harmonic function, $\phi(x,y,z,t)$, which satisfies Laplace's equation (eq 20) in the region occupied by the liquid, and the following surface conditions.

At the free surface, if it exists, there are two conditions to be satisfied. If $F(x,y,z,t)$ is the equation of the surface, we have

$$\frac{\partial F}{\partial t}+u\frac{\partial F}{\partial x}+v\frac{\partial F}{\partial y}+w\frac{\partial F}{\partial z}=0, \tag{13}$$

where u, v, w are the velocities at the surface. The second condition states that the pressure is atmospheric at the free surface; we then have from eq 34

$$p_a/\rho=\frac{\partial \phi}{\partial t}-\Omega-\frac{1}{2}q^2+f(t). \tag{35}$$

At the fixed boundaries,

$$\frac{\partial \phi}{\partial n}=0, \tag{36}$$

n being the normal drawn to the boundary.

The function, ϕ, which satisfies eq 13, 20, 35, and 36 is unique, except for an additive constant. For references to proofs see [4, p. 59].

III. FORMULATION OF THE WAVE PROBLEM—WAVES IN WATER OF SMALL DEPTH

We consider a rectangular horizontal channel of uniform cross-section and infinite length, containing a perfect liquid initially at rest. We assume that some external agency acting for a short time produces a deformation of the free surface of the liquid in the channel. If the action of the external agency is such that the associated forces exerted on a portion of the water in the channel are essentially in the direction parallel to the direction of the channel and are constant throughout the whole depth of the liquid, the particles in a normal section under the deformed surface will be moving with a constant velocity. Under these conditions the deformed free surface constitutes a translation wave.

The liquid of the channel being initially at rest, we infer from the theorems previously explained that the resulting motion of the liquid under the deformed free surface is irrotational and possesses a velocity potential, ϕ. Let the axis of x be drawn in the bottom plane of the channel parallel to the channel axis; let the axis of z be drawn upwards. Denoting the velocity components in the direction of x and z by u and w, respectively, we have

$$u=-\frac{\partial\phi}{\partial x}, \tag{37}$$

and

$$w=-\frac{\partial\phi}{\partial z}, \tag{38}$$

where ϕ is a function of x, z, and t and satisfies Laplace's equation

$$\frac{\partial^2\phi}{\partial x^2}+\frac{\partial^2\phi}{\partial z^2}=0. \tag{39}$$

The pressure equation (35) reduces to

$$\frac{p}{\rho}=\frac{\partial\phi}{\partial t}-gz-\frac{1}{2}(u^2+w^2)+F(t), \tag{40}$$

where g is the intensity of gravity.

Let the z coordinate of the free surface be denoted by $h+H$, where H is the initial undisturbed depth of water in the channel, and h is the elevation (or depression) of the wave.

To evaluate $F(t)$, let us consider the point at infinity on the free surface; at such a point $\partial\phi/\partial t=u=w=h=0$, $z=H$, and $p=p_a$. Substituting in eq 40 there results

$$F(t)=\frac{p_a}{\rho}+gH.$$

At the surface, since $p=p_a$, we obtain the dynamical surface condition from eq 40, neglecting the effect of surface tension:

$$\frac{\partial\phi}{\partial t}-gh-\frac{1}{2}(u^2+w^2)=0,\ z=H+h. \tag{41}$$

Although the last equation has been derived for the case where the liquid at infinity is at rest, it is equally applicable to the case where u^2+w^2 and $\partial\phi/\partial t$ vanish at the points on the surface where $h=0$, as, for example, in an intumescence consisting of an infinite number of undulations of the same dimensions moving without change of form.

We obtain the kinematic surface condition, that a fluid particle of the free surface always remains on the free surface, by substituting $F(x,y,z,t)=z-H-h=0$ in eq 13, obtaining

$$w=\frac{\partial h}{\partial t}+u\frac{\partial h}{\partial x},\ z=H+h. \tag{42}$$

At the bottom surface of the channel the velocity component normal to the bottom vanishes, that is, at $z=0$,

$$\frac{\partial\phi}{\partial z}=0. \tag{43}$$

In view of this last condition, we adopt for the potential ϕ the power series

$$\phi=\sum_{n=0}^{\infty}\phi_n z^n,\ \phi_1=0, \tag{44}$$

where ϕ_n is a function of x and t only. Substituting this expression for ϕ in eq 39, and equating the coefficients of z^n to zero, term by term, we arrive at the convergent series

$$\phi=\phi_0-\frac{z^2}{2!}\frac{\partial^2\phi_0}{\partial x^2}+\frac{z^4}{4!}\frac{\partial^4\phi_0}{\partial x^4}-\frac{z^6}{6!}\frac{\partial^6\phi_0}{\partial x^6}+\cdots. \tag{45}$$

Differentiating with respect to z,

$$\frac{\partial\phi}{\partial z}=-z\frac{\partial^2\phi_0}{\partial x^2}+\frac{z^3}{3!}\frac{\partial^4\phi_0}{\partial x^4}-\frac{z^5}{5!}\frac{\partial^6\phi_0}{\partial x^6}+\cdots. \tag{46}$$

The function ϕ_0, as stated above, depends only on x and t. If we denote the velocity of particles of water at the bottom of the channel at x by u_0, then

$$\phi_0=(\phi_0)_\infty-\int_x^\infty\frac{\partial\phi_0}{\partial x}dx=(\phi_0)_\infty+\int_x^\infty u_0dx, \tag{47}$$

where $(\phi_0)_\infty$ is the value of ϕ at $x=\infty$. Since the liquid in the channel at infinity is at rest, we may take the value of $(\phi_0)_\infty$ as zero: then,

$$\phi_0=\int_x^\infty u_0dx. \tag{48}$$

In the above formulation, h and ϕ_0 are functions specifying a translation wave. They can be determined by integrating the two simultaneous differential eq 41 and 42 representing the dynamical and kinematical surface conditions.

IV. LONG WAVES OF NEGLIGIBLE HEIGHT AND CURVATURE

1. VELOCITY OF PROPAGATION

If u^2 and w^2 are negligible in comparison with gh (assumptions I, II) and $u\partial h/\partial x$ in comparison with $\partial h/\partial t$ (assumption III), then the surface conditions given by eq 41 and 42 reduce to

$$gh-\frac{\partial\phi}{\partial t}=0, \tag{49}$$

and

$$\frac{\partial\phi}{\partial z}+\frac{\partial h}{\partial t}=0. \tag{50}$$

Also, if in the expansions of ϕ and $\partial\phi/\partial z$ given in eq 45 and 46, only the first term is retained (assumption IV), we have

$$\phi=\phi_0, \tag{51}$$

and

$$\frac{\partial\phi}{\partial z}=-z\frac{\partial^2\phi_0}{\partial x^2}. \tag{52}$$

198881—40——5

Here, then, we have the basis for a first approximation to a solution of a wave configuration. The horizontal component of the velocity in a normal section is constant and equals the bottom velocity u_0; the vertical component varies linearly with z.

Substituting eq 51 and 52 in eq 49 and 50, we obtain

$$gh-\frac{\partial\phi_0}{\partial t}=0, \tag{53}$$

and

$$-H\frac{\partial^2\phi_0}{\partial x^2}+\frac{\partial h}{\partial t}=0, \tag{54}$$

assuming that h is small in comparison with H and hence can be neglected (assumption V). Eliminating ϕ_0 from eq 53 and 54, we obtain the differential equation

$$\frac{\partial^2 h}{\partial t^2}=c^2\frac{\partial^2 h}{\partial x^2}, \tag{55}$$

where

$$c=\sqrt{gH}. \tag{56}$$

Eliminating h similarly and writing

$$u_0=-\frac{\partial\phi_0}{\partial x}, \tag{57}$$

there results for u_0 the relation

$$\frac{\partial^2 u_0}{\partial t^2}=c^2\frac{\partial^2 u_0}{\partial x^2}. \tag{58}$$

Equations 55 and 58, which are well known, possess complete solutions, which also satisfy eq 53 and 54:

$$\frac{h}{H}=F_1(x-ct)+F_2(x+ct), \tag{59}$$

and

$$\frac{u_0}{c}=F_1(x-ct)-F_2(x+ct), \tag{60}$$

where F_1 and F_2 are two arbitrary functions.

These results have a very simple geometrical interpretation. Consider the motion represented by the function F_1 in eq 60. When x and t are increased by $c\tau$ and τ, respectively, the value of the function is not changed; the disturbance h which existed at the place x and at time t has moved during the time interval τ to the place $x+c\tau$. Therefore, the function F_1 represents a wave traveling in the positive x-direction without change of form at a constant velocity of propagation[2] $c=\sqrt{gH}$.

Similarly, F_2 represents another wave propagated in the opposite direction with the same velocity. Any motion whatever subject to the conditions assumed above for the approximate solution will be made up of waves of these types. F_1 and F_2 are determinate when

[2] The question of the meaning of velocity of propagation when the wave does not retain its form will be discussed later in section V-1.

h and u_0 are known for every value of t, and at a single point $x=x_1$; or when h and u_0 are known for every value of x and for a single time $t=t_1$.

If h and u_0 represent the surface elevation and velocity of particles in either the progressive or regressive wave (F_1 or $F_2\equiv 0$) it is seen from eq 59 and 60 that

$$u_0=\pm c\frac{h}{H}, \tag{61}$$

where the plus sign applies to a wave moving in the positive x-direction ($F_2\equiv 0$) and the minus sign to a wave moving in the negative x-direction ($F_1\equiv 0$).

We shall now examine the restrictions assumed in obtaining our approximate solution:

$$u^2 \ll gh, \tag{I}$$

$$w^2 \ll gh, \tag{II}$$

and

$$u\frac{\partial h}{\partial x} \ll \frac{\partial h}{\partial t}. \tag{III}$$

The two series converge rapidly; that is,

$$\frac{z^2}{2!}\frac{\partial^2\phi_0}{\partial x^2} \ll \phi_0, \tag{IV}$$

and

$$\frac{h}{H} \ll 1. \tag{V}$$

It can be demonstrated that the following physical restrictions lead to the above mathematical assumptions:

(A) The ratio of the wave amplitude to the depth of the channel is small: $(h/H) \ll 1$.

(B) The slope of the wave is small: $(\partial h/\partial x) \ll 1$.

(C) The radius of curvature of the waves is large with respect to $H^2/2h$.

2. ENERGY OF AN INTUMESCENCE

A single wave is called an *intumescence*. The potential energy per unit width of an intumescence, at time t, due to the elevation or depression of the fluid surface above or below the level of the previously undisturbed liquid in a channel is

$$\frac{g\rho}{2}\int_{x_1}^{x_2} h^2 dx, \tag{62}$$

where x_1 and x_2 denote the extremities of the intumescence. The kinetic energy per unit width of the liquid under the free surface of the intumescence is

$$\frac{\rho H}{2}\int_{x_1}^{x_2} u_0^2 dx. \tag{63}$$

Substituting for u_0 its value in eq 61, eq 63 becomes

$$\frac{\rho g}{2}\int_{x_1}^{x_2} h^2\,dx. \tag{64}$$

Comparing eq 64 and 62, it is seen that the potential and kinetic energy of an intumescence are equal and that the total energy is

$$g\rho\int_{x_1}^{x_2} h^2\,dx. \tag{65}$$

The integral in eq 65 without the multiplier $g\rho$ will be of special interest, and will be subsequently referred to as the energy, E, of an intumescence.

3. DISPLACEMENT OF THE PARTICLES

The liquid particles in the cross section at x, before the arrival of an intumescence, are at rest. At the moment when the intumescence is passing, the particles in the section are moving with the velocity u_0, to a first approximation. Thus, the volume of flow through the section during the passage of the intumescence is

$$V=\int_{t_1}^{t_2} u_0 H dt. \tag{66}$$

Since

$$c\,dt=dx, \tag{67}$$

we have

$$V=\int_{x_1}^{x_2}\frac{u_0 H}{C}dx. \tag{68}$$

Substituting for u_0 from eq 61, we obtain

$$V=\int_{x_1}^{x_2} h dx. \tag{69}$$

The volume of flow through a cross section equals the volume of the intumescence. Hence, during the passage of an intumescence, the particles in a cross section are moved forward a distance δx, the magnitude of which is given by the ratio of the volume of the intumescence to the area of the channel cross section.

4. EFFECT OF AN ARBITRARY INITIAL DISTURBANCE

If for $t=0$ the velocity of the liquid particles in the channel and the form of the disturbed surface are known:

$$\frac{u}{c}=\theta(x),\ -\infty<x<+\infty, \tag{70}$$

and

$$\frac{h}{H}=\psi(x),\ -\infty<x<+\infty, \tag{71}$$

then the functions F_1 and F_2 occurring in eq 59 and 60 are

$$\left.\begin{aligned} F_1(x) &= \frac{1}{2}[\theta(x)+\psi(x)], \\ \text{and} \\ F_2(x) &= \frac{1}{2}[-\theta(x)+\psi(x)]. \end{aligned}\right\} \tag{72}$$

To determine the form of the wave profile, $h/H=\psi(x,t_1)$ for any subsequent time, $t=t_1$, the curve representing $F_1(x)$ is displaced in the positive x-direction by a distance ct_1, the curve representing $F_2(x)$ by the same distance in the opposite direction, and the ordinates of the two displaced curves are added algebraically.

Consider disturbances confined initially to a finite segment of the channel of length l. Resolution of the initial disturbance into F_1 and F_2 indicates that after the lapse of the time interval $\tau=c/2$, two waves of equal length l will be traveling in opposite directions. In general, resolved waves will have unequal heights at corresponding points. If, however, in the initial state, $u=0$, that is, $\theta(x)\equiv 0$, then $F_1(x)\equiv F_2(x)$, and the two component waves have the same shape. If, on the other hand, $u=\pm ch/H$ initially, then either F_1 or F_2 is zero, and the result is a single wave traveling in one direction.

5. REFLECTION AND TRANSMISSION OF WAVES

A wave is reflected when it reaches a barrier in a channel. We take the origin, $x=0$, at the barrier and note that $u=0$ at the barrier. Utilizing this fact in the general eq 60, we obtain the condition that

$$F_1(-ct)=F_2(+ct) \tag{73}$$

for the incident and reflected waves.

Applying this last condition to the general eq 59 and 60, we obtain

$$\frac{h}{H}=F_2(ct-x)+F_2(ct+x), \tag{74}$$

and

$$\frac{u_0}{c}=F_2(ct-x)-F_2(ct+x), \tag{75}$$

which are the equations for reflected waves or for identical waves traveling in opposite directions. Here, if $F_2(ct+x)$ is taken as the incident wave, $F_2(ct-x)$ will be the reflected wave. At $x=x_1$, and $t=t_1$, the elevation or depression of the wave is

$$\frac{h}{H}=F_2(ct_1+x_1). \tag{76}$$

The corresponding elevation or depression of the reflected wave will reach the point $x=x_1$ at the time $t=t_1+2x_1/c$, and the value of the elevation or depression is

$$\frac{h}{H}=F_2(c\{t_1+2x_1/c\}-x_1)=F_2(ct_1+x_1). \tag{77}$$

Hence, elevations and depressions are reflected without change. It can be shown in a similar manner that corresponding velocities are reversed with their magnitudes unchanged.

When a wave reaches a point in a channel where there is an abrupt change in the cross section of the channel, either in width or in depth, a part of the approaching wave is transmitted and a part is reflected. Taking the origin at the point of the abrupt change of section, we may write from the general eq 59 and 60 for the side from which the wave approaches, moving in the positive x-direction,

$$\frac{h_1}{H_1}=F(x-c_1t)+f(c_1t+x), \tag{78}$$

and

$$\frac{u_1}{c_1}=F(x-c_1t)-f(c_1t+x), \tag{79}$$

in which the first term in the right member of each equation applies to the approaching wave, and the second term to the reflected wave.

For the transmitted wave we have

$$\frac{h_2}{H_2}=g(x-c_2t), \tag{80}$$

and

$$\frac{u_2}{c_2}=g(x-c_2t). \tag{81}$$

In the above equations H_1 and H_2 are the depths of the channel on the two sides of $x=0$, and c_1 and c_2 the velocities of propagation for the corresponding portions of the channel. At $x=0$, $h_1=h_2$, since the surface is continuous, and therefore,

$$H_1[F(-c_1t)+f(c_1t)]=H_2g(-c_2t). \tag{82}$$

Also, the conservation of matter requires that $B_1H_1u_1=B_2H_2u_2$, where B_1 and B_2 are the widths of the channel on the two sides of $x=0$. This condition gives

$$B_1H_1c_1[F(-c_1t)-f(c_1t)]=B_2H_2c_2g(-c_2t). \tag{83}$$

We deduce from eq 83 and 84 the ratio of the elevations in the corresponding parts of the reflected and incident waves and of the transmitted and incident waves. These are

$$\frac{f}{F}=\frac{B_1c_1-B_2c_2}{B_1c_1+B_2c_2}, \tag{84}$$

and

$$\frac{g}{F}=\frac{2B_1c_1H_1}{(B_1c_1+B_2c_2)H_2}, \tag{85}$$

respectively.

A wave traveling in a channel connected to a body of water in a basin of infinite depth and width may be considered as a special case. For this case it is evident by inspection that $g/F=0$ and $f/F=-1$. Hence the incident wave is completely reflected at the juncture, and the elevations are reflected as depressions.

V. WAVES OF APPRECIABLE HEIGHT AND CURVATURE

1. TWO DEFINITIONS OF VELOCITY OF PROPAGATION

For long waves of infinitesimal height, the concept of velocity of propagation entails no ambiguity, because such waves are propagated without change of form. However, when a traveling wave is undergoing deformation, the meaning of velocity of propagation must be clearly defined. We may adopt either of two distinct definitions. The first definition will be developed on a purely formal basis. In a given wave system we consider the quantities $\partial h/\partial t$ and $\partial h/\partial x$ for an arbitrary x and t, and write the following relation from eq 13:

$$\frac{\partial h}{\partial t}+\omega_1\frac{\partial h}{\partial x}=0,\ h=h(x,t). \tag{86}$$

In effect, this relation defines the quantity ω_1, which we may call the *velocity of propagation of a wave-height element.* When the traveling wave is undergoing a change of form at a given instant, t, ω_1 is a function of h.

A second definition, which is due to Boussinesq, considers the volume of an intumescence. The volume of an intumescence is the quantity of liquid in the entire intumescence between the free surface and the undisturbed primitive level of the liquid in channel. We have, therefore

$$\Sigma=\int_{x_0}^{\infty} h dx, \tag{87}$$

where x_0 is the rear of the intumescence, assumed moving in the positive x-direction. The intumescence may be limited posteriorly; that is, for all values of $x\leqq x_0$, h is negligible, and in this case Σ has a finite value. On the other hand, the intumescence may be unlimited; in this case we consider the volume, Σ, included between the head and an abscissa, x_0, considerably removed from the head, and moving in such a way that Σ remains constant.

We now consider a partial volume, σ, of Σ, between the head of the intumescence and an abscissa, x:

$$\sigma=\int_{x}^{\infty} h dx,\ x\leqq x_0. \tag{88}$$

We assume that a plane originally at x moves in such a way that it always has in front of it the same partial volume σ of the intumescence. We refer to the velocity at which this plane moves as the *velocity of propagation of an element of volume of an intumescence,* and denote this velocity by ω.

The relation between ω and h may be obtained from eq 88 by differentiating the right-hand member of the equation with respect to t and equating to zero. However, it may be more instructive to obtain the desired relation in the following manner (see fig. 1). The curves *abc* and *a'b'c'* represent the free surface of the moving intumescence at the times t and $t+\Delta t$, respectively. A plane at x having in front of it, at time t, the partial volume, σ, of the intumescence, moves to the position $x+\omega\Delta t$ at time $t+\Delta t$ and still has the same par-

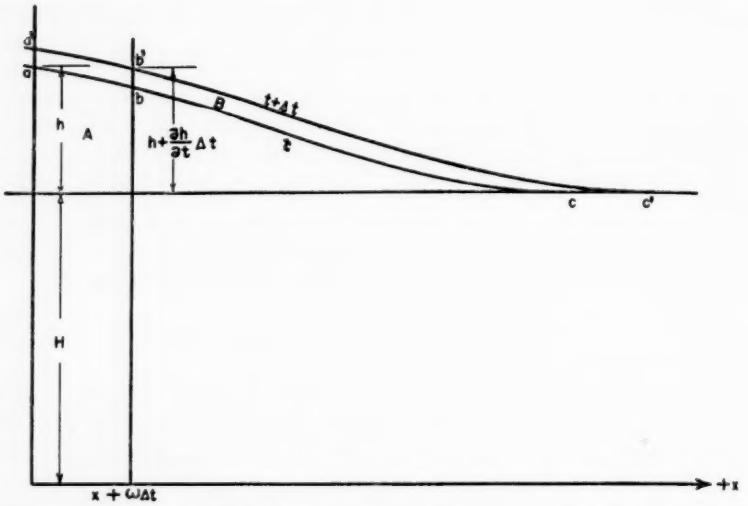

FIGURE 1.—*Diagram illustrating the velocity of propagation of a volume element.*

tial volume, σ, in front of it. The areas A and B are equal to each other. Consequently,

$$h\omega\Delta t=\int_x^\infty \frac{\partial h}{\partial t}\Delta t dx. \tag{89}$$

Dividing by Δt,

$$h\omega=\int_x^\infty \frac{\partial h}{\partial t}dx,\ x\leqq x_0,$$

and then differentiating with respect to x, we obtain

$$\frac{\partial h}{\partial t}+\frac{\partial}{\partial x}(h\omega)=0, \tag{90}$$

which is the relation connecting ω with h.

Eliminating $\partial h/\partial t$ between eq 86 and 90, we find that the difference between the two velocities of propagation is

$$\omega_1-\omega=h\frac{\partial \omega}{\partial x}\Big/\frac{\partial h}{\partial x}. \tag{91}$$

If a wave is moving without change of form, ω is constant, and the two definitions give identical values for the two velocities of propagation, a fact that is self-evident.

2. MEAN VELOCITY OF PARTICLES

If U and q, respectively, denote the mean velocity of the particles in, and the discharge through, a cross section at x, then

$$q=U(H+h) \tag{92}$$

Consider the inflow and outflow in a time interval, Δt, for the volume between two cross sections separated by a distance, Δx; Δx

and Δt having the same order of magnitude. The mean discharge at x in the time Δt is

$$q+\frac{\Delta t}{2}\frac{\partial q}{\partial t},$$

omitting infinitesimals in Δt of the second and higher orders. The volume of the inflow in the time Δt is then

$$q\Delta t+\frac{(\Delta t)^2}{2}\frac{\partial q}{\partial t}.$$

Similarly, the mean discharge at $x+\Delta x$ in the time Δt is

$$q+\frac{\partial q}{\partial x}\Delta x+\frac{\Delta t}{2}\frac{\partial q}{\partial t}$$

omitting infinitesimals in Δx and Δt of the second and higher orders. The volume of the outflow at $x+\Delta x$ in the time Δt is

$$q\Delta t+\frac{\partial q}{\partial x}\Delta x\Delta t+\frac{(\Delta t)^2}{2}\frac{\partial q}{\partial t},$$

and the accumulation of liquid in the volume is

$$-\frac{\partial q}{\partial x}\Delta x\Delta t.$$

The increase of volume of the liquid is also

$$\frac{\partial h}{\partial t}\Delta x\Delta t,$$

omitting infinitesimals of the same orders as before.

Therefore,

$$\frac{\partial q}{\partial x}=-\frac{\partial h}{\partial t}, \tag{93}$$

or from eq 92

$$\frac{\partial}{\partial x}[U(H+h)]=-\frac{\partial h}{\partial t}.$$

Substituting from eq 90

$$\frac{\partial}{\partial x}[U(H+h)]=\frac{\partial}{\partial x}(h\omega), \tag{94}$$

which when integrated becomes

$$U(H+h)=h\omega+C. \tag{95}$$

Since the liquid is assumed to be undisturbed at infinity, the constant of integration vanishes, and the equation for the mean velocity is

$$U=\frac{h\omega}{H+h}. \tag{96}$$

3. EFFECT OF CURVATURE AND HEIGHT ON VELOCITY OF PROPAGATION OF A VOLUME ELEMENT

When the ratio h/H and the curvature of the wave profile are appreciable, the first approximation is no longer satisfactory, and in such cases recourse to a second approximation becomes necessary. The method which will now be presented is due essentially to Boussinesq.

In the surface conditions, eq 41 and 42, we neglect w^2 and replace u by the value of u_0 in the first approximation, eq 61, replacing c by its value in eq 56:

$$u=\sqrt{\frac{g}{H}}h. \tag{97}$$

These conditions now become

$$gh-\frac{\partial\phi}{\partial t}+\frac{1}{2}\frac{g}{H}h^2=0, \tag{98}$$

and

$$\frac{\partial\phi}{\partial z}+\frac{\partial h}{\partial t}+\sqrt{\frac{g}{H}}h\frac{\partial h}{\partial x}=0. \tag{99}$$

Retaining the first two terms in the expressions for ϕ and $\partial\phi/\partial z$, eq 45 and 46, and neglecting h in the terms having the smaller values, we obtain

$$\phi=\phi_0-\frac{H^2}{2}\frac{\partial^2\phi_0}{\partial x^2}, \tag{100}$$

and

$$\frac{\partial\phi}{\partial z}=-(h+H)\frac{\partial^2\phi_0}{\partial x^2}+\frac{H^3}{6}\frac{\partial^4\phi_0}{\partial x^4}. \tag{101}$$

We differentiate eq 100 with respect to t, replacing $\partial\phi_0/\partial t$ in the second term of the right-hand member by its value in the first approximation given by eq 53, that is, by gh. In this manner we obtain

$$\frac{\partial\phi}{\partial t}=\frac{\partial\phi_0}{\partial t}-\frac{H^2}{2}g\frac{\partial^2 h}{\partial x^2}. \tag{102}$$

We next consider eq 101. In the right-hand member there are two small terms. In these terms we replace $\partial\phi_0/\partial x$ by its first approximation from eq 57 and 61, that is, by $-\sqrt{\frac{g}{H}}h$. In this manner, restricting ourselves to waves propagated in the positive x-direction, we obtain

$$\frac{\partial\phi}{\partial z}=-H\frac{\partial^2\phi_0}{\partial x^2}+\sqrt{\frac{g}{H}}h\frac{\partial h}{\partial x}-\frac{H^3}{6}\sqrt{\frac{g}{H}}\frac{\partial^3 h}{\partial x^3}. \tag{103}$$

Substituting from eq 102 and 103, we obtain from eq 98 and 99:

$$gh-\frac{\partial\phi_0}{\partial t}+\frac{g}{2}\left[\frac{h^2}{H}+H^2\frac{\partial^2 h}{\partial x^2}\right]=0, \tag{104}$$

and

$$\frac{\partial h}{\partial t}-H\frac{\partial^2\phi_0}{\partial x^2}+\sqrt{gH}\frac{\partial}{\partial x}\left[\frac{h^2}{H}-\frac{H^2}{6}\frac{\partial^2 h}{\partial x^2}\right]=0. \tag{105}$$

To eliminate ϕ_0 between these, we differentiate eq 104 twice with respect to x and multiply through by H, and differentiate eq 105 with respect to t. In place of actually differentiating with respect to t, however, we differentiate with respect to x and multiply[3] by $-\sqrt{gH}$. Subtracting eq 105 from eq 104, there results:

$$\frac{\partial^2 h}{\partial t^2}=gH\frac{\partial^2 h}{\partial x^2}+gH\frac{\partial^2}{\partial x^2}\left(\frac{3}{2}\frac{h^2}{H}+\frac{H^2}{3}\frac{\partial^2 h}{\partial x^2}\right), \tag{106}$$

which is the fundamental wave equation to the second approximation, in which the effects of the wave height and of curvature of wave profile are included.

Although this equation has been derived for the case where the liquid in the channel is undisturbed at infinity, it remains valid for the case where the liquid at infinity is in motion, provided $u=\sqrt{g/H}\,h$, to a first approximation (eq 97).

Equation 106 becomes integrable once with respect to x when $\partial h/\partial t$ is introduced from eq 90. Performing the integration with respect to x and remembering that h and its derivatives vanish for $x=\infty$, we obtain

$$\frac{\partial}{\partial t}(h\omega)+gH\frac{\partial h}{\partial x}+gH\frac{\partial}{\partial x}\left(\frac{3h^2}{2H}+\frac{H^2}{3}\frac{\partial^2 h}{\partial x^2}\right)=0, \tag{107}$$

which permits the determination of ω, the velocity of propagation of a wave-volume element, in terms of h and $\partial^2 h/\partial x^2$.

We adopt as an expression for ω the product

$$\omega=\sqrt{gH}(1+\epsilon), \tag{108}$$

where ϵ is a small quantity. Multiplying the two members by h and differentiating with respect to t, we obtain, remembering that ϵ is a small quantity and applying the same reasoning used in differentiating eq 105,

$$\frac{\partial}{\partial t}(h\omega)=\sqrt{gH}\frac{\partial h}{\partial t}-gH\frac{\partial}{\partial x}(\epsilon h).$$

Introducing $\partial h/\partial t$ from eq 90, this may be written,

$$\frac{\partial}{\partial t}(h\omega)=-\sqrt{gH}\frac{\partial}{\partial x}(h\omega)-gH\frac{\partial}{\partial x}(\epsilon h); \tag{109}$$

or, in view of eq 108,

$$\frac{\partial}{\partial t}(h\omega)=-gH\frac{\partial}{\partial x}[(1+2\epsilon)h]. \tag{110}$$

[3] The justification for replacing the operator $\partial/\partial t$ by $-\sqrt{gH}\,\partial/\partial x$ can be seen from the following: Assuming that the wave retains its form, that is, that $dF/dt=0$, where F is a function of $(x-ct)$, we have the relation

$$\frac{dF}{dt}=\frac{\partial F}{\partial t}+c\frac{\partial F}{\partial x}=0,$$

from which it is obvious that

$$\frac{\partial F}{\partial t}=-c\frac{\partial F}{\partial x}=-\sqrt{gH}\frac{\partial F}{\partial x}.$$

While the present discussion relates to waves that may change their form, the above relation can be applied to small terms in the wave equation, to a first approximation.

The substitution of eq 110 in eq 107 makes the latter expression immediately integrable with respect to x. Integrating, putting the constant of integration equal to zero, since h and its derivatives vanish at $x=\infty$, and then dividing by h, we find

$$2\epsilon=\frac{3}{2}\frac{h}{H}+\frac{H^2}{3h}\frac{\partial^2 h}{\partial x^2}. \tag{111}$$

Hence

$$\omega=\sqrt{gH}\left(1+\frac{3}{4}\frac{h}{H}+\frac{H^2}{6h}\frac{\partial^2 h}{\partial x^2}\right), \tag{112}$$

which is the expression for the velocity of propagation of a volume element of an intumescence moving in still water.

We next derive the expressions for u_0, the horizontal velocity component at the bottom, and u, w, the velocity components at a point having the ordinate z. To determine u_0 we consider eq 105, replacing $\partial h/\partial t$ by $-\partial(h\omega)/\partial x$ from eq 90, and then integrating with respect to x, the constant of integration being equated to zero. In this manner we obtain, since $u_0=-\partial\phi_0/\partial x$,

$$u_0=\sqrt{\frac{g}{H}}\left(h-\frac{h^2}{4H}+\frac{H^2}{3}\frac{\partial^2 h}{\partial x^2}\right). \tag{113}$$

From eq 45, after differentiating with respect to x, and from eq 46, retaining only the first two terms of the right members, we obtain:

$$u=u_0-\frac{z^2}{2}\frac{\partial^2 u_0}{\partial x^2}, \tag{114}$$

and

$$w=-z\frac{\partial u_0}{\partial x}+\frac{z^3}{6}\frac{\partial^3 u_0}{\partial x^3}, \tag{115}$$

which give, after substituting for u_0 from eq 113, and neglecting quantities of small order:

$$u=\sqrt{gH}\left[\frac{h}{H}-\frac{h^2}{4H^2}+\left(\frac{H}{3}-\frac{z^2}{2H}\right)\frac{\partial^2 h}{\partial x^2}\right], \tag{116}$$

and

$$w=-z\sqrt{gH}\left[\left(\frac{1}{H}-\frac{h}{2H^2}\right)\frac{\partial h}{\partial x}+\frac{1}{3}\left(H-\frac{z^2}{2H}\right)\frac{\partial^3 h}{\partial x^3}\right]. \tag{117}$$

4. DEFORMATION OF THE WAVE PROFILE

The expression for ω, eq 112, and the relation in eq 90 permit the evaluation of the change in h occurring during a short interval of time to a sufficient approximation. Denoting $\sqrt{gH}$ by ω_0, eq 90 may be written as

$$\frac{\partial h}{\partial t}+\omega_0\frac{\partial h}{\partial x}+\frac{\partial}{\partial x}[h(\omega-\omega_0)]. \tag{118}$$

The integral of this expression is

$$h=f(x-\omega_0 t)-t\frac{\partial}{\partial x}[h(\omega-\omega_0)], \tag{119}$$

when t is small. This may be proved by differentiating eq 119 and substituting in eq 118. In the process of differentiating the second term in the right member, the relation $\partial/\partial t=\omega_0\partial/\partial x$ is used, this being valid if t is small. Eq 119 enables us to trace the wave profile curve as it would be for time t_1+t, if it is given for time t_1.

We next take an element of the intumescence, $d\sigma$, having the height h and base dx and follow its motion. We denote the time-rate of variation of h during the motion by dh/dt. From the definition of ω we obtain

$$\frac{dh}{dt}=\frac{\partial h}{\partial t}+\omega\frac{\partial h}{\partial x}. \tag{120}$$

Multiplying by h and using eq 90, we obtain

$$h\frac{dh}{dt}=-h^2\frac{\partial\omega}{\partial x}. \tag{121}$$

Introducing the value of ω from eq 112, we obtain

$$h\frac{dh}{dt}=-\sqrt{gH}\left[\frac{3h^2\partial h}{4H\partial x}-\frac{H^2}{6}\frac{\partial h\partial^2 h}{\partial x\partial x^2}+\frac{hH^2}{6}\frac{\partial^3 h}{\partial x^3}\right],$$

which may be written, after dividing through by h,

$$\frac{dh}{dt}=-\sqrt{gH}\frac{1}{h}\frac{\partial}{\partial x}\left\{\frac{h^3}{4H}+\frac{H^2}{6}\left[h\frac{\partial^2 h}{\partial x^2}-\left(\frac{\partial h}{\partial x}\right)^2\right]\right\}. \tag{122}$$

This expression gives the rate of variation of the height of an intumescence element.

5. MOTION OF THE CENTER OF GRAVITY OF A WAVE

The last section treated of the motion of an element, $d\sigma$, of a wave. We may also discuss the motion of a volume, V, between two abscissas, x_1 and x_2 where $x_2>x_1$. Then

$$V=\int_{x_1}^{x_2} d\sigma.$$

Let ξ denote the horizontal coordinate of the center of gravity of the volume and η the elevation of the center of gravity above the level of the undisturbed liquid in the channel. By definition,

$$\xi=\frac{\int_{x_1}^{x_2} x\,d\sigma}{V}, \text{ and } \eta=\frac{\int_{x_1}^{x_2} h\,d\sigma}{2V}. \tag{123}$$

Differentiating with respect to t, we obtain

$$\frac{d\xi}{dt}=\frac{\int_{x_1}^{x_2}\omega\,d\sigma}{V}, \text{ and } \frac{d\eta}{dt}=\frac{\int_{x_1}^{x_2}\frac{dh}{dt}d\sigma}{2V}, \tag{124}$$

which are expressions for the velocity of the center of gravity of the

volume. The two integrals $\int_{x_1}^{x_2} \omega\, d\sigma$ and $\int_{x_1}^{x_2} \frac{dh}{dt} d\sigma$ are readily evaluated by means of eq 112 and 122. Writing $h dx$ for $d\sigma$, we obtain

$$\int_{x_1}^{x_2} \omega\, d\sigma = \sqrt{gH}\left[V + \frac{3}{4H}\int_{x_1}^{x_2} h\, d\sigma + \frac{H^2}{6}\left(\frac{\partial h}{\partial x}\right)_{x_1}^{x_2}\right],$$

and

$$\int_{x_1}^{x_2} \frac{dh}{dt} d\sigma = -\sqrt{gH}\left[\frac{h^3}{4H} + \frac{H^2}{6}\left\{h\frac{\partial^2 h}{\partial x^2} - \left(\frac{\partial h}{\partial x}\right)^2\right\}\right]_{x_1}^{x_2}.$$

When these expressions are substituted in eq 123 and 124, we obtain for the velocity components of the center of gravity

$$\frac{d\xi}{dt} = \sqrt{gH}\left[1 + \frac{3\eta}{2H} + \frac{H^2}{6V}\left(\frac{\partial h}{\partial x}\right)_{x_1}^{x_2}\right], \tag{125}$$

and

$$\frac{d\eta}{dt} = -\frac{\sqrt{gH}}{2V}\left[\frac{h^3}{4H} + \frac{H^2}{6}\left\{h\frac{\partial^2 h}{\partial x^2} - \left(\frac{\partial h}{\partial x}\right)^2\right\}\right]_{x_1}^{x_2}. \tag{126}$$

Equation 125 simplifies if the slopes $\partial h/\partial x$ vanish at the end points of the intumescence considered, or if the volume V is large, yielding

$$\left(\frac{d\xi}{dt}\right)^2 = g(H + 3\eta). \tag{127}$$

Equation 126 likewise simplifies if applied to the entire body of an intumescence. If the intumescence is unlimited, V is infinitely large, and the right-hand member vanishes. It also vanishes if the intumescence is limited, for then both h and $\partial h/\partial x$ vanish at the anterior and posterior ends of the intumescence. Therefore, the center of gravity of an intumescence is maintained at a constant height above the primitive free surface, and the velocity of propagation of this center of gravity is constant. [5, p. 84].

6. VARIATION IN ENERGY OF AN INTUMESCENCE

It may be inferred from the invariability of η that the integral $\int h\, d\sigma$, when applied to an entire intumescence, is independent of time; that is, the integral

$$\int_{x_0}^{\infty} h^2\, dx$$

is independent of time. When this integral is multiplied by $\rho g/2$, the product represents the potential energy of the intumescence, eq 62. On the other hand, the kinetic energy of the entire liquid is given by the double integral

$$\rho/2 \int_{x_0}^{\infty} dx \int_0^{H+h} (u^2 + w^2) dz.$$

The velocity components, u and w, are given by eq 114 and 115. From these equations, neglecting quantities of small order, we obtain

$$\int_0^{H+h} (u^2 + w^2) dz = g\left[h^2 + \frac{h^3}{2H} + \frac{H^2}{3}\frac{\partial}{\partial x}\left(h\frac{\partial h}{\partial x}\right)\right],$$

which we multiply by $\rho dx/2$ and integrate between the limits $x=x_0$ and $x=\infty$. The integral $h\partial h/\partial x$ vanishes at infinity and also, when the intumescence is limited, at x_0. It also vanishes at x_0 when the intumescence is unlimited, because this integral is negligible in comparison with the first two terms owing to the length of the intumescence. Thus the kinetic energy of the wave system is

$$\frac{\rho g}{2}\int_{x_0}^{\infty} h^2\,dx+\frac{\rho g}{4H}\int_{x_0}^{\infty} h^3\,dx.$$

The total energy of wave, E, consequently, is

$$\rho g E=\rho g\int_{x_0}^{\infty} h^2\,dx+\frac{\rho g}{4H}\int_{x_0}^{\infty} h^3\,dx. \tag{128}$$

It consists of two terms, of which the first is independent of time, and the second which is small in comparison with the other, may be shown to vary very slowly with time.

7. THE MOMENT OF INSTABILITY OF AN INTUMESCENCE

It was seen that every intumescence is characterized by two integrals, $E=\int h d\sigma$ and $V=\int d\sigma$, which are independent of time. (See eq 65, 69, and 88). In addition to these, there also exists another integral

$$M_s=\int_{x_0}^{\infty}\left[\left(\frac{\partial h}{\partial x}\right)^2-\frac{3h^3}{H^3}\right]dx, \tag{129}$$

which is independent of time. The invariant character of this integral was discovered by Boussinesq, who referred to it as the *moment of instability* [5, p. 97].

We consider the integral

$$M_s-\frac{6}{H^2}E=\int_{x_0}^{\infty}\left[\left(\frac{\partial h}{\partial x}\right)^2-\frac{3h^3}{H^3}-\frac{6h^2}{H^2}\right]dx, \tag{130}$$

where E is the integral representing the energy of the intumescence. Differentiating both members of the equation, we obtain, since $dE/dt=0$,

$$\begin{aligned}\frac{dM_s}{dt}=&-\left[\left\{\left(\frac{\partial h}{\partial x}\right)^2-\frac{3h^3}{H^3}-\frac{6h^2}{H^2}\right\}\omega+2\frac{\partial h}{\partial x}\frac{\partial h}{\partial t}\right]_{x_0}\\&-\int_{x_0}^{\infty}\frac{\partial h}{\partial t}\left(12\frac{h}{H^2}+\frac{9h^2}{H^3}+2\frac{\partial^2 h}{\partial x^2}\right)dx.\end{aligned} \tag{131}$$

The term in the brackets vanishes when the intumescence is limited; in the contrary case it is negligible in comparison with the integral, owing to the great length of the intumescence. Therefore,

$$\frac{dM_s}{dt}=-\int_{x_0}^{\infty}\frac{\partial h}{\partial t}\left(12\frac{h}{H^2}+\frac{9h^2}{H^3}+2\frac{\partial^2 h}{\partial x^2}\right)dx, \tag{132}$$

or, in view of eq 112,

$$\frac{dM_s}{dt}=-\frac{12}{\sqrt{gH^5}}\int_{x_0}^{\infty}\frac{\partial h}{\partial t}h\omega dx. \tag{133}$$

Now, introducing $\partial h/\partial t$ from eq 90, and then integrating, we obtain

$$\frac{dM_s}{dt}=\frac{6}{\sqrt{gH^5}}(h\omega)_{x_0}{}^2. \tag{134}$$

If the intumescence is limited, the right-hand member vanishes: if it is unlimited, this member is a quantity of the order which is neglected in this analysis. Therefore, to this approximation, the moment of instability of an intumescence is independent of time.

8. SOLITARY WAVES

The effect of height and curvature on the deformation of waves was discussed in the previous section on the basis of the assumption that deformation actually occurs. It may well be that configurations exist with appreciable height and curvature which are propagated with no deformation whatever. As a matter of fact, such waves were first discovered by experiment. The solitary wave of J. Scott Russell, consisting of a single elevation whose height may be of the same order of magnitude as the depth, may travel considerable distances without appreciable deformation [6, p. 505; 7, p. 324; 9, p. 289]. This property is called *longevity* and the law governing it may be derived from eq 106.

Putting new variables

$$(x-\omega t)=\zeta H,$$

$$h=\eta H,$$

and

$$\left(\frac{\omega^2}{gH}-1\right)=b$$

into eq 106, we get, since $\frac{\partial^2}{\partial t^2}=\omega^2\frac{\partial^2}{\partial x^2}$ on the basis of the assumption that the wave does not deform,

$$\frac{\partial^2}{\partial\zeta^2}\left(6b\eta-9\eta^2-2\frac{\partial^2\eta}{\partial\zeta^2}\right)=0, \tag{135}$$

which when integrated twice gives

$$6b\eta-9\eta^2-2\frac{\partial^2\eta}{\partial\zeta^2}+c_1\zeta+c_2=0. \tag{136}$$

Since η and $\frac{\partial^2\eta}{\partial\zeta^2}$ are finite, $c_1=0$. If we restrict ourselves to the case where at $\zeta=\infty$, $\eta=0$ and $\frac{\partial^2\eta}{\partial\zeta^2}=0$, then $c_2=0$ and we have

$$6b\eta-9\eta^2-2\frac{d^2\eta}{d\zeta^2}=0. \tag{137}$$

Multiplying by $\frac{d\eta}{d\zeta}d\zeta$ and integrating:

$$3b\eta^2-3\eta^3=\left(\frac{d\eta}{d\zeta}\right)^2. \tag{138}$$

Denoting the maximum height of the wave by h_1, and the corresponding value of η by η_1,

$$\eta_1=\frac{h_1}{H}. \tag{139}$$

At the crest of the wave, $\eta=\eta_1$, and the wave surface is parallel to the bed, $d\eta/d\zeta=0$. Substituting these values in eq 138 we obtain the relation between b and η_1,

$$\eta_1=b=\left(\frac{\omega^2}{gH}-1\right). \tag{140}$$

Replacing this value of b in eq 138:

$$\left(\frac{d\eta}{d\zeta}\right)^2=3\eta^2\,\eta_1-3\eta^3, \tag{141}$$

and integrating twice:

$$\eta=\eta_1\,\mathrm{sech}^2\left[\sqrt{\frac{3}{4}\eta_1}\zeta\right].$$

Reverting to the original variables, we obtain the equation of the wave profile

$$h=h_1\,\mathrm{sech}^2\left[\sqrt{\frac{3h_1}{4H^3}}(x-\omega t)\right]. \tag{142}$$

The free surface is symmetrical about the normal at $x=\omega t$, and approaches the primitive surface as $x-\omega t$ approaches $\pm\infty$ (fig. 2).

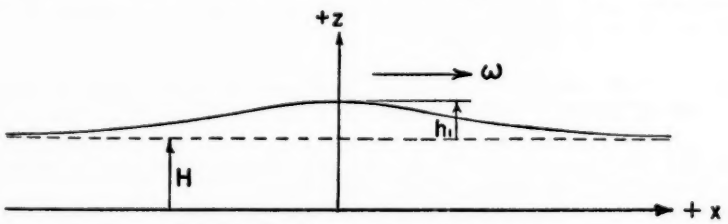

FIGURE 2.—*Diagram of a solitary wave.*

The velocity of propagation, ω, which may be interpreted either as that of the volume element or height element since the wave does not deform, is obtained from eq 140:

$$\omega^2=g(H+h_1), \tag{143}$$

which is the formula adopted by Russell [7, p, 328; 8, p. 423], on empirical grounds and confirmed by the experiments of Bazin [6, p. 496, 515].

A comparison of theory and experiment, based upon 117 observations by Bazin [6, p. 510–514], shows the error of the formula to be -0.91 ± 5.10 percent. Similar calculations based upon 77 observations by Russell [8, p. 440–442] give $+0.78\pm2.30$ percent. The $\pm$ term indicates the standard deviation, and this usage will be followed in subsequent comparisons. It will be noted that in each case zero error is well within the limits determined by the standard deviation.

From eqs 127 and 143 we will now show that the center of gravity of a wave propagated without change of form is $h_1/3$ above the primitive surface, where h_1 is the maximum height of the wave. Since the wave retains its form,

$$\frac{d\xi}{dt}=\omega \tag{144}$$

and is constant. Substituting from eq 143 in eq 127, we obtain

$$\eta=\frac{h_1}{3}. \tag{145}$$

A relation connecting the height at any arbitrary point with the partial volumes of the wave on each side of the perpendicular at this point is derived as follows. By virtue of the relation $(1/h)(\partial/\partial x)=\partial/\partial\sigma$, when dh/dt is placed equal to zero, eq 122 yields the result:

$$h^3\left(1+\frac{2H^3}{3}\frac{d^2h}{d\sigma^2}\right)=\text{constant}.$$

The constant is zero, since h vanishes at infinity; therefore,

$$1+\frac{2H^3}{3}\frac{d^2h}{d\sigma^2}=0. \tag{146}$$

Integrating and employing the boundary conditions $\sigma=0$, $h=0$; $\sigma=Q$, $h=0$, we obtain the solution

$$h=\frac{3}{4H^3}(Q-\sigma)\sigma. \tag{147}$$

Since the wave is symmetrical, the maximum ordinate, h_1, divides the wave into equal parts: $\eta=h_2$, $\sigma=Q/2$.
Therefore,

$$h_1=\frac{3Q^2}{16H^3}, \tag{148}$$

which is the relation between the maximum height of the wave and its total volume. It was demonstrated in section IV–2 that the potential and kinetic energies of an intumescence are equal, to within a small term of the order of h^3; consequently

$$E=2\eta Q=\frac{Q^3}{8H^3}. \tag{149}$$

From eq 148 and 149 we derive the following relations:

$$h_1=\frac{3\sqrt[3]{E^2}}{4H}, \text{ and } \frac{Q}{h_1}=\frac{8H^2}{3\sqrt[3]{E}}. \tag{150}$$

These relations will now be used to explain the phenomena of waves traveling up a channel of slowly decreasing depth. Considering eq 85, we see that the quantity c_1-c_2 is small, since dH/dx is small. Consequently, the reflected wave is negligible, and the energy of the transmitted wave remains sensibly constant. From eq 150 we deduce that h_1 continually increases, and Q/h_1 continually decreases. The wave gets higher and higher, and its base narrows continually. As a result, the wave becomes unstable and finally breaks. A quantitative analysis of this phenomenon will be given in section V–19.

9. CNOIDAL WAVES

In the theory developed thus far, extensive use has been made of the assumption that the liquid is undisturbed at infinity; that is, that the wave profile $x=f(h)$ vanishes at infinity together with all its derivatives. In the previous section this assumption was utilized in deriving eq 137, and it was found that the only wave fulfilling this condition and propagated without change of form was the solitary wave. We now wish to eliminate this restriction and determine the form of a wave of appreciable height, governed by eq 106 and propagated without change of form.

We therefore assume that at $h=0$, the derivatives $\partial h/\partial x$, $\partial^2 h/\partial x^2$, . . . do not all necessarily vanish. The constant c_2 is consequently retained in eq 136, and we write

$$6b\eta-9\eta^2-\frac{d^2\eta}{d\zeta^2}+3c_2=0. \tag{151}$$

Multiplying both members of eq 151 by $(d\eta/d\zeta)\,d\zeta$ and integrating:

$$\left(\frac{d\eta}{d\zeta}\right)^2=3b\eta^2-3\eta^3+3c_2\eta+3c_1, \tag{152}$$

where $3c_1$ is another constant of integration. Since $d\eta/d\zeta$ is real at $\eta=0$, then c_1 is positive, and if η', η'', η''' are the roots of the polynomial, then

$$\eta'\eta''\eta'''=c_1.$$

Either all the roots are positive, or one is positive and two negative, or one is positive and two complex. There is at least one positive value of η, say η', for which $d\eta/d\zeta$ vanishes. If this is the only value of η for which the profile is horizontal, then the wave profile must become infinite with ζ, which is physically impossible. The third case is therefore excluded. If all the roots are positive, then the wave profile must be included between the extreme values, since otherwise it would become infinite. This requires that the wave surface be everywhere above the primitive surface, which is likewise physically impossible, and the first case is also excluded. Therefore η'' and η''' are both negative. Writing the three roots $\eta_1, -\eta_2, -\eta_3$, $\eta_3 \geqq \eta_2$, we have

$$\left(\frac{d\eta}{d\zeta}\right)^2=3(\eta_1-\eta)(\eta+\eta_2)(\eta+\eta_3), \tag{153}$$

and

$$\left.\begin{aligned} b&=\eta_1-\eta_2-\eta_3,\\ c_2&=-\eta_2\eta_3+\eta_1\eta_3+\eta_1\eta_2,\\ c_1&=\eta_1\eta_2\eta_3. \end{aligned}\right\} \tag{154}$$

Introducing the new variable, χ,

$$\eta=\eta_1\cos^2\chi-\eta_2\sin^2\chi, \tag{155}$$

eq 153 becomes

$$\beta\left(\frac{d\chi}{d\zeta}\right)=\sqrt{1-k^2\sin^2\chi}, \tag{156}$$

where

$$\beta=\sqrt{\frac{4}{3(\eta_1+\eta_3)}}=\sqrt{\frac{4H}{3(h_1+h_3)}}, \tag{157}$$

and

$$k^2=\frac{\eta_1+\eta_2}{\eta_1+\eta_3}=\frac{h_1+h_2}{h_1+h_3}. \tag{158}$$

Selecting $\zeta=0$ at the apex, then $\eta=\eta_1$ and $\chi=0$, and we have

$$\zeta=\beta\int_0^{\chi}\frac{d\chi}{\sqrt{1-k^2\sin^2\chi}}=\beta F(\chi, k), \tag{159}$$

where F is an incomplete elliptic integral of the first kind. Introducing Jacobian elliptic functions, since $\cos\chi=\mathrm{cn}(\zeta/\beta, k)$, $\sin\chi=\mathrm{sn}(\zeta/\beta, k)$ and $\mathrm{sn}^2u+\mathrm{cn}^2u=1$, we have

$$\eta=-\eta_2+(\eta_1+\eta_2)\,\mathrm{cn}^2\left(\frac{\zeta}{\beta}, k\right), \tag{160}$$

or reverting to the original coordinates

$$h=-h_2+(h_1+h_2)\,\mathrm{cn}^2\left[\sqrt{\frac{3(h_1+h_3)}{4H^3}}\,(x-\omega t), \sqrt{\frac{h_1+h_2}{h_1+h_3}}\right]. \tag{161}$$

This equation represents an infinite number of undulations of identical size and shape, each symmetrical about a vertical plane passing through the apex. The existence of these periodic waves moving without change of form was first indicated by Boussinesq [10, p. 392], and the name, *cnoidal waves*, from the cn function by analogy with sinusoidal, is due to Korteweg and de Vries [11].

The relative wave length, λ/H, is given by

$$\frac{\lambda}{H}=2\beta\int_0^{\pi/2}\frac{d\chi}{\sqrt{1-k^2\sin^2\chi}}=2\beta F_1(k), \tag{162}$$

F_1 being the complete elliptic integral of the first kind.

The initial depth of the water in the channel being H, we must have

$$\int_0^{\frac{\lambda}{H}} \eta d\zeta = 0,$$

or from eq 155 and eq 156

$$2\int_0^{\frac{\pi}{2}} \frac{(\eta_1 \cos^2 \chi - \eta_2 \sin^2 \chi)\beta}{\sqrt{1-k^2 \sin^2 \chi}} d\chi = 0,$$

which from eq 158 reduces to

$$(h_1+h_3)E_1(k) = h_3 F_1(k), \tag{163}$$

where E_1 is the complete elliptic integral of the second kind. The form of the waves is completely determined by λ/H, and h_1/H, the relative wave length and height of the crest above the initial surface of the water, since h_2/H and h_3/H are determined by eq 158, 162, and 163.

From eq 162 we see that the wave length of the undulations becomes infinite when $k=1$. From eq 163 if $k=1$, $h_2=h_3=0$. Since $\mathrm{cn}(\chi, 1)=\mathrm{sech}\ \chi$, then for $k=1$, eq 161 reduces to the equation of the solitary wave (eq 142), and the latter appears as a special case of the cnoidal wave.

From the definition of b (eq 136) and from eq 154, we have

$$\frac{\omega^2}{gH} = 1+\frac{h_1}{H}-\frac{h_2}{H}-\frac{h_3}{H}, \tag{164}$$

which is the expression for the velocity of the wave profile. Since we are now dealing with an infinite number of undulations moving in a channel of finite depth, a question arises as to the meaning of the velocity of propagation. Stokes [12, p. 202], has given two definitions applicable to this case, and we adopt the second one; namely, the velocity of propagation is the velocity of the wave profile with respect to the center of inertia of the fluid mass included between two vertical planes separated by a distance equal to the wave length.

Writing this velocity as ω_c:

$$\omega_c = \omega - \frac{1}{H\lambda}\int_0^{\lambda} U(H+h)dx, \tag{165}$$

where U is the mean velocity in a vertical section. If U_0 is the mean velocity in the section at $h=0$, we have from eq 95

$$U(H+h) = h\omega + U_0 H. \tag{166}$$

Substituting in eq 165, we have for the velocity of propagation

$$\omega_c = \omega - U_0 \tag{167}$$

or

$$\omega_c^2 = \omega^2\left(1-2\frac{U_0}{\omega}\right). \tag{168}$$

We now evaluate U_0. Integrating eq 114, we have

$$U_0 = u_0 - \frac{H^2}{6}\frac{\partial^2 u_0}{\partial x^2}, h=0,$$

u_0 being the velocity at the bottom. It has been assumed in the analysis that at $h=0$, the surface velocity u_1 vanishes (see the discussion of eq 41); hence from eq 114,

$$u_0=\frac{H^2}{2}\frac{\partial^2 u_0}{\partial x^2},\ h=0,$$

and

$$U_0=\frac{H^2}{3}\left(\frac{\partial^2 u_0}{\partial x^2}\right),\ h=0. \tag{169}$$

From eq 104, since we can write $\partial/\partial t=-\omega\,(\partial/\partial x)$, we obtain by differentiating twice with respect to x, and neglecting the term containing $\partial^4 h/\partial x^4$:

$$\frac{\partial^2 u_0}{\partial x^2}=\frac{g}{\omega}\left(\frac{\partial^2 h}{\partial x^2}\right),\ h=0.$$

Substituting in eq 169, we finally have

$$U_0=\frac{1}{3}\frac{gH^2}{\omega}\frac{\partial^2 h}{\partial x^2},\ h=0$$

and eq 168 becomes

$$\omega_c^2=\omega^2\left[1-\frac{2gH^2}{3\omega^2}\left(\frac{\partial^2 h}{\partial x^2}\right)_{h=0}\right],$$

or from eq 151, 154, 164, in terms of h_1, h_2, and h_3, within the approximation of the analysis, that is, neglecting $h_1h_2h_3/H^3$,

$$\omega_c^2=gH\left[1+\frac{h_1}{H}\right]\left[1-\frac{h_2}{H}\right]\left[1-\frac{h_3}{H}\right]. \tag{170}$$

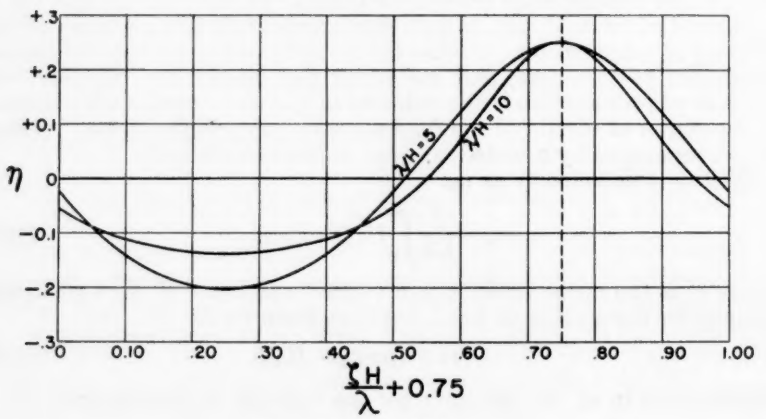

FIGURE 3.—*Cnoidal waves.*

Relative displacemen of the free surface as a function of the fractional part of the relative wave length.

This, then, is the velocity of propagation of the wave profile with respect to the center of inertia of the fluid mass included between two vertical planes separated by a distance equal to the wave length, λ.

For other treatments of this subject reference may be made to Boussinesq [10, p. 390], Korteweg and de Vries [11], and Lamb [4, p. 402].

Figures 3 and 4 represent two typical cnoidal waves. Figure 3 shows on an arbitrary scale one complete undulation for two values of λ/H, and figure 4 shows extended profiles of the same two waves at the correct height above the bottom, but compressed horizontally 5 times. In both cases, $h_1/H=0.25$.

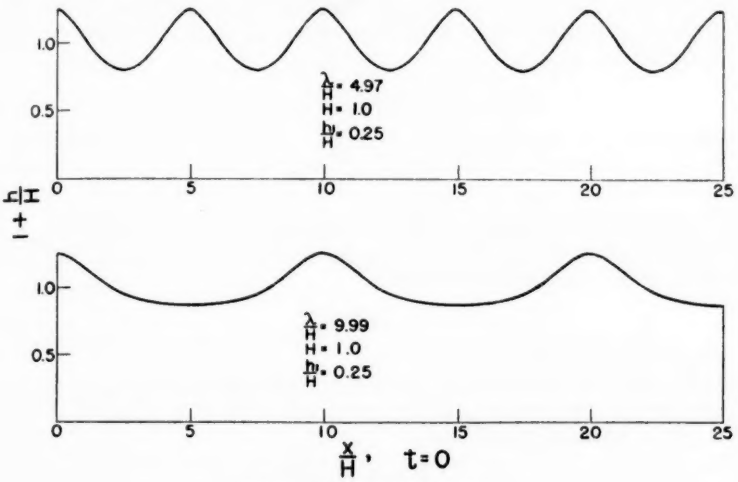

FIGURE 4.—*Cnoidal waves.*
Relative height above the bottom as a function of relative horizontal dimension.

10. MOMENT OF INSTABILITY OF A SOLITARY WAVE

Of all the intumescences of equal energy, the solitary wave is the only one for which the moment of instability

$$M_s=\int_{x_0}^{\infty}\left[\left(\frac{\partial h}{\partial x}\right)^2-\frac{3h^3}{H^3}\right]dx \tag{129}$$

is a minimum.

The theorem may be proved by the methods of the calculus of variations for the solution of isometric problems. By an isometric problem, we mean one of the following kind:

Among all curves joining two points (x_0, h_0) and (x_1, h_1) for which the definite integral

$$K=\int_{s_0}^{s_1} G(x, h, x', h')ds \tag{171}$$

takes on a given value l, to determine the one

$$\left.\begin{aligned} &C_0,\ x=x(s),\ x_0=x(s_0)\\ &\quad h=h(s),\ h_0=h(s_0)\end{aligned}\right\} \tag{172}$$

which minimizes (or maximizes) another definite integral

$$J=\int_{s_0}^{s_1} F(x, h, x', h')ds. \tag{173}$$

Here s is a parametric variable, and the primes indicate differentiation with respect to s.

Putting

$$H=F+\lambda G, \tag{174}$$

where λ is a numerical constant, the first necessary condition for a minimum or maximum is that the curve C_0 in eq 172 must satisfy the differential equation

$$H_{xh'}-H_{x'h}+H_1(x'h''-x''h')=0, \tag{175}$$

where

$$H_1=-\frac{H_{x'h'}}{x'h'}. \tag{176}$$

The subscripts indicate partial differentiation with respect to the variables represented by the subscripts. The second necessary condition for a minimum is that

$$H_1 \gtrless 0 \tag{177}$$

at every point of the curve C_0.

Obviously, in the present isometric problem, the integral K corresponds to the energy of an intumescence and the integral J to the moment of instability; that is,

$$K=\int_{x_0}^{\infty} h^2\,dx, \tag{178}$$

and

$$J=\int_{x_0}^{\infty}\left[\left(\frac{\partial h}{\partial x}\right)^2-\frac{3h^3}{H^3}\right]dx. \tag{179}$$

We select the parametric variable s so that

$$\left.\begin{aligned} x&=s, \\ \text{and}\quad h&=h(s). \end{aligned}\right\} \tag{180}$$

The above integrals, eq 178 and 179, become

$$K=\int_{s_0}^{\infty} h^2 x'\,ds, \tag{181}$$

and

$$J=\int_{s_0}^{\infty}\left(\frac{h'^2}{x'}-\alpha h^3 x'\right)ds, \tag{182}$$

where $\alpha=3/H^3$. Hence,

$$G=h^2x', \tag{183}$$

$$F=\frac{h'^2}{x}-\alpha h^3 x', \tag{184}$$

$$H_1=\frac{2}{x'^3}, \tag{185}$$

and

$$H=\frac{h_1'^2}{x'}-\alpha h^3 x'+\lambda h^2 x'. \tag{186}$$

The first necessary condition for a minimum, eq 175, after some simplifications, yields

$$3\alpha h^2-2\lambda h+2\frac{\partial^2 h}{\partial x^2}=0, \tag{187}$$

which also may be written as

$$\frac{3}{4}h+\frac{1}{6}\frac{H^3}{h}\frac{\partial^2 h}{\partial x^2}=\frac{1}{6}\lambda H^3, \tag{188}$$

if α is replaced by $3/H^3$. Since the left-hand member is a constant, we see on comparing eq 188 with eq 112 that the intumescence having a maximum or a minimum moment of instability for a given energy is one that is propagated without change of form. The only wave which is propagated with constant velocity is the solitary wave. The second necessary condition, eq 177, is likewise satisfied; hence the moment of instability is a minimum.

11. MOMENT OF INSTABILITY AND WAVE FORMATION

The frequent occurrence of the solitary wave, owing to its production by a broad class of different initial disturbances, was observed by Scott Russell [7, p. 351; 8, p. 423]. This frequent formation of the solitary wave has been explained by Boussinesq [5, p. 99; 10, p. 401], utilizing the theorem just proved—that the solitary wave is the only intumescence for which the moment of instability is a minimum. An integration would show that this minimum is

$$(M_s)_1=\frac{27E^{5/3}}{20H^4}, \tag{189}$$

where E is the energy of the wave and H is the depth of the channel.

If one considers an intumescence of arbitrary form, and a solitary wave, both having the same energy, E, the excess of the integral M_s of the intumescence over that of the solitary wave, $M_s-(M_s)_1$ may be regarded as a measure of the rapidity with which the intumescence will deform during its propagation and also of the extent of the deformation taking place. This is why Boussinesq named the integral the *moment of instability*.

If $M_s-(M_s)_1$ is small, the profile of the intumescence will oscillate about that of a solitary wave having the same energy, E. The form of the intumescence cannot change very markedly, as this would require M_s to increase, contrary to the theory. Friction, which has been ignored in the theory, will damp out these oscillations and the intumescence will eventually assume the shape of a solitary wave.

It should be noted that there does not exist a solitary wave having an arbitrary energy, since there is a maximum height, above which a solitary wave cannot be propagated without breaking (see section V-19). This limiting factor serves to determine the class of disturbances which can produce a solitary wave.

12. NEGATIVE WAVES

Let us now examine the circumstances governing the motion of a negative wave limited in extent and propagated in the positive x-direction, negative signifying that the surface is depressed. The longitudinal profile of such a wave in its simplest form will consist at the moment of the formation of the wave of a main concave portion in the center and two convex arcs at the posterior and the anterior ends of the wave. As long as the form is not altered, the center of gravity of the wave is located at one-third of its maximum depth; that is, $\eta=h_1/3$. According to eq 127, the velocity of propagation of this wave would be

$$\omega^2=g(H-h_1), \tag{190}$$

a law that is confirmed very nearly in the experiments of Bazin. Calculations based upon 18 observations, [6, p. 521] give as the error of the formula, -1.54 ± 2.09 percent, where the $\pm$ term indicates the standard deviation.

The initial simple form of the wave, however, is soon modified. In fact, eq 112 shows that since h is negative, the third term is nega-

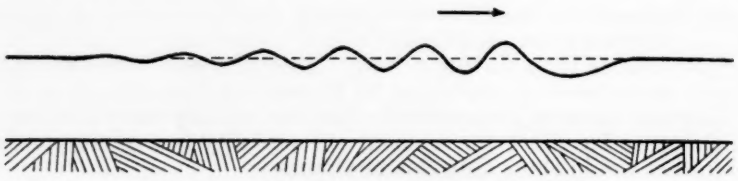

FIGURE 5.—*Negative wave as observed by Bazin.*

tive in the concave portion and positive in the convex portion. The second term is more negative in the concave portion than in the convex portion, since h is smaller in absolute magnitude in the latter case. Thus the head of the depression, being both at a higher elevation than the center of the cavity and convex, while the latter is concave, is propagated faster than the center and becomes elongated. The tail of the wave also travels faster than the center for the same reasons and is therefore shortened as long as the requisite initial conditions obtain. However, the process of shortening cannot be indefinite. Furthermore, a convex portion is necessary for the continuity of the surface slope; hence the convex portion is finally raised above the level of the primitive free surface. Since h is now positive, the last term of eq 112 is negative; and if either h is small enough or $\partial^2 h/\partial x^2$ large enough, it can exceed the second term, so that a condition is reached such that ω of the elevated convex portion is the same as ω of the lowest point of the depressed body. But the elevation thus produced at the posterior end of the main negative body of the wave requires an intermediate concave portion in order to join the free primitive surface with a continuous slope. Such a concave portion cannot exist and cannot be formed if its velocity of propagation is greater than that of the positive wave preceding it. Equation 112 indicates that if these velocities are to be equal, the convex positive wave must be followed by a negative wave. Continuing the argument, we see that a given negative wave is followed by a series of smaller waves, alternatively positive and negative, and entirely convex and

concave, with inflection points on the level of the primitive surface (fig. 5). For additional figures, see [6, plate 2, fig. 3; 7, plate 52, fig. 10].

13. INTUMESCENCES OF FINITE HEIGHT BUT NEGLIGIBLE CURVATURE

For an intumescence of finite height but having a free surface of negligible curvature, the expression of the velocity of propagation of volume element, eq 112, assumes the simple form

$$\omega=\sqrt{gH}\left(1+\frac{3}{4}\frac{h}{H}\right). \tag{191}$$

As an immediate consequence of this simplification, differential equation 90 can be integrated and the equation of the intumescence profile obtained. Introducing eq 191, eq 90 becomes

$$\frac{\partial h}{\partial t}+\sqrt{gH}\left(1+\frac{3}{2}\frac{h}{H}\right)\frac{\partial h}{\partial x}=0, \tag{192}$$

which possesses the integral

$$x-\sqrt{gH}\left(1+\frac{3}{2}\frac{h}{H}\right)t=f(h), \tag{193}$$

where $f(h)$ is an arbitrary function of h. The integral may be interpreted as follows: If h is the elevation of the free surface at x at time t, then the same elevation is reproduced at $x+\Delta x$ at time $t+\Delta t$; but, from eq 193:

$$\Delta x=\sqrt{gH}\left(1+\frac{3}{2}\frac{h}{H}\right)\Delta t,$$

and, therefore, the intumescence height is propagated with the velocity

$$\omega_1=\sqrt{gH}\left(1+\frac{3}{2}\frac{h}{H}\right), \tag{194}$$

which is Airy's expression [4, p. 243] for the velocity of propagation for waves of finite height. It should be noted that eq 194 represents the velocity of propagation of the height of an element.

The arbitrary function, f, in eq 193 can be determined in two ways, depending on whether the canal is infinite in one or both directions. In the latter case, h is usually given for all values of x at some instant, t. If the relationship is in the form $h=f_1(x)$, we may invert the function and obtain $f_2(h)=x$, which is the desired function.

In the former case, assume the channel in communication with an infinitely large basin and that the water level of the basin is a known function of time, say, $h=F(t)$. Inverting this function, we have $t=F_1(h)$, and, if we take the point where the channel meets the basin as the origin of x, the arbitrary function is

$$f(h)=-\sqrt{gH}\left(1+\frac{3}{2}\frac{h}{H}\right)F_1(h).$$

In intumescences of this type, the mean velocity, U, of the fluid particles in a cross section is

$$U=\sqrt{gH}\cdot\frac{h}{H}\left(1-\frac{h}{4H}\right), \tag{195}$$

which follows from eq 96 and 191.

14. HORIZONTAL CHANNEL IN COMMUNICATION WITH THE OCEAN

Boussinesq has applied the method of the last article to a horizontal channel in communication with the ocean to determine the mean elevation of the ocean surface above the bed of the channel.

We may write for the elevation of the surface water of the ocean above the bed of channel,

$$H+h=a\left(1+\alpha\sin\frac{2\pi t}{T}\right),\ x=0, \tag{196}$$

where H is the depth of water in the channel at points so remote from the mouth that the disturbances of the ocean are not felt, a is the elevation of the mean level of the surface waters of the ocean above the channel bed, α the ratio of the half amplitude of the tidal oscillations to the elevation, a, and T the period of the tides. Using eq 171, we obtain for the arbitrary function, $f(h)$, in eq 193,

$$-f(h)=\sqrt{gH}\left(1+\frac{3}{2}\frac{h}{H}\right)\frac{T}{2\pi}\sin^{-1}\frac{H+h-a}{a\alpha}, \tag{197}$$

and for the free surface of water in the channel,

$$x=\sqrt{gH}\left(1+\frac{3}{2}\frac{h}{H}\right)\left(t-\frac{T}{2\pi}\sin^{-1}\frac{H+h-a}{a\alpha}\right). \tag{198}$$

After a certain length of time, the transients will die out and the total volume of water entering the channel during each period T will be zero; that is,

$$\int_0^T U(H+h)dt=0,\ x=0. \tag{199}$$

This condition permits the determination of H. Since $U(H+h)=\omega h$, eq 199 gives, substituting for ω from eq 191,

$$\int_0^T\left(h+\frac{3}{4}\frac{h^2}{H}\right)dt=0. \tag{200}$$

Introducing h from eq 196 and integrating, we obtain

$$H-a-\frac{3}{4}\frac{(H-a)^2}{H}=\frac{3}{8}\frac{\alpha^2 a^2}{H},$$

which can be simplified further since $H-a$ is a small quantity:

$$H-a=\frac{3}{8}\alpha^2 a. \tag{201}$$

This is the desired relation. The mean level of the surface water of the ocean is below the level of the water in the horizontal channel at large distances from the mouth by the small amount (3/8) $\alpha^2 a$.

15. WAVES DUE TO SUDDEN INCREASE OF DISCHARGE

Let us examine the case in which a positive intumescence of infinite length is produced in a body of still water in a channel when a discharge of constant value is established at the entrance. After the initial disturbances have died down, the wave is of constant elevation, h, except in the anterior portion, and the front of the wave moves with a constant velocity, ω. As the curvature of the layer representing the intumescence is negligible at points sufficiently removed from the front, the velocity of propagation of the wave front must be from eq 191,

$$\omega=\sqrt{g\left(H+\frac{3}{2}h\right)}, \tag{202}$$

since h/H is small.

Bazin's experiments verify this formula closely. From his data [6, p. 539–541], velocities were computed and were compared with the theoretical values. The mean values of h and H at the two points of the channel between which the wave traveled when its elapsed time was observed were substituted in the formula. The method of obtaining h from the data is described on page 96.

The data gave sufficient information to make 37 comparisons. Observations on eight intervals were rejected, since the observers reported that the wave had completely broken and reported h as zero.

The average error of the theoretical values was -0.98 ± 2.71 percent, where the $\pm$ term indicates the standard deviation. These values were plotted as a function of h/H in figure 6, in an attempt to discover a systematic variation. The lines connect observations on the same wave in different intervals. The results were essentially negative, although there is a suggestion of an error changing in sign from minus to plus, as h/H increases. It will be noted that the formula applies equally well to unstable waves on the point of breaking as well as to those having a definite h_1/h ratio of 3/2. (See fig. 9.)

St. Venant, using the principle of momentum, has derived for the celerity of this type of wave,

$$\omega^2=gH\left(1+\frac{3}{2}\frac{h}{H}+\frac{1}{2}\frac{h^2}{H^2}\right), \tag{203}$$

an expression which reduces to eq 202 when the last term is neglected.

16. EFFECT OF CHANNEL VELOCITY DISTRIBUTION

We may now consider a discharge wave superposed on a current and determine the effect of the velocity distribution in the current on the celerity of the wave.

We shall assume (1) that the profile of wave does not deform during the motion and (2) that at the two sections, each at a distance s from the wave front, the velocity distributions are characteristic of the channel. (See fig. 7.) Let the mean velocities at these sections

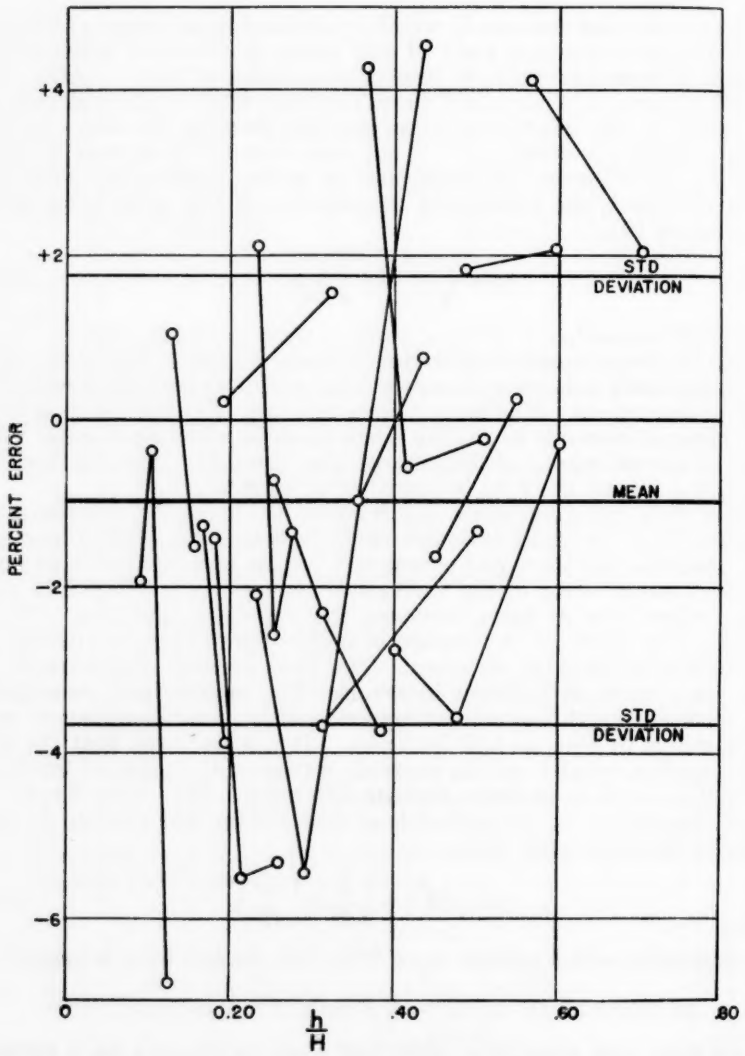

FIGURE 6.—*Percentage of error of eq 202 compared with experiment, as a function of the relative height.*

be U_1 and U_2, the local velocities at any height z be u_1 and u_2, and the depths H and $H+h$. We consider the body of water included at the instant t between the sections AB and DC. The distance between AB and the section containing the wave front is s; the distance between DC and the wave front is $s+\omega\Delta t$, where ω is the celerity of the wave, and Δt an interval of time. The momentum of the body of

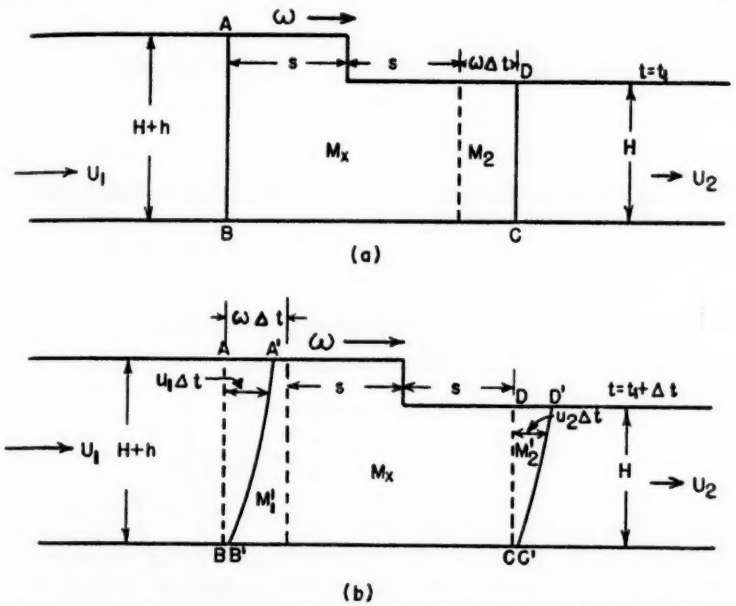

FIGURE 7.—*Diagram illustrating the effect of channel velocity distribution.*
(*a*) Configuration at time t_1; (*b*) Configuration at time $t_1+\Delta t$.

water thus delimited may be denoted by M_x+M_2, where M_2 is given by

$$M_2=\rho\omega\Delta t\int_0^H u_2 dz=\rho\omega\Delta t U_2 H.$$

At the instant of time $t+\Delta t$, the particles originally at AB have reached the position $A'B'$, and the particles originally at DC have reached the position $D'C'$. (See fig. 7.) The liquid contained between $A'B'$ and $D'C'$ has the momentum $M_x+M'_1+M'_2$, where

$$M'_1=\rho\int_0^{H+h}(\omega\Delta t-u_1\Delta t)u_1\,dz,$$

and

$$M'_2=\rho\int_0^H u_2^2\Delta t\,dz.$$

Introducing the *Boussinesq number*, η, the coefficient of the excess of the mean of the velocities squared over the square of the mean velocity, which we assume to be unaffected by depth,

$$\int_0^{H+h} u_1^2\, dz = (1+\eta)\, U_1^2\, (H+h),$$

and

$$\int_0^{H} u_2^2\, dz = (1+\eta)\, U_2^2\, H.$$

We have, therefore,

$$M_1' = \rho U_1 (H+h)\omega\Delta t - \rho U_1^2\, (H+h)(1+\eta)\Delta t,$$

and

$$M_2' = \rho(1+\eta)\, U_2^2\, H\Delta t.$$

Thus the increase of momentum of the body of water under consideration during the time interval Δt is

$$M_x + M_1' + M_2' - (M_x + M_2) = \rho\Delta t[U_1(H+h)(\omega - U_1) + U_2 H(U_2 - \omega) - \eta\{U_1^2\, (H+h) - U_2^2 H\}]. \tag{204}$$

We may eliminate U_1 by the equation of continuity,

$$U_1(H+h) = U_2 H + \omega h, \tag{205}$$

and obtain for the rate of change of momentum:

$$\frac{\rho(\omega - U_2)^2 Hh}{H+h}\left[1+\eta\left\{1-\frac{\omega^2}{(\omega-U_2)^2}\right\}\right], \tag{206}$$

neglecting h/H with respect to unity.

The force which produces this rate of change of momentum is the difference between the total hydrostatic pressures acting on the sections AB and DC, which is

$$\rho g H h\left[1+\frac{h}{2H}\right]. \tag{207}$$

Equating 206 and 207, and assuming that the effect of the η term is small, we obtain

$$(\omega - U_2)^2 = gH\left(1+\frac{3}{2}\frac{h}{H}+\frac{h^2}{2H^2}\right)\left[1-\eta\left\{1-\frac{\omega^2}{(\omega-U_2)^2}\right\}\right],$$

or

$$\omega = U_2 \pm \sqrt{gH}\left(1+\frac{3}{4}\frac{h}{H}\right)\left(1-\frac{\eta}{2}\left[1-\frac{\omega^2}{(\omega-U_2)^2}\right]\right). \tag{208}$$

This is the expression for the celerity of a discharge wave or a depression wave, which takes into account the height, h, and u_2, the channel velocity distribution. For a wave moving downstream the plus sign holds; for a wave moving upstream the negative sign holds. For a positive wave h represents an elevation and is positive; for a negative wave h represents a depression and is negative.

Equation 208 can be further simplified when the approximation $\omega = U_2 \pm \sqrt{gH}$ is used. Accordingly, we obtain for a wave moving downstream

$$\omega = U_2 - \sqrt{gH}\left(1+\frac{3}{4}\frac{h}{H}\right)\left(1+\frac{\eta}{2}\left[\frac{U_2^2}{gH}+\frac{2U_2}{\sqrt{gH}}\right]\right), \tag{209}$$

and for a wave moving upstream

$$\omega = U_2 - \sqrt{gH}\left(1+\frac{3}{4}\frac{h}{H}\right)\left(1+\frac{\eta}{2}\left[\frac{U_2^2}{gH}-\frac{2U_2}{\sqrt{gH}}\right]\right). \tag{210}$$

It is now seen that the effect of velocity distribution is appreciable only when the ratio U_2^2/gH is larger than unity, and for the ordinary case, in which U_2^2/gH is a small fraction, this effect is negligible.

17. INITIAL WAVES

Bazin observed that in waves of constant discharge moving in still water, the initial part of the wave is made up of a series of relatively short, alternately convex and concave, intumescences. (See fig. 8.)

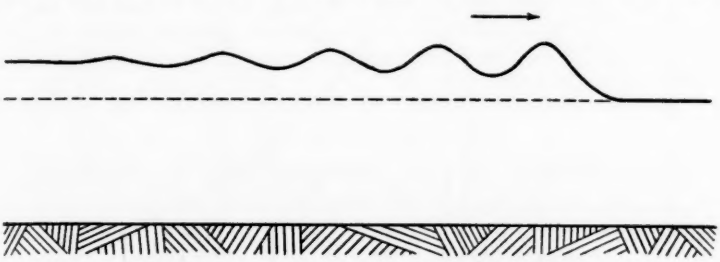

FIGURE 8.—*Initial wave as observed by Bazin.*

The foremost intumescence is convex, and its crest is at a higher lever than that of the constant elevation of the free surface of the main intumescence. Bazin refers to this initial part as the *initial wave*. The mechanical basis of the phenomenon was discussed by Boussinesq in the following manner, which is similar to the treatment in section V-12.

At the head of the intumescence it is not possible for the depth to equal the depth of the main layer. The anterior part of the wave being convex, the curvature $\partial^2 h/\partial x^2$ is negative and according to eq 112,

$$\omega = \sqrt{gH}\left(1+\frac{3}{4}\frac{h}{H}+\frac{H^2}{6h}\frac{\partial^2 h}{\partial x^2}\right), \tag{112}$$

the velocity of propagation there is less than that part of the layer which follows. This layer moves with a greater velocity and thus overruns the anterior portion of the wave until the augmented height compensates for the effect of the negative curvature. This explains the formation of the initial wave. It is known that the height of the initial wave tends to oscillate around a height equal to 3/2 of the height, h, of the long layer. The height of the initial wave will increase until the velocity of propagation of its center of gravity becomes sensibly equal to that of the layer. But the form of this wave indicates that the center of gravity, η, is to be placed at 1/3 of its height, h_0; and, on the other hand, eq 127, which is applicable in the present

case, gives for the square of the velocity of the propagation, $g(H+h_a)$. Equating this to the square of the velocity of the layer, $g(H+3h/2)$, eq 202, it is seen that $h_a=3h/2$.

The ratio $h_1/h=3/2$ has been investigated by Bazin [6]. The experiments were made in a rectangular channel having a bottom slope of 1.5 in 1,000. The percentage change in depth being the least at the deep end, where the waves were generated, the motion at this end will nearly approximate flow in a channel of uniform depth. Calcu-

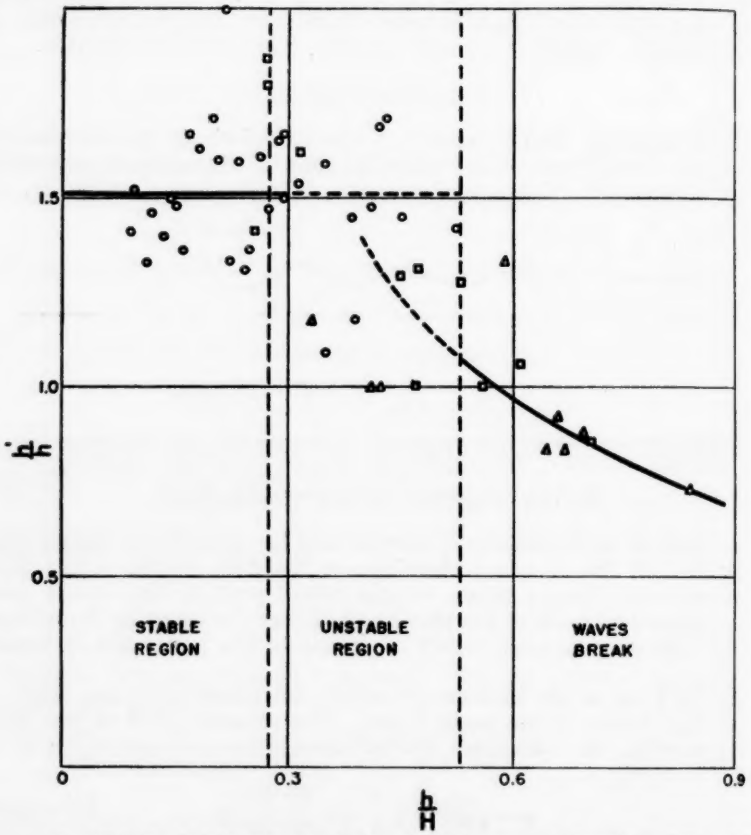

FIGURE 9.—*Relative height of the head of an initial wave as a function of the relative depth of the main layer.*

lations made by the authors from data taken at his end of the channel [6, p. 542] give $h_1/h=1.61\pm0.18$. Bazin [6, p. 550] considers 3/2 to be the approximate value.

Inasmuch as the waves are found to break as they ascend the channel if the original depth of the water is small enough, it is instructive to consider this aspect of the phenomenon. Observations were taken on the wave at four points in the channel. The complete data [6, p. 539–541] have been employed to plot h_1/h as a function of the dimensionless ratio h/H, the relative height of the wave layer. The average value of h was utilized in order to approximate the

steady height of the layer, eliminating the undulations behind the head of the wave. These data are represented in figure 9. The circles represent observations on waves which have no tendency to break; the squares, those in which breaking is imminent; the triangles, those in which breaking has occurred. An average of the 33 points with circles gives $h_1/h=1.51\pm0.17$. Although the data do not provide a clearly defined function, the following conclusions seem justified.

1. As would be expected, for increasing h/H the waves become unstable and eventually break. The critical value is about 0.275.
2. The value $h_1/h=1.5$ is a reasonable approximation in the stable region.
3. The ratio h_1/h definitely decreases with increasing h/H, outside the stable region.

Recent experiments [2, p. 158–159] indicate that h_1/h is a function of h/H in the stable region, increasing from 1 to 2 at the critical value 0.28, then decreasing asymptotically toward unity in the unstable region.

Where the initial wave joins the main layer, the condition of continuity of slope requires a concave curve, that is, a curve for which $\partial^2 h/\partial x^2$ is positive. The positive curvature would entail a velocity of propagation greater than that of the layer as a whole, unless h is less than in the remainder of the layer. Hence a depression is produced immediately following the initial wave.

Continuing the argument, it is seen that the initial wave is followed by convexities and concavities all above the undisturbed surface. Because of the internal friction of the liquid, the heights of these convexities and concavities decrease in the posterior direction until they become insensible. The inflexion points where $\partial^2 h/\partial x^2$ vanish are in a plane containing the free surface of the main layer.

18. FAVRE'S EXPERIMENTS ON THE UNDULATIONS IN A POSITIVE SURGE

In 1934, Favre [2] made an elaborate series of experiments on translation waves. Several of these experiments were undertaken to investigate the undulations composing the head of a discharge wave [2, ch. IV]. The experiments established the following facts:

1. The undulations are not formed immediately, but require a certain amount of time to establish themselves.
2. After the undulations are formed, they are of similar size and shape.
3. The final configuration is a stable one.
4. The height of the undulation at x is independent of Θ, the time in which the flow is established, for a considerable range of values of x, provided $\Theta\omega/x<0.2$. In other words, within certain limits, a discharge which is not created instantaneously will behave like a theoretically sudden increase of flow.
5. The wave length of the undulations depends only on the mean height of the layer above the primitive surface. The former decreases as the latter increases.

These results suggest that the undulations composing the head of a discharge wave have a very general character, in the same sense that the solitary wave has a general character. Within certain limits, they are formed independently of the rate at which the discharge is

increased, and depend only on the final discharge rate; they assume a stable configuration after a short initial interval, that is, they are propagated without change of form. In section V–9, it was mathematically demonstrated that the only wave propagated without change of form is the cnoidal wave, which includes the solitary wave as a special limiting case. It is also true that the solitary wave is a special case of the discharge wave from the physical point of view. The solitary wave may be formed by a sudden increase of discharge which soon decreases to zero, while the discharge wave is caused by a sudden increase of discharge which is maintained. All these considerations inevitably suggest the question: Are the undulations composing the head of a discharge wave cnoidal waves?

A comparison of figure 4 with Favre's figure 48 [2, p. 156] supports an affirmative answer. The wave profiles are very similar. However, there is a more significant comparison which may be made, namely, one between the theoretical velocity of propagation, ω_c, and that observed by experiment. This is accomplished by using eq 167 and 170. From the values of η_1 and λ/H given by the experimental data, we determine η_3, k, and η_2 by eq 163, 162, and 158, and then calculate ω_c from eq 170. Equation 191 written in the form

$$\omega=\sqrt{gH'}\left(1+\frac{3}{4}\frac{h'}{H'}\right), \tag{191}$$

is used to compute ω. This equation, in the form of eq 202, has already been verified in section V–15. In order to calculate U_0, we write

$$\omega h'=U_0(H'+h'), \tag{211}$$

where h' is the average height of the layer, and H' is the undisturbed depth of the liquid. It should be noted that this H' is different from the H in eq 170. U_0 is computed from eq 211 with the assistance of eq 191. From eq 167 we have $\omega_c=\omega-U_0$. These two values are compared in the following tables for nine nonbreaking waves. Table 1 gives the experimental data from Favre [2, p. 157], and table 2 gives the results of the calculations. The explanation of the symbols is clearly indicated in figure 10.

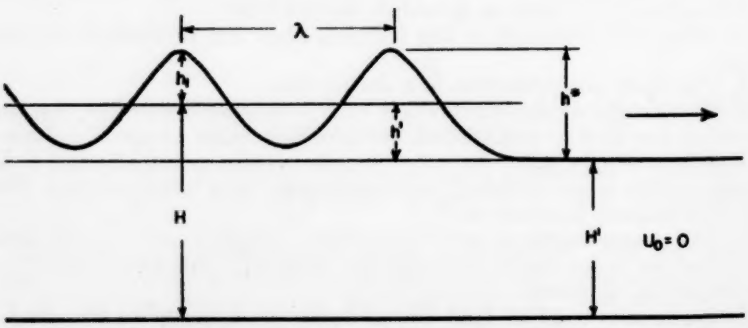

FIGURE 10.—*Diagram illustrating the notation used in the studies of the positive surge.*

TABLE 1.—*Favre's experimental data on positive surges*

Experiment No.	Undisturbed depth, H'	Mean height of layer h'	Crest height, h^*, 1st wave	2d wave	3d wave	4th wave	Mean h^*	Wave length	h'/H'
	cm	*cm*	*cm*	*cm*	*cm*	*cm*	*cm*	*cm*	
4	20.55	2.29	3.90	3.60	------	------	3.75	222	0.111
6	20.22	3.08	6.00	6.00	5.90	------	5.97	194	.152
8	20.19	4.08	8.10	8.00	------	------	8.05	192	.202
10	20.38	4.84	9.80	8.70	9.90	------	9.47	185	.238
12	20.57	5.72	11.70	11.40	10.90	------	11.33	176	.278
21	10.78	0.86	1.30	1.20	1.00	1.05	1.14	119	.080
22	10.73	1.50	2.80	2.70	2.85	2.70	2.76	101	.140
23	10.79	2.48	4.95	4.70	4.70	4.45	4.70	91	.230
24	10.74	3.02	6.25	6.10	5.70	6.10	6.04	86	.281

TABLE 2.—*Velocity comparisons between cnoidal waves and positive surges*

Experiment No.	h_1=mean h^*-h'	$H=H'+h'$	λ/H	η_1	η_2	η_3	$\sin^{-1}k$	ω	U_0	$\omega-U_0$	ω_c	Percentage of difference
	cm	*cm*						*cm/sec*	*cm/sec*	*cm/sec*	*cm/sec*	
4	1.46	22.84	9.72	0.064	0.052	0.142	48.6°	153.8	15.4	138.4	139.2	+0.58
6	2.89	23.30	8.33	.124	.094	.197	55.4°	156.9	20.7	136.2	136.7	+.37
8	3.97	24.27	7.91	.164	.118	.222	58.8°	162.0	27.2	134.8	137.9	+2.30
10	4.63	25.22	7.34	.184	.126	.257	58.1°	166.7	32.0	134.7	137.9	+2.38
12	5.61	26.29	6.69	.213	.157	.307	57.5°	171.7	37.4	134.3	135.2	+0.67
21	0.28	11.64	10.22	.024	.022	.126	33.6°	109.0	8.0	101.0	100.0	−.99
22	1.26	12.23	8.26	.103	.081	.198	51.5°	113.4	13.9	99.5	98.7	−.80
23	2.22	13.27	6.86	.167	.129	.289	53.7°	120.6	22.5	98.1	97.0	−1.12
24	3.02	13.76	6.25	.219	.166	.349	55.4°	124.3	27.3	97.0	94.5	−2.58

The average percentage error of ω_c as compared to $\omega-U_0$ is $+0.09 \pm 1.53$, where the $\pm$ term indicates the standard deviation. This is further evidence that the undulations in the head of a discharge wave are cnoidal waves. Inasmuch as these experiments were not intended to shed light on this particular problem, other points of verification cannot be easily attempted. An experiment made especially to investigate this problem would be more suitable.

19. THEORY OF BREAKERS

As was indicated at the end of section V–8, there is a limiting height for a solitary wave, dependent on the depth of the liquid in the channel. If an attempt is made to form a higher wave, it breaks at the crest. If ω is the velocity of propagation of the solitary wave, and u_1 is the absolute velocity of the liquid particle at the apex, that is, at the point $h=h_1$, it is evident that the limiting height is represented by the relation

$$u_1-\omega=0, \tag{212}$$

since if $u_1>\omega$, the particle at the crest of the wave is traveling faster than the wave itself, and consequently the wave is breaking.

Equating eq 112 and 143 and neglecting terms in $(h_1/H)^2$ or higher powers, we obtain for the curvature at the apex of the wave

$$\left(\frac{\partial^2 h}{\partial x^2}\right)_{h=h_1}=-\frac{3}{2}\frac{h_1^2}{H^3}.$$

Substituting this value in eq 116, putting $z=H+h_1$ and neglecting terms of the order of $(h_1/H)^4$, the resulting velocity of the particle is

$$u_1=\sqrt{gH}\left\{\frac{h}{H}+\frac{3}{2}\left(\frac{h}{H}\right)^2\right\}. \tag{213}$$

Putting this value and that from eq 143 in eq 212, the limiting height is a root of the equation

$$\frac{h_1}{H}+\frac{3}{2}\left(\frac{h_1}{H}\right)^2=\sqrt{1+\frac{h_1}{H}}. \tag{214}$$

The only positive real root of this equation is $h_1/H=0.731$, and this is the limiting height of the solitary wave.

This figure is confirmed reasonably well by experiment. Calculations made by the authors from Bazin's data [6, p. 510–514] give 0.71. Scott Russell [7, p. 352; 8, p. 425, 426, 445, 450] surmised that the wave broke when its height was approximately equal to the depth, and McCowan [13, p. 56] states that for his experiments 0.75 is a closer approximation for the relative elevation at the breaking point.

The above result may now be applied to the ultimate breaking of waves rolling in on a gently sloping bottom. Assuming that the waves are solitary, we obtain from eq 148 the following limiting condition involving the volume Q:

$$\frac{3Q^2}{16H^3}=\frac{h_1}{H}=0.73,$$

or

$$H=0.71\sqrt{Q}. \tag{215}$$

This gives the depth at which the waves will break as a function of the volume. If the waves travel up a channel with a sloping bed, the larger waves break first, and the depths at which they break is proportional to the square root of their volume.

The authors express their appreciation to Herbert N. Eaton of the National Bureau of Standards for his valuable criticisms and review of the paper.

VI. REFERENCES

[1] Ph. Forchheimer, Hydraulik, [ed. 3] p. 295 (B. G. Teubner, Leipzig and Berlin, 1930).
[2] H. Favre, Étude Théorique et Expérimentale des Ondes de Translation dans les Canaux Découverts (Dunod, Paris, 1935).
[3] P. Massé, Hydrodynamique Fluviale Régimes Variables (Hermann, Paris, 1935).
[4] H. Lamb, Hydrodynamics, [ed. 5] (Cambridge University Press, Cambridge, England, 1924).

[5] J. Boussinesq, *Théorie des ondes et des remous qui se propagent le long d'un canal rectangulaire horizontal, en communiquant au liquide contenu dans ce canal de vitesses sensiblement pareilles de la surface au fond*, Liouville's J. Math. **17**, 55 (1872).
[6] H. Bazin, *Recherche expérimentales sur la propagation des ondes*, Mém. divers Savants a L'Acad. des Sci. **19**, 495 (1865).
[7] J. Scott Russell, Report on Waves. Report of the fourteenth meeting of the Brit. Assn. Adv. Sci., p. 311. (John Murray, London, 1845.)
[8] J. Scott Russell, Report of the Committee on Waves. Report of the seventh meeting of the Brit. Assn. Adv. Sci., p. 417. (John Murray, London, 1838.)
[9] H. Bouasse, Houle, Rides, Seiches et Marées (Delagrave, Paris, 1924).
[10] J. Boussinesq, *Essai sur la théorie des eaux courantes*, Mém. divers Savants a L'Acad. des Sci. **32**, 56 (1891).
[11] D. J. Korteweg and G. de Vries, *On the change of form of long waves*. Phil. Mag. [5] **39**, 422 (1895).
[12] G. G. Stokes, Mathematical and Physical Papers, **1** (Cambridge University Press, Cambridge, England, 1880).
[13] J. McCowan, *On the solitary wave*, Phil. Mag. [5] **32**, 56 (1891).

WASHINGTON, October 24, 1939.